PHYSIOLOGICAL AND MORPHOLOGICAL EFFECTS OF LED SPECTRUM ON LETTUCE: APPLICATIONS IN CONTROLLED ENVIRONMENT AGRICULTURE

by

JUN LIU

(Under the Direction of Marc W van Iersel)

ABSTRACT

Within photosynthetically active radiation (PAR), green photons had a lower quantum yield of photosynthesis than blue and red photons at low *PPFD*. Once absorbed, green photons drove photosynthesis as efficiently as red photons and more efficiently than blue photons. At high *PPFD*, low absorptance of green photons by leaves allowed more even distribution of green photons throughout the depth of leaves, resulting in higher quantum yield of photosynthesis than blue or red photons. Far-red photons supplemented to background white light induced leaf expansion and canopy enlargement of 'Cherokee', 'Green Saladbowl' and 'Little Gem' lettuces. Supplemental far-red photons only increased light interception of 'Cherokee' throughout the whole life cycle and increased that of 'Green Saladbowl' and 'Little Gem' transiently, which resulted in increased dry weight of 'Cherokee' and 'Little Gem' but not 'Green Saladbowl'. Our study with 'Little Gem' lettuce grown under lights with the same ePAR but different fractions of far-red photons (%FR), showed that far-red photons affected canopy-level photosynthesis depending on plant density. At high plant density, far-red photons resulted in limited increase in light interception. The effect of higher light interception on canopy-level photosynthesis was likely compensated by lower absorptance of far-red photons by lettuce plants and %FR did not

affect canopy-level photosynthesis. At low plant density, far-red photons increased light interception more dramatically, which resulted in increased canopy-level photosynthesis despite lower absorptance. Far-red photons also had lower canopy-level quantum yield of photosynthesis than red photons (0.57 times of that of red photons), due to lower absorptance and the fact that they can only excite PSI. The change in canopy-level photosynthetic rates was not reflected in the dry weight of the plants. Carbon use efficiency changed dramatically through life cycle of 'Little Gem' lettuce plants, ranging from 0.05 to 0.76. CUE initially increased with plant size, then decreased steadily during active vegetative growth. This steady decrease in CUE was due to the increasing percentage of maintenance respiration in total respiration, which competed with growth and growth respiration for carbon. CUE is important for modelling crop growth, as canopy-level photosynthetic rates alone cannot accurately predict crop growth and yield.
INDEX WORDS: Leafy green, Sole-source lighting, Indoor production, Photosynthesis, Green photon, Far-red photon

PHYSIOLOGICAL AND MORPHOLOGICAL EFFECTS OF LED SPECTRUM ON LETTUCE: APPLICATIONS IN CONTROLLED ENVIRONMENT AGRICULTURE

by

JUN LIU

BA, Nanjing Agricultural University, People's Republic of China, 2014

MS, University of Georgia, 2017

A Dissertation Submitted to the Graduate Faculty of The University of Georgia in Partial Fulfillment of the Requirements for the Degree

DOCTOR OF PHILOSOPHY

ATHENS, GEORGIA

2022

PHYSIOLOGICAL AND MORPHOLOGICAL EFFECTS OF LED SPECTRUM ON LETTUCE: APPLICATIONS IN CONTROLLED ENVIRONMENT AGRICULTURE

by

JUN LIU

Major Professor:	Marc W van Iersel
Committee:	Timothy W Coolong
	Joshua Craver
	Juan Carlos Diaz Perez
	Daniel M Johnson

Electronic Version Approved:

Ron Walcott
Vice Provost for Graduate Education and Dean of the Graduate School
The University of Georgia
August 2022

ACKNOWLEDGEMENTS

I would like to express my sincere gratitude to my advisor, Dr. Marc van Iersel, for his guidance, patience, and encouragement. I consider myself very lucky to be Marc's student. Few have bigger hearts and kinder soul than him.

I deeply appreciate support from all my friends, Leynar, Shuyang, He, Yi-wen, Yongjun and YYY. My heartfelt appreciation goes to my families as well, who were always supporting me and encouraging me. Only for their unconditional support, was it possible for me to finish my PhD study.

I would also like to thank my committee members, Drs. Tim Coolong, Josh Craver, Juan Carlos Diaz-Perez, and Dan Johnson, for generously sharing their knowledge with me and all the amazing and inspiring conversation. I thank all our past and current lab members, TC, Claudia, Laura, , Ruqayah, Changhyeon, Kahlin, Geoff, Shane, Reeve, Justin, Suyun, Andrés, Dr. Michael Martin and Sue Dove, for their help along my journey and all the good times we had in lab. I also thank Dr. Nambeesan and John for their help.

TABLE OF CONTENTS

Page

LIST OF TABLES

Page

LIST OF FIGURES

Page

CHAPTER 1

INTRODUCTION

In controlled environment agriculture (CEA), electricity to power supplemental lighting is expensive. In greenhouse production, the electrical cost for lighting can account for as much as 30% of its operating cost (van Iersel and Gianino, 2017). Therefore, reducing the cost of electricity and enhancing the efficiency of supplemental lighting is crucial to increasing profitability of CEA.

Light emitting diodes (LEDs) have received widespread attention in recent years in CEA. Owing to advancing technology, LEDs have superior efficacy over traditional lighting technologies in CEA (Pattison et al., 2018). They thus offer great potential to reduce energy cost and increase profitability for growers. In 2017, the U.S. Department of Energy estimated that by changing all horticultural lighting to LED lights, the industry would reduce 40% of its energy for horticultural lighting, equivalent to $240 million of saving (Pattison et al., 2018). Greenhouse growers, in particular, can benefit from such transformation, since only 2% of supplemental lighting used in greenhouse production is LED lights, which represent a much slower transition than vertical farms and indoor farms (Pattison et al., 2018).

Application of LED technology in CEA production, however, requires a thorough understanding of spectral effect on crop growth and development. Growers lack information on crop performance under these LED grow lights, which have a substantially different spectrum than traditional grow lights and therefore are hesitant to make such transition. Furthermore, many commercially-available LED grow lights contain only red and blue LEDs, because of their

high efficacy of converting electricity into photons, as compared to white LEDs (Nelson and Bugbee, 2014). Abnormal growth and development was reported under these LED grow lights for many crops (Lin et al., 2013; Wollaeger and Runkle, 2015).

Furthermore, the unique features of LEDs with narrow spectrum and controllability also provide an unprecedented opportunity to manipulate crop growth and development. Numerous studies suggested that by altering the light spectrum, growers can regulate crop yield and quality, crop height, flowering, etc. (Gómez and Mitchell, 2015; Wollaeger and Runkle, 2015; Snowden et al., 2016; Ohtake et al., 2018; Zhang and Runkle, 2019). The spectrum of LED grow lights can be easily and precisely tailored by combining LEDs with different wavebands to meet the needs of specific crops. It is also possible to control light level of individual colors in a LED light to create a grow light with dynamic spectrum. This feature of LED lighting provides unique opportunity for growers to increase yield, improve crop quality, shorten or extend crop cycle to meet market window, and overall increase profitability. Therefore, it is of great importance to investigate effect of LED spectrum on crops and identify the most economical way of providing LED lighting.

Much current research interest focuses on increasing carbon assimilation of crop to increase growth and yield. However, not all assimilated carbon through photosynthesis can be incorporated into biomass: a fraction of carbon is lost through respiration. To accurately translate carbon assimilation into growth and yield, carbon use efficiency (CUE) is a critical parameter to consider. CUE is the conversion efficiency of turning assimilated carbon into biomass. CUE of many species is similar, ranging from 0.4 to 0.6 (Gifford, 1994; Monje and Bugbee, 1998; Frantz et al., 2004; Zhen and Bugbee, 2020b). But other literature reported a large variation in CUE at

different developmental stages (van Iersel and Seymour, 2002; van Iersel, 2003). Therefore, more knowledge is needed to successfully predict plant growth from photosynthesis.

Background

I. Green light can excite more photosynthetic reaction centers in canopy

The photosynthetic action spectrum, or McCree spectrum, suggests that light in red and blue regions (600 – 700 nm and 400 – 500 nm, respectively) have the highest quantum yield of CO_2 assimilation across the whole light spectrum over 22 species of crop species surveyed (McCree, 1971). It also shows that within the range of photosynthetically active radiation (PAR, 400-700 nm), photons in the green region (500 – 600 nm) have a lower quantum yield of CO_2 assimilation than red photons (McCree, 1971). Therefore, green light is commonly considered to be photosynthetically inefficient.

The low leaf absorption of green light is primarily responsible for the low quantum yield of CO_2 assimilation. Within the PAR range, a green leaf has the highest absorptance in the blue waveband, followed by red. Green light has the lowest absorptance, which gives plants their green appearance (McCree, 1971; Zhen et al., 2018). The low absorption, however, also gives green light the ability to penetrate deeper into leaf tissues (Terashima et al., 2009; Brodersen and Vogelmann, 2010), and it thus has the potential to excite more cell layers for photosynthetic reactions. At the leaf scale, carbon fixation of spinach leaves under blue light peaks in the palisade mesophyll cells (top 20% of leaf depth), then decreases rapidly with increasing leaf depth (Sun et al., 1998). Peak carbon fixation location under green light was observed deeper in leaves (35-40% of leaf depth); and carbon fixation rate decrease more gradually with increasing leaf depth. Maximum carbon fixation location under red light was coincident with blue light, but

carbon fixation decreased slower than that of blue light but faster than that of green light with increasing leaf depth (Sun et al., 1998; Nishio, 2000).

Not only do green photons penetrate deeper into leaves, absorbed green photons are used with high photosynthetic efficiency. Cucumber leaves absorb green photons more poorly than red and blue photons, resulting in a lower quantum yield of CO_2 assimilation under green light than under red or blue light on an *incident* photon basis. On an *absorbed* photon basis, the quantum yield of CO_2 assimilation under red and green light were similar, and higher than that of blue light (Hogewoning et al., 2012).

The advantage of green photons is even more pronounced at high light level. Since green photons can excite more photosynthetic reaction centers, the light saturation point under green light is likely higher than red and blue light. Red and blue photons can excite fewer reaction centers, thus saturating those reaction centers at lower light intensity, while not exciting many reactions centers deeper in the leaves. That may result in a lower maximum photosynthetic capacity under red or blue light, as compared to green light. This is supported by a study that measured 'differential quantum yield' (Terashima et al., 2009). The differential quantum yield was measured by adding red or green light to leaves illuminated by white light of different intensities, and the quantum yield of CO_2 assimilation of the added light was quantified (Terashima et al., 2009). The differential quantum yield under red light was higher than the differential quantum yield under green light at low background white light levels, due to low absorption of green light. But as the background light level increased, the differential quantum yield under green light decreased more slowly than that of red, and was eventually higher than the differential quantum yield under red light (Terashima et al., 2009). Red light likely was absorbed very efficiently by the uppermost chloroplasts that were already partially saturated by

the high level background white light. Green light, on the other hand, was able to reach the chloroplasts deeper in the mesophyll and excited those chloroplasts that were under lower light conditions. Therefore, green light was able to drive more leaf photosynthesis under a high background white light level (Terashima et al., 2009).

The interactive effect of light quality and light intensity on photosynthesis has rarely been studied. Based on previous discussion, green light shows great potential to enhance photosynthesis at high light levels and when combined with other photons. However, a more comprehensive study is needed to fully investigate the magnitude of this enhancement effect of green light and to elucidate the underlying photosynthetic mechanism.

II. Far-red light can enhance both photosynthetic efficiency and light energy harvesting

The far-red waveband (700 – 750 nm) was long considered as photosynthetically ineffective, but recently has been shown to have great benefits for photosynthesis, growth, and development (Park and Runkle, 2017; Zhen and van Iersel, 2017; Zhen et al., 2018; Zhang and Runkle, 2019; Zhen and Bugbee, 2020a; b). The McCree spectrum showed that light of wavelengths longer than 685 nm has an extremely low quantum yield of CO_2 assimilation, known as the 'red drop' (Emerson and Lewis, 1943; McCree, 1971). When the wavelength of photons exceeds 685 nm, they contain insufficient energy to excite P680 (the photosystem II primary electron donor). Far-red light alone therefore has very little photosynthetic activity in green plants and is not included in the definition of PAR (McCree, 1971; 1972).

Although light from this far-red region has little photosynthetic activity when applied alone, it can nevertheless benefit photosynthesis and carbon assimilation of plants, by 1) enhancing photochemical efficiency when combined with light of shorter wavelengths (Emerson,

1957; Myers, 1971; Zhen and van Iersel, 2017; Zhen et al., 2018; Zhen and Bugbee, 2020a; b), and 2) improving light interception of canopy by inducing shade responses in various vegetable (Li and Kubota, 2009; Kubota et al., 2011; Lee et al., 2015; Lee et al., 2019; Meng and Runkle, 2019b; a; Zou et al., 2019; Elkins and van Iersel, 2020; Zhen and Bugbee, 2020b; Legendre and van Iersel, 2021) and ornamental crops (Park and Runkle, 2017; Craver et al., 2018; Park and Runkle, 2018; Zhang and Runkle, 2019), especially under sole-source lighting.

In the light-dependent reactions of photosynthesis, two photosystems, PSI and PSII, work in a linear manner. They need to operate at matching rates to achieve high electron transport rates and high photosynthetic rates. As discussed before, far-red light does not excite PSII effectively. But far-red light can excite PSI, since PSI absorbs light of 700 nm but PSII does not. When combining far-red light with light that preferentially excites PSII (e.g. blue light), these two photosystems can be harmonically excited and a high quantum yield of PSII (ϕ_{PSII}) can be achieved.

This concept is not unfamiliar to researchers. Over 60 years ago, far-red was empirically shown to enhance the photosynthetic rate when added to light of shorter wavelengths, known as the 'Emerson enhancement effect' (Emerson, 1957; Myers, 1971). This synergistic effect has been long overlooked, partially due to the influential findings of McCree (1971). In recent years, the application of the Emerson enhancement effect by adding far-red light to PAR to improve quantum efficiency of CO_2 assimilation is getting more and more attention.

The photosynthetic enhancement effect of adding far-red light to either white or red and blue light is well quantified at both the leaf and canopy level (Zhen and van Iersel, 2017). Adding 110 $\mu mol \cdot m^{-2} \cdot s^{-1}$ of far-red photons to warm-white and red/blue light significantly increased the ϕ_{PSII} and net photosynthetic rate (P_n) of lettuce (*Lactuca sativa* L.) leaves across a

PPFD range from 0 – 800 $\mu mol \cdot m^{-2} \cdot s^{-1}$ (Zhen and van Iersel, 2017). This benefit of far-red light for photochemistry and overall photosynthesis appears to be a true enhancement effect rather than additive effect, since P_n increased in a greater degree/magnitude than the increase of total photon flux density (Zhen and van Iersel, 2017). At the canopy level, when combined with light of shorter wavelengths, far-red photons were shown to have equal photosynthetic efficiency as PAR (Zhen and Bugbee, 2020a). When adding up to140 $\mu mol \cdot m^{-2} \cdot s^{-1}$ far-red photons to 400 $\mu mol \cdot m^{-2} \cdot s^{-1}$ cool white LED light, net photosynthetic rate increased at an equivalent amount of as adding the same amount of white light. This relationship held true across 14 different crops, including from C_3 plants and C_4 plants (Zhen and Bugbee, 2020a). In addition, when supplying different intensities of far-red light to 200 $\mu mol \cdot m^{-2} \cdot s^{-1}$ red and blue light, 50 $\mu mol \cdot m^{-2} \cdot s^{-1}$ far-red light restored the excitation balance between PSI and PSII of lettuce, while adding more far-red light yielded no further increase in photosynthesis (Zhen and van Iersel, 2017). This relationship between red and blue light and far-red light is yet to be tested on plants adapted to far-red enriched environment at the canopy level, which can provide information to determine the optimal amount of far-red light for crop production.

For plants adapted to high far-red light conditions, there are added layers of complexity that affect carbon assimilation. Lettuce plants grown under 350 $\mu mol \cdot m^{-2} \cdot s^{-1}$ white or red/blue light had similar quantum yield of CO_2 assimilation at the canopy level as plants grown under the same amount of ePAR (extended PAR, 400 - 750 nm), but with 50 $\mu mol \cdot m^{-2} \cdot s^{-1}$ far-red photons substituting white or red/blue light (Zhen and Bugbee, 2020b). Other than the photosynthetic activity, far-red light can also induce leaf and stem elongation and increase light capture, known as shade avoidance response (Park and Runkle, 2017). Since leaves absorb relatively little far-red light, plants shaded by other canopies can detect high far-red light conditions as environmental

signal (McCree, 1971; Holmes and Smith, 1977) and adjust their growth and development to increase light interception and ultimately overall canopy carbon assimilation (Valladares and Niinemets, 2008; Ruberti et al., 2012; Gommers et al., 2013; Park and Runkle, 2017; Craver et al., 2018). Far-red light also induces other shade responses, such as lower chlorophyll concentration and consequentially lower light absorptance (Park and Runkle, 2018; Zou et al., 2019; Zhen and Bugbee, 2020b). But the negative effect on light energy harvesting did not negate the benefit of far-red light on carbon assimilation in previous studies, as the biomass still increased with far-red light inclusion despite lower light absorptance by leaves (Zou et al., 2019; Zhen and Bugbee, 2020b). For many vegetable and ornamental crops, adding far-red light to white and red/blue light increased dry weight (Li and Kubota, 2009; Kubota et al., 2011; Lee et al., 2015; Park and Runkle, 2017; Craver et al., 2018; Park and Runkle, 2018; Lee et al., 2019; Meng and Runkle, 2019a; b; Zhang and Runkle, 2019; Zou et al., 2019; Elkins and Iersel, 2020; Zhen and Bugbee, 2020b; Legendre and van Iersel, 2021).

Although the benefit of adding far-red light to growing light spectrum has been shown in many studies, there is a lack of studies that quantify and distinguish the contributions from the Emerson enhancement effect versus increased leaf elongation and light capture on the photosynthesis, growth, and yield resulting from far-red light inclusion. The optimal amount of far-red light to apply with PAR light to elicit the full benefit of far-red lights inclusion on crops is also unclear.

III. Carbon use efficiency is an important parameter that affects crop growth

Much research has been done to investigate ways to improve photosynthesis of plants to increase growth. However, a fraction of carbon assimilated through photosynthesis is lost through respiration. Therefore, to accurately estimate growth from assimilated carbon through

photosynthesis, CUE is a critical parameter in modeling plant growth. CUE is calculated as the amount of carbon incorporated into biomass divided by the amount of carbon assimilated through photosynthesis.

CUE was previously reported to be fairly constant (Gifford, 1994) and changed only slightly in response to changes in environmental conditions, once the plants were adapted to those conditions (Monje and Bugbee, 1998; van Iersel and Seymour, 2002; Frantz et al., 2004; Kim and van Iersel, 2011; Zhen and Bugbee, 2020b). However, CUE was reported to change dramatically throughout life cycle of plants (van Iersel and Seymour, 2002; van Iersel, 2003). For example, lettuce CUE ranged from 0.2 to 0.6 depending on age, meaning that 80% to 40% of assimilated carbon was lost through respiration (van Iersel, 2003). Studies in wheat (*Triticum aestivum* L. Veery 10), vinca (*Catharanthus roseus*), marigold (*Tagetes patula*), and lettuce all reported changes in CUE throughout the life cycle of plants (Monje and Bugbee, 1998; van Iersel and Seymour, 2000; van Iersel and Seymour, 2002; van Iersel, 2003; Zhen and Bugbee, 2020b). However, despite the large changes in CUE throughout the life cycle of plants, the underlying physiological mechanism has rarely been studies.

Studies overview

We conducted a short-term study to investigate the interactive effect of light intensity (0 – 1500 $\mu mol \cdot m^{-2} \cdot s^{-1}$) and light spectrum (blue, green, red, and mixtures of the three lights) on photosynthesis, and explored the underlying physiological mechanisms by constructing photosynthetic light-response curves and CO_2-response curves.

To further explore the effect of supplemental far-red light on crop growth and yield and to quantify the optimal amount of far-red light to apply, we studied the long-term effect of far-red light inclusion on plant growth and development. We supplemented a wide range of far-red

light (ranging from 0 to 70 $\mu mol \cdot m^{-2} \cdot s^{-1}$) to 200 $\mu mol \cdot m^{-2} \cdot s^{-1}$ PAR light and evaluated morphological and physiological changes of lettuce from seedling to mature stage and yield of lettuce plants.

We also aim to disentangle the effect of far-red light on crop growth and development through promoting canopy enlargement and through photosynthetic activity of far-red light. To do so, we grew lettuce plants in a whole-plant gas exchange system under light with different fractions of far-red light. We measured photosynthetic rate at the whole plant level and tracked morphological and physiological responses of lettuce grown under different far-red light fractions.

Last, to connect carbon assimilation with plant growth and crop yield, we quantified CUE of lettuce from the seedling to the mature stage and determined how CUE is affected by growth and maintenance respiration.

References:

Brodersen, C.R., and Vogelmann, T.C. (2010). Do changes in light direction affect absorption profiles in leaves? *Functional Plant Biology* 37(5)**,** 403-412. doi: 10.1071/fp09262.

Craver, J.K., Boldt, J.K., and Lopez, R.G. (2018). Radiation Intensity and Quality from Sole-source Light-emitting Diodes Affect Seedling Quality and Subsequent Flowering of Long-day Bedding Plant Species. *HortScience* 53(10)**,** 1407-1415.

Elkins, C., and Iersel, M.W.v. (2020). Supplemental Far-red Light-emitting Diode Light Increases Growth of Foxglove Seedlings Under Sole-source Lighting. 1. doi: 10.21273/horttech04661-20.

Emerson, R. (Year). "Dependence of yield of photosynthesis in long-wave red on wavelength and intensity of supplementary light", in: *Science*: AMER ASSOC ADVANCEMENT SCIENCE 1200 NEW YORK AVE, NW, WASHINGTON, DC 20005), 746-746.

Emerson, R., and Lewis, C.M. (1943). The dependence of the quantum yield of Chlorella photosynthesis on wave length of light. *American Journal of Botany* 30(3)**,** 165-178.

Frantz, J.M., Cometti, N.N., and Bugbee, B. (2004). Night temperature has a minimal effect on respiration and growth in rapidly growing plants. *Annals of Botany* 94(1)**,** 155-166.

Gifford, R. (1994). The global carbon cycle: a viewpoint on the missing sink. *Functional Plant Biology* 21(1)**,** 1-15.

Gómez, C., and Mitchell, C.A. (2015). Growth Responses of Tomato Seedlings to Different Spectra of Supplemental Lighting. *HortScience* 50(1)**,** 112-118.

Gommers, C.M.M., Visser, E.J.W., Onge, K.R.S., Voesenek, L.A.C.J., and Pierik, R. (2013). Shade tolerance: when growing tall is not an option. *Trends in Plant Science* 18(2)**,** 65-71. doi: 10.1016/j.tplants.2012.09.008.

Hogewoning, S.W., Wientjes, E., Douwstra, P., Trouwborst, G., Van Ieperen, W., Croce, R., et al. (2012). Photosynthetic quantum yield dynamics: from photosystems to leaves. *The plant cell* 24(5)**,** 1921-1935. doi: 10.1105/tpc.112.097972.

Holmes, M., and Smith, H. (1977). The function of phytochrome in the natural environment—II. The influence of vegetation canopies on the spectral energy distribution of natural daylight. *Photochemistry and Photobiology* 25(6)**,** 539-545.

Kim, J., and van Iersel, M.W. (2011). Slowly developing drought stress increases photosynthetic acclimation of Catharanthus roseus. *Physiologia Plantarum* 143(2)**,** 166-177. doi: 10.1111/j.1399-3054.2011.01493.x.

Kubota, C., Chia, P., Yang, Z., and Li, Q. (Year). "Applications of far-red light emitting diodes in plant production under controlled environments", in: *International Symposium on Advanced Technologies and Management Towards Sustainable Greenhouse Ecosystems: Greensys2011 952*), 59-66.

Lee, M.-J., Park, S.-Y., and Oh, M.-M. (2015). Growth and cell division of lettuce plants under various ratios of red to far-red light-emitting diodes. *Horticulture, Environment, and Biotechnology* 56(2)**,** 186-194.

Lee, M., Xu, J., Wang, W., and Rajashekar, C. (2019). The Effect of Supplemental Blue, Red and Far-Red Light on the Growth and the Nutritional Quality of Red and Green Leaf Lettuce. *American Journal of Plant Sciences* 10(12)**,** 2219-2235.

Legendre, R., and van Iersel, M.W. (2021). Supplemental Far-Red Light Stimulates Lettuce Growth: Disentangling Morphological and Physiological Effects. *Plants* 10(1)**,** 166.

Li, Q., and Kubota, C. (2009). Effects of supplemental light quality on growth and phytochemicals of baby leaf lettuce. *Environmental and Experimental Botany* 67(1)**,** 59-

64.

Lin, K.-H., Huang, M.-Y., Huang, W.-D., Hsu, M.-H., Yang, Z.-W., and Yang, C.-M. (2013). The effects of red, blue, and white light-emitting diodes on the growth, development, and edible quality of hydroponically grown lettuce (Lactuca sativa L. var. capitata). *Scientia Horticulturae* 150**,** 86-91.

McCree, K.J. (1971). The action spectrum, absorptance and quantum yield of photosynthesis in crop plants. *Agricultural Meteorology* 9(Supplement C)**,** 191-216. doi: 10.1016/0002-1571(71)90022-7.

McCree, K.J. (1972). Test of current definitions of photosynthetically active radiation against leaf photosynthesis data. *Agricultural Meteorology* 10**,** 443-453. doi: 10.1016/0002-1571(72)90045-3.

Meng, Q., and Runkle, E.S. (2019a). Far-red radiation interacts with relative and absolute blue and red photon flux densities to regulate growth, morphology, and pigmentation of lettuce and basil seedlings. *Scientia Horticulturae* 255**,** 269-280. doi: 10.1016/j.scienta.2019.05.030.

Meng, Q., and Runkle, E.S. (2019b). Regulation of flowering by green light depends on its photon flux density and involves cryptochromes. *Physiologia Plantarum* 166(3)**,** 762-771. doi: 10.1111/ppl.12832.

Monje, O., and Bugbee, B. (1998). Adaptation to high CO2 concentration in an optimal environment: radiation capture, canopy quantum yield and carbon use efficiency. *Plant, Cell & Environment* 21(3)**,** 315-324. doi: https://doi.org/10.1046/j.1365-3040.1998.00284.x.

Myers, J. (1971). Enhancement studies in photosynthesis. *Annual Review of Plant Physiology*

22(1), 289-312.

Nelson, J.A., and Bugbee, B. (2014). Economic analysis of greenhouse lighting: light emitting diodes vs. high intensity discharge fixtures. *PloS one* 9(6), e99010.

Nishio, J. (2000). Why are higher plants green? Evolution of the higher plant photosynthetic pigment complement. *Plant, Cell & Environment* 23(6), 539-548. doi: 10.1046/j.1365-3040.2000.00563.x.

Ohtake, N., Ishikura, M., Suzuki, H., Yamori, W., and Goto, E. (2018). Continuous Irradiation with Alternating Red and Blue Light Enhances Plant Growth While Keeping Nutritional Quality in Lettuce. *HortScience* 53(12), 1804-1809. doi: 10.21273/hortsci13469-18.

Park, Y., and Runkle, E.S. (2017). Far-red radiation promotes growth of seedlings by increasing leaf expansion and whole-plant net assimilation. *Environmental and experimental botany* 136, 41-49. doi: 10.1016/j.envexpbot.2016.12.013.

Park, Y., and Runkle, E.S. (2018). Far-red radiation and photosynthetic photon flux density independently regulate seedling growth but interactively regulate flowering. *Environmental and Experimental Botany* 155, 206-216.

Pattison, P., Lee, K., stober, k., and Yamada, M. (2018). *Energy Savings Potential of SSL in Horticultural Applications.*

Ruberti, I., Sessa, G., Ciolfi, A., Possenti, M., Carabelli, M., and Morelli, G. (2012). Plant adaptation to dynamically changing environment: the shade avoidance response. *Biotechnology advances* 30(5), 1047-1058.

Snowden, M.C., Cope, K.R., and Bugbee, B. (2016). Sensitivity of Seven Diverse Species to Blue and Green Light: Interactions with Photon Flux. *PLOS ONE* 11(10), e0163121. doi: 10.1371/journal.pone.0163121.

Sun, J., Nishio, J.N., and Vogelmann, T.C. (1998). Green light drives CO2 fixation deep within leaves. *Plant and Cell Physiology* 39(10)**,** 1020-1026. doi: 10.1093/oxfordjournals.pcp.a029298.

Terashima, I., Fujita, T., Inoue, T., Chow, W.S., and Oguchi, R. (2009). Green light drives leaf photosynthesis more efficiently than red light in strong white light: revisiting the enigmatic question of why leaves are green. *Plant and cell physiology* 50(4)**,** 684-697. doi: 10.1093/pcp/pcp034.

Valladares, F., and Niinemets, Ü. (2008). Shade Tolerance, a Key Plant Feature of Complex Nature and Consequences. *Annual Review of Ecology, Evolution, and Systematics* 39(1)**,** 237-257. doi: 10.1146/annurev.ecolsys.39.110707.173506.

van Iersel, M., and Seymour, L. (Year). "Temperature effects on photosynthesis, growth respiration, and maintenance respiration of marigold", in: *XXVI International Horticultural Congress: Elegant Science in Floriculture 624*), 549-554.

van Iersel, M.W. (2003). Carbon use efficiency depends on growth respiration, maintenance respiration, and relative growth rate. A case study with lettuce. *Plant, Cell & Environment* 26(9)**,** 1441-1449. doi: doi:10.1046/j.0016-8025.2003.01067.x.

van Iersel, M.W., and Gianino, D. (2017). An Adaptive Control Approach for Light-emitting Diode Lights Can Reduce the Energy Costs of Supplemental Lighting in Greenhouses. *HortScience* 52(1)**,** 72-77.

van Iersel, M.W., and Seymour, L. (2000). Growth Respiration, Maintenance Respiration, and Carbon Fixation of Vinca: A Time Series Analysis. *Journal of the American Society for Horticultural Science* 125(6)**,** 702-706.

Wollaeger, H.M., and Runkle, E.S. (2015). Growth and acclimation of impatiens, salvia, petunia,

and tomato seedlings to blue and red light. *HortScience* 50(4)**,** 522-529.

Zhang, M., and Runkle, E.S. (2019). Regulating Flowering and Extension Growth of Poinsettia Using Red and Far-red Light-emitting Diodes for End-of-day Lighting. 54(2)**,** 323. doi: 10.21273/hortsci13630-18.

Zhen, S., and Bugbee, B. (2020a). Far‐red photons have equivalent efficiency to traditional photosynthetic photons: implications for redefining photosynthetically active radiation. *Plant, Cell & Environment*.

Zhen, S., and Bugbee, B. (2020b). Substituting Far-Red for Traditionally Defined Photosynthetic Photons Results in Equal Canopy Quantum Yield for CO2 Fixation and Increased Photon Capture During Long-Term Studies: Implications for Re-Defining PAR. *Frontiers in Plant Science* 11(1433). doi: 10.3389/fpls.2020.581156.

Zhen, S., Haidekker, M., and van Iersel, M.W. (2018). Far‐red light enhances photochemical efficiency in a wavelength‐dependent manner. *Physiologia plantarum*.

Zhen, S., and van Iersel, M.W. (2017). Far-red light is needed for efficient photochemistry and photosynthesis. *Journal of plant physiology* 209**,** 115-122. doi: 10.1016/j.jplph.2016.12.004.

Zou, J., Zhang, Y., Zhang, Y., Bian, Z., Fanourakis, D., Yang, Q., et al. (2019). Morphological and physiological properties of indoor cultivated lettuce in response to additional far-red light. *Scientia Horticulturae* 257**,** 108725. doi: 10.1016/j.scienta.2019.108725.

CHAPTER 2

PHOTOSYNTHETIC PHYSIOLOGY OF BLUE, GREEN AND RED LIGHT: LIGHT INTENSITY EFFECTS AND UNDERLYING MECHANISMS[1]

[1]Liu, J. and M.W. van Iersel. Accepted by *Frontiers in Plant Sciences*. Reprinted here with permission of publisher.

Abstract

Red and blue light are traditionally believed to have a higher quantum yield of CO_2 assimilation (*QY*, moles of CO_2 assimilated per mole of photons) than green light, because green light is absorbed less efficiently. However, because of its lower absorptance, green light can penetrate deeper and excite chlorophyll deeper in leaves. We hypothesized that, at high photosynthetic photon flux density (*PPFD*), green light may achieve higher *QY* and net CO_2 assimilation rate (A_n) than red or blue light, because of its more uniform absorption throughout leaves. To test the interactive effects of *PPFD* and light spectrum on photosynthesis, we measured leaf A_n of "Green Tower" lettuce (*Lactuca sativa*) under red, blue, and green light, and combinations of those at *PPFD*s from 30 to 1300 $\mu mol \cdot m^{-2} \cdot s^{-1}$. The electron transport rates (*J*) and the maximum Rubisco carboxylation rate ($V_{c,max}$) at low (200 $\mu mol \cdot m^{-2} \cdot s^{-1}$) and high *PPFD* (1000 $\mu mol \cdot m^{-2} \cdot s^{-1}$) were estimated from photosynthetic CO_2 response curves. Both $QY_{m,inc}$ (maximum *QY* on incident *PPFD* basis) and *J* at low *PPFD* were higher under red light than under blue and green light. Factoring in light absorption, $QY_{m,abs}$ (the maximum *QY* on absorbed *PPFD* basis) under green and red light were both higher than under blue light, indicating that the low $QY_{m,inc}$ under green light was due to lower absorptance, while absorbed blue photons were used inherently least efficiently. At high *PPFD*, the QY_{inc} [gross CO_2 assimilation (A_g)/incident *PPFD*] and *J* under red and green light were similar, and higher than under blue light, confirming our hypothesis. $V_{c,max}$ may not limit photosynthesis at a *PPFD* of 200 $\mu mol \cdot m^{-2} \cdot s^{-1}$ and was largely unaffected by light spectrum at 1000 $\mu mol \cdot m^{-2} \cdot s^{-1}$. A_g and *J* under different spectra were positively correlated, suggesting that the interactive effect between light spectrum and *PPFD* on photosynthesis was due to effects on *J*. No interaction between the three colors of light was detected. In summary, at low *PPFD*, green light had the lowest photosynthetic efficiency because of its low absorptance. Contrary, at high *PPFD*, QY_{inc} under green light was among the

highest, likely resulting from more uniform distribution of green light in leaves.

1 Introduction

The photosynthetic activity of light is wavelength dependent. Based on McCree's work (McCree, 1971; 1972), photosynthetically active radiation is typically defined as light with a wavelength range from 400 to 700 nm. Light with a wavelength shorter than 400 nm or longer than 700 nm was considered as unimportant for photosynthesis, due to its low quantum yield of CO_2 assimilation, when applied as a single waveband (Fig. 2.1). Within the 400 – 700 nm range, McCree (1971) showed that light in the red region (600 - 700 nm) resulted in the highest quantum yield of CO_2 assimilation of plants. Light in the green region (500 - 600 nm) generally resulted in a slightly higher quantum yield than light in the blue region (400 - 500 nm) (Fig. 2.1) (McCree, 1971). The low absorptance of green light is partly responsible for its low quantum yield of CO_2 assimilation. Within the visible spectrum, green leaves have the highest absorptance in the blue region, followed by red. Green light is least absorbed by green leaves, which gives leaves their green appearance (McCree, 1971; Zhen et al., 2019).

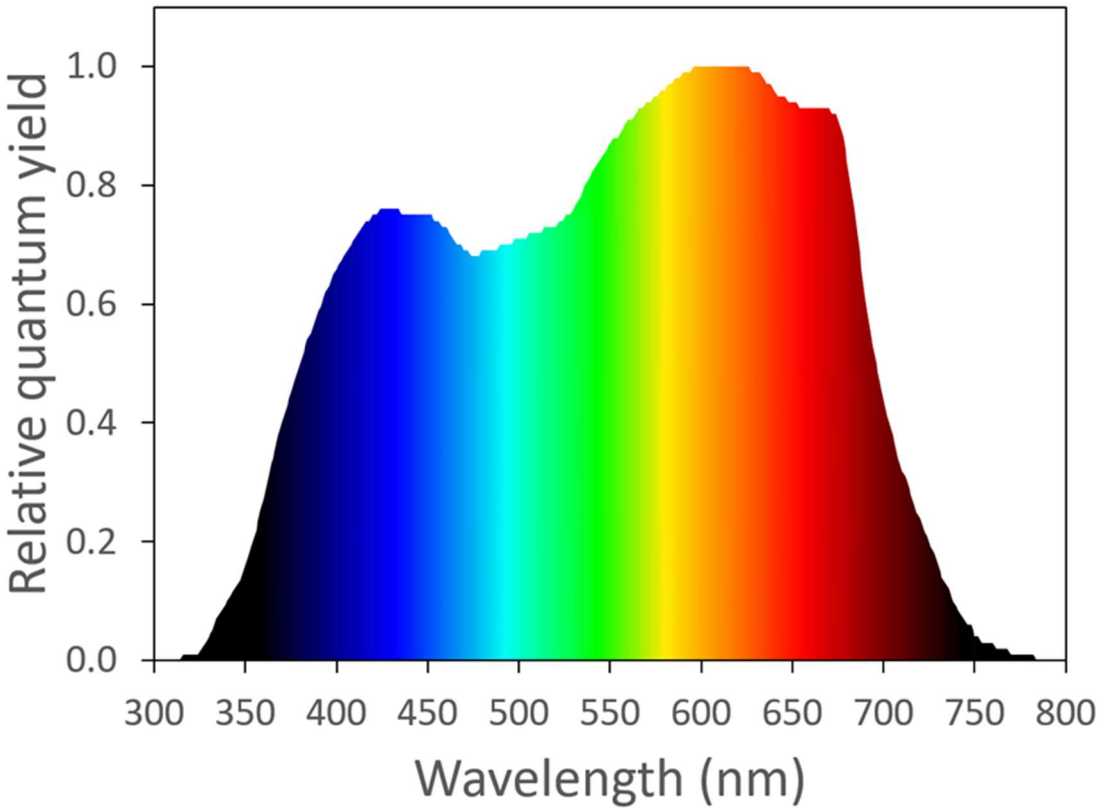

Figure 2.1. The normalized action spectrum of the maximum quantum yield of CO_2 assimilation for narrow wavebands of light from ultra-violet to far-red wavelengths (McCree, 1971). Redrawn using data from Sager et al (1988).

Since red and blue light are absorbed more strongly by photosynthetic pigments than green light, they are predominantly absorbed by the top few cell layers, while green light can penetrate deeper into leaf tissues (Nishio, 2000; Vogelmann and Evans, 2002; Terashima et al., 2009; Brodersen and Vogelmann, 2010), thus giving it the potential to excite photosystems in deeper cell layers. Leaf photosynthesis may benefit from the more uniform light distribution throughout a leaf under green light. Absorption of photons by chloroplasts near the adaxial surface may induce heat dissipation of excess excitation energy in those chloroplasts, while

chloroplasts deeper into the leaf receive little excitation energy (Sun et al., 1998; Nishio, 2000). Blue and red photons, therefore, may be used less efficiently and are more likely to be dissipated as heat than green photons.

The misconception that red and blue light are used more efficiently by plants than green light still occasionally appears (Singh et al., 2015), often citing McCree's action spectrum or the poor absorption of green light by chlorophyll extracts. The limitations of McCree's action spectrum were explained in his original paper: the quantum yield was measured under low photosynthetic photon flux density (*PPFD*), using narrow waveband light, and expressed on an incident light basis (McCree, 1971), but these limitations are sometimes ignored. The importance of green light for photosynthesis has been well established in more recent studies (Sun et al., 1998; Nishio, 2000; Terashima et al., 2009; Hogewoning et al., 2012; Smith et al., 2017).

From those studies, one trend has emerged that has not received much attention: there is an interactive effect of light quality and intensity on photosynthesis (Sun et al., 1998; Evans and Vogelmann, 2003; Terashima et al., 2009). At low *PPFD*, green light has the lowest QY_{inc} (quantum yield of CO_2 assimilation on incident light basis) because of its low absorptance; at high *PPFD*, on the other hand, red and blue light have a lower QY_{inc} than green light, because of their high absorptance by photosynthetic pigments, which shifts much of the light absorption closer to the upper leaf surface. This reduces both the quantum yield of CO_2 assimilation in cells in the upper part of a leaf and light availability in the bottom part of a leaf.

The interactive effect between light quality and intensity was illustrated in an elegant study that quantified the differential quantum yield, or the increase in leaf CO_2 assimilation per unit of additional light (Terashima et al., 2009). The differential quantum yield was measured by adding red or green light to a background illumination of white light of different intensities. At

low background white light levels, the differential quantum yield of red light was higher than that of green light, due to the low absorptance of green light. But as the background light level increased, the differential quantum yield of green light decreased more slowly than that of red light, and was eventually higher than that of red light (Terashima et al., 2009). The red light was absorbed efficiently by the chloroplasts in the upper part of leaves. With a high background level of white light, those chloroplasts already received a large amount of excitation energy from white light and up-regulated non-photochemical quenching (NPQ) to dissipate excess excitation energy as heat, causing the additional red light to be used inefficiently. Green light, on the other hand, was able to reach the chloroplasts deeper in the mesophyll and excited those chloroplasts that received relatively little excitation energy from white light. Therefore, with high background white light intensity, additional green light increased leaf photosynthesis more efficiently than red light (Terashima et al., 2009).

In this paper, we present a comprehensive study to explore potential interactive effect of light intensity and light quality on C_3 photosynthesis and underlying processes. We quantified the photosynthetic response of plants to blue, green, and red light over a wide *PPFD* range to better describe how light intensity and waveband interact. In addition, we examined potential interactions among blue, green, and red light, using light with different ratios and intensities of the three narrow waveband lights. To get a better understanding of the biochemical reasons for the effects of light spectrum and intensity on CO_2 assimilation, we constructed assimilation – internal leaf CO_2 (C_i) response curves (A/C_i curves) under blue, green, and red light, as well as combinations of the three narrow waveband lights at both high and low *PPFD*. We hypothesized that effects of different light spectra would be reflected in the electron transport rate (J) required

to regenerate consumed ribulose 1,5-bisphosphate (RuBP), rather than the maximum carboxylation rate of ribulose-1,5-bisphosphate carboxylase/oxygenase (Rubisco) ($V_{c,max}$).

2 Materials and Methods

2.1 Plant Material

Lettuce 'Green Towers' plants were grown from seed in 1.7 L round pots filled with soilless substrate (Fafard 4P Mix, Sun Gro Horticulture, Agawam, MA, USA). The plants were grown in a growth chamber (E15, Conviron, Winnipeg, Manitoba, Canada) at 23.2 ± 0.8 ˚C (mean ± SD), under white fluorescent light with a 14-hr photoperiod, vapor pressure deficit (VPD) of 1.20 ± 0.43 kPa and a *PPFD* of 200-230 $\mu mol \cdot m^{-2} \cdot s^{-1}$ at the floor level, and ambient CO_2 concentration. Plants were sub-irrigated when necessary with a nutrient solution containing 100 $mg \cdot L^{-1}$ N, made with a complete, water-soluble fertilizer (Peter's Excel 15-5-15 Cal-Mag fertilizer, Everris, Marysville, OH, USA).

2.2 Leaf absorptance, Transmittance, and Reflectance

Leaf absorptance was determined using a method similar to that of Zhen et al. (2019). Three plants were randomly selected. A newly expanded leaf from each plant was illuminated with a broad-spectrum halogen bulb (70W; Sylvania, Wilmington, MA, USA) for leaf transmittance measurement. Transmittance was measured with a spectroradiometer (SS-110, Apogee, Logan, UT, USA). The halogen light spectrum was taken as reference measurement with the spectroradiometer placed directly under the halogen bulb in a dark room. Then, a lettuce leaf was placed between the halogen bulb and spectroradiometer, with its adaxial side facing the halogen bulb and transmitted light was measured. Leaf transmittance was then calculated on 1 nm resolution. Light reflectance of the leaves was measured using a spectrometer with a leaf clip (UniSpec, PP systems, Amesbury, MA, USA). Light absorptance was calculated as 1 −

$reflectance - transmittance$. We verified that this method results in similar absorptance spectra as the use of an integrating sphere. Absorptance of each of the nine light spectra used in this study were calculated from the overall leaf absorptance spectrum and the spectra of the red, green, and blue LEDs.

2.3 Leaf Photosynthesis Measurements

All gas exchange measurements were made with a leaf gas exchange system (CIRAS-3, PP Systems). Light was provided by the LEDs built into the chlorophyll fluorescence module (CFM-3, PP Systems). This module has dimmable LED arrays of different colors, with peaks at 653 nm [red, full width at half maximum (FWHM) of 17 nm], 523 nm (green, FWHM of 36 nm), and 446 nm (blue, FWHM of 16 nm). Nine different combinations of red, green, and blue light were used in this study (Table 2.1). Throughout the measurements, the environmental conditions inside the cuvette were controlled by the leaf gas exchange system. Leaf temperature was 23.0 ± 0.1 ˚C, CO_2 concentration was 400.5 ± 4.1 μmol·mol^{-1}, and the VPD of air in the leaf cuvette was 1.8 ± 0.3 kPa (mean ± SD).

Table 2.1. List of light spectrum abbreviations and their spectral composition

Light spectrum	Fraction of total photon flux (%)		
	Blue	Green	Red
100B	100	0	0
80B20G	80	20	0
20B80G	20	80	0
100G	0	100	0
80G20R	0	80	20
20G80R	0	20	80
100R	0	0	100
20B80R	20	0	80
16B20G64R	16	20	64

2.3.1 Photosynthesis - Light Response Curves

To explore photosynthetic efficiency of light with different spectra, we constructed light response curves for lettuce plants using each light spectrum. Lettuce plants were exposed to 10 *PPFD* levels ranging from 30 to 1300 μmol·m^{-2}·s^{-1} (30, 60, 90, 120, 200, 350, 500, 700, 1000, and 1300 μmol·m^{-2}·s^{-1}) in ascending orders for light response curves. Photosynthetic measurements were taken on 40 – 66 days old lettuce plants. Lettuce plants were taken out of the growth chamber and dark-adapted for 30 min. Starting from the lowest *PPFD*, one newly expanded leaf was exposed to all nine spectra. Net CO_2 assimilation rate (A_n) of the leaf was measured using the leaf gas exchange system. Under each light spectrum, three A_n readings were recorded at 10 s intervals after readings were stable (about 4-20 min depending on *PPFD* after changing *PPFD* and spectrum). The three A_n readings were averaged for analysis. After A_n measurements under all nine light spectra were taken, the leaf was exposed to the next *PPFD* level and A_n measurements were taken with the light spectra in the same order, until measurements were completed at all *PPFD* levels. Throughout the light response curves, C_i decreased with increasing *PPFD*, from 396 ± 10 μmol·mol^{-1} at a *PPFD* of 30 μmol·m^{-2}·s^{-1} to 242 ± 44 μmol·mol^{-1} at a *PPFD* of 1300 μmol·m^{-2}·s^{-1}. To account for the potential effect of plants and the order of the spectra on assimilation rates, the order of the different spectra was re-randomized for each light response curve, using a Latin square design with plant and spectrum as the blocking factors. Data were collected on nine different plants.

Regression curves (exponential rise to maximum) were fitted to the data for each light spectrum and replication (plant):

$$A_n = A_{g,max} \times (1 - e^{-QY_{m,inc} \times \frac{PPFD}{A_{g,max}}}) - R_d \quad \cdots\cdots\cdots\cdots \textit{Equation 1}$$

where R_d is the dark respiration rate, $QY_{m,inc}$ is the maximum quantum yield of CO_2 assimilation (initial slope of light response curve, mol of CO_2 fixed per mol of incident photons) and $A_{g,max}$ is the light-saturated gross assimilation rate. The $A_{n,max}$ is the light-saturated net assimilation rate and was calculated as $A_{n,max} = A_{g,max} - R_d$. The maximum quantum yield of CO_2 assimilation was also calculated on absorbed light basis as $QY_{m,abs} = \frac{QY_{m,inc}}{light\ absorptance}$.

The instantaneous quantum yield of CO_2 assimilation based on incident *PPFD* (QY_{inc}) was calculated as $\frac{A_g}{PPFD}$ for each *PPFD* at which A_n was measured, where the gross CO_2 assimilation rate (A_g) was calculated as $A_g = A_n + R_d$. To account for differences in absorptance among the different light spectra, the quantum yield of CO_2 assimilation was also calculated based on absorbed light base, as $QY_{abs} = \frac{A_g}{PPFD \times light\ absorptance}$, where light absorptance is the absorptance of lettuce leaves for each specific light spectrum. The *differential QY*, the increase in assimilation rate per unit of additional incident *PPFD*, was calculated as the derivative of equation 1:

$$Differential\ QY = QY_{m,inc} \times e^{-QY_{m,inc} \times \frac{PPFD}{A_{g,max}}} \cdots\cdots\cdots\cdots \text{Equation 2}$$

2.3.2 Photosynthesis – Internal CO_2 Response (A/C_i) Curves

To explore the underlying physiological mechanisms of assimilation responses to different light spectra, we constructed A/C_i curves. Typically, A/C_i curves are collected under saturating *PPFD*. We collected A/C_i curves at two *PPFD*s (200 and 1000 μmol·m^{-2}·s^{-1}) to explore interactive effects of light spectrum and *PPFD* on the assimilation rate. At a *PPFD* of 200 μmol·m^{-2}·s^{-1}, red light has the highest A_n and green light the lowest A_n, while at *PPFD* of 1000 μmol·m^{-2}·s^{-1}, red and green light resulted in the highest A_n and blue light in the lowest A_n.

We used the rapid A/C_i response (RACiR) technique that greatly accelerates the process of constructing A/C_i curves (Stinziano et al., 2017). We used a Latin square design, similar to the light response curves. A/C_i curves were measured under the same nine spectra used for the light response curves. Nine lettuce plants were used as replicates. For each A/C_i curve, CO_2 concentration in the leaf cuvette started from 0 μmol·mol^{-1}, steadily ramping to 1200 μmol·mol^{-1} over 6 min. A reference measurement was also taken at the beginning of each replication with an empty cuvette to correct for the reaction time of the leaf gas exchange system. Post-ramp data processing was used to calculate the real A and C_i with the spreadsheet provided by PP systems, which yielded the actual A/C_i curves with C_i range of about 100 – 950 μmol·mol^{-1}. Throughout the data collection, leaf temperature was 24.4 ± 1.3 ˚C and VPD in the cuvette was 1.4 ± 0.2 kPa.

Curve fitting for A/C_i curves was done by minimizing the residual sum of squares, following the protocol developed by Sharkey et al. (2007). Among our nine replicates, four plants did not show clear Rubisco limitations at low *PPFD* and for those plants Rubisco limitation ($V_{c,max}$) was not included in the model (Sharkey et al., 2007). We therefore report $V_{c,max}$ values for high *PPFD* only. The J was determined for all light spectra at both *PPFD*s. We therefore report $V_{c,max}$ was determined for all light spectra only at high *PPFD*. The quantum yield of electron transport [$QY(J)$] was calculated on both incident and absorbed *PPFD* basis as $QY(J)_{inc} = \frac{J}{PPFD}$ and $QY(J)_{abs} = \frac{QY(J)_{inc}}{light\ absorptance}$, respectively. We did not estimate triose phosphate utilization, because the A/C_i curves often did not show a clear plateau.

2.4 Data Analysis

The $QY_{m,inc}$, $QY_{m,abs}$, and $A_{g,max}$ were analyzed with ANOVA to determine the effects of light spectrum using SAS (SAS University Edition; SAS Institute, Cary, NC, USA). A_n, QY_{inc}, and QY_{abs} at each *PPFD* level and $V_{c,max}$ and J estimated from A/C_i curves were similarly

analyzed with ANOVA using SAS. A_n at different *PPFD* levels were analyzed with regression analysis to detect interactive effect of blue, green, and red light on leaf assimilation rates using the fractions of red, blue, and green light as explanatory variables (JMP Pro 15, SAS Institute).

3 Results

3.1 Leaf Absorptance

A representative spectrum of light absorptance, reflectance and transmittance of a newly fully expanded lettuce leaf is shown in Fig. 2.2. In the blue region, 400 - 500 nm, the absorptance by 'Green Towers' lettuce leaves was high and fairly constant, averaging 91.6%. The leaf absorptance decreased as the wavelength increased from 500 to 551 nm where the absorptance minimum was 69.8%. Absorptance increased again at longer wavelengths, with a second peak at 666 nm (92.6%). Above 675 nm, the absorptance decreased steadily to <5% at 747 nm (Fig. 2.2). The absorptance spectrum of our lettuce leaves is similar to what McCree (1971) obtained for growth chamber-grown lettuce, with the exception of slightly higher absorptance in the green part of the spectrum in our lettuce plants. Using this spectrum, the absorptance of the blue, green, and red LED lights were calculated to be 93.2 ± 1.0%, 81.1 ± 1.9% and 91.6 ± 1.1%, respectively. Absorptance of all nine spectra was calculated based on their ratios of red, green, and blue light (Table 2.2).

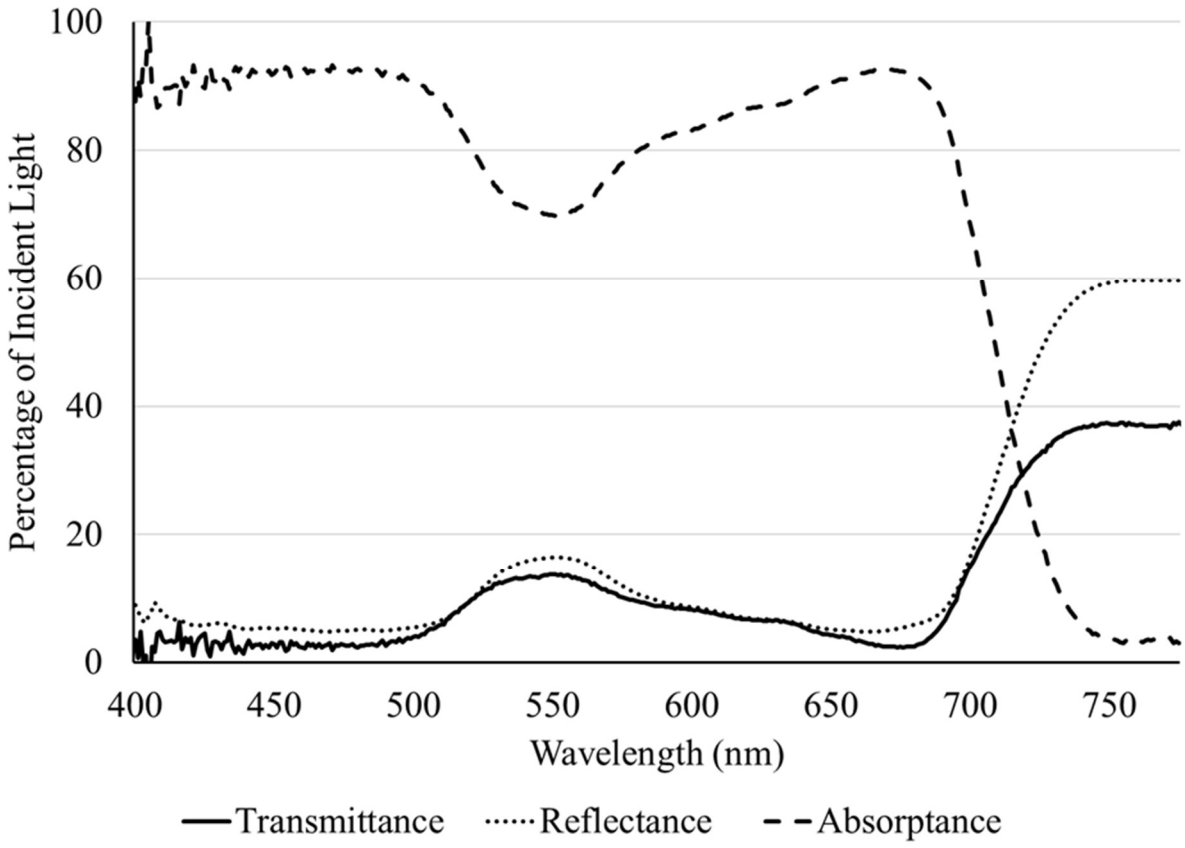

Figure 2.2. Light absorptance, reflectance, and transmittance spectrum of a newly fully-expanded 'Green Towers' lettuce leaf.

Table 2.2. Light absorptance and transmittance of new fully-expanded 'Green towers' lettuce leaves under nine light spectra. See Fig. 2.2 for the leaf absorptance spectrum.

Light spectrum*	LIGHT ABSORPTANCE (%)	LIGHT TRANSMITTANCE (%)
100B	93.2	2.2
80B20G	90.8	3.6
20B80G	83.6	7.8
100G	81.1	9.1
80G20R	83.2	8.1
20G80R	89.5	4.9
100R	91.6	3.9
20B80R	91.9	3.5
16B20G64R	89.8	4.7

See spectral composition in Table 2.1

3.2 Light Quality and Intensity Effects on Photosynthetic Parameters

Light response curves of lettuce under all nine spectra are shown in Fig. 2.3, with regression coefficients in Table S2.1. It is worth noting that a few plants showed photoinhibition under 100B (decrease in A_n with $PPFD > 1000$ µmol·m^{-2}·s^{-1}). Those data were excluded in curve fitting for light response curves to better estimate asymptotes. Photoinhibition was not observed under other spectra.

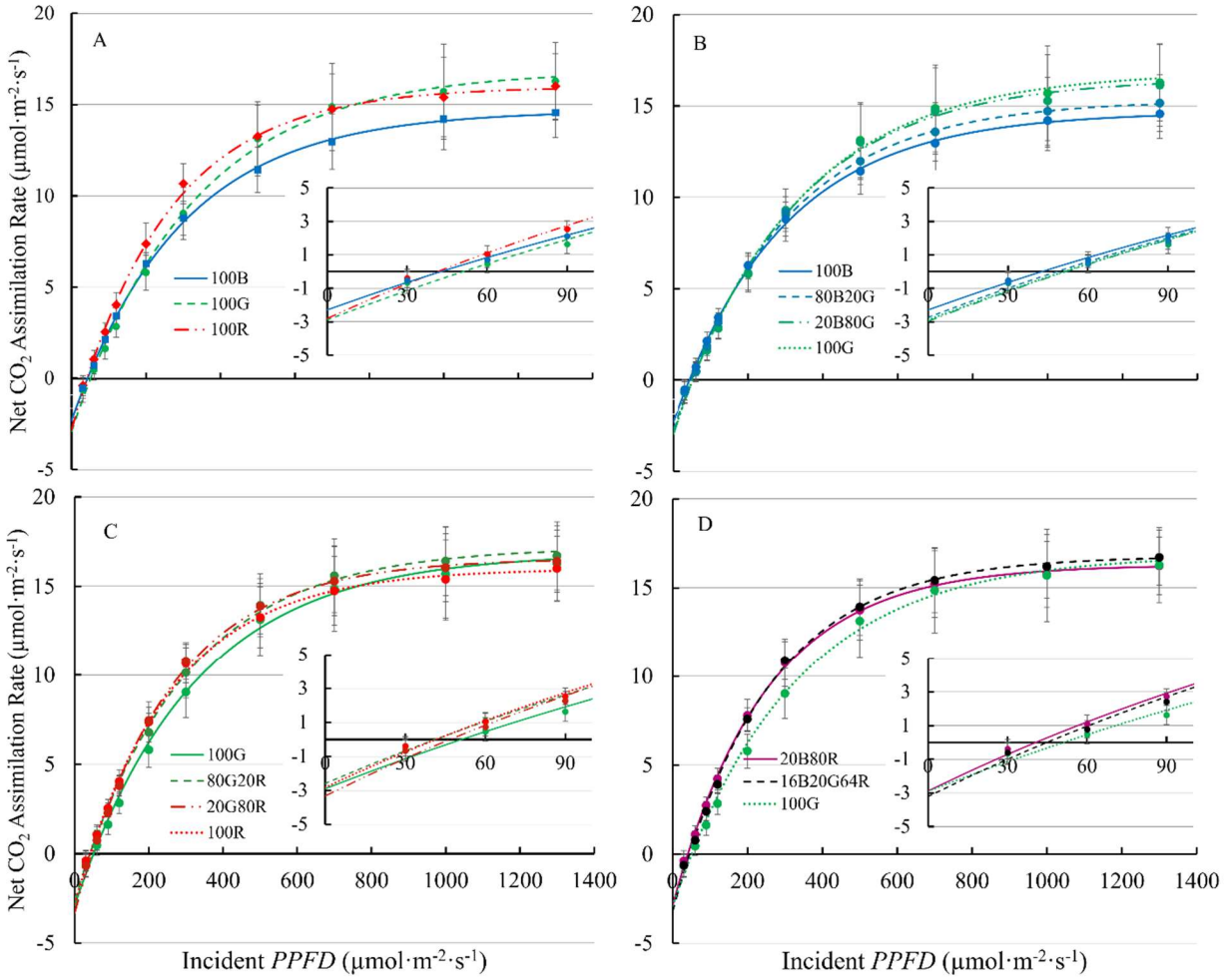

Figure 2.3. Net assimilation (A_n) - light response curves of 'Green Towers' lettuce under nine light spectra. Error bars represent the standard deviation (n = 9). Inserts show A_n against *PPFD* of 30-90 µmol·m^{-2}·s^{-1}s to better show the initial slopes of curves. The composition of the nine light spectra is shown in Table 2.1. The light spectra in the graphs are (A)100B, 100G and 100R;

(B)100B, 80B20G, 20B80G and 100G; (C)100G, 80G20R, 20G80R and 100R; and (D)20B80R, 16B20G64R and 100G.

The $QY_{m,inc}$ of lettuce plants was 22% and 27% higher under red light (74.3 mmol·mol^{-1}) than under either 100G (60.8 mmol·mol^{-1}) or 100B (58.4 mmol·mol^{-1}), respectively (Fig. 2.4A, Table S2.1). Spectra with a high fraction of red light (64% or more) resulted in a high $QY_{m,inc}$ (Fig. 2.4A), while 80G20R resulted in an intermediate $QY_{m,inc}$ (Fig. 2.4A). To determine whether differences in $QY_{m,inc}$ were due to differences in absorptance or in the ability of plants to use the absorbed photons for CO_2 assimilation, we also calculated $QY_{m,abs}$. On an absorbed light basis, 100B light still resulted in the lowest $QY_{m,abs}$ (62.7 mmol·mol^{-1}) and red light resulted in the highest $QY_{m,abs}$ (81.1 mmol·mol^{-1}) among narrow waveband lights (Fig. 2.4B). Green light resulted in a $QY_{m,abs}$ (74.9 mmol·mol^{-1}) similar to that under red light, but significantly higher than that of blue light (Fig. 2.4B). We did not find any interactions (synergism or antagonism) between lights of different colors, with all physiological responses under mixed spectra being similar to the weighted average of responses under single colors. Thus, for the rest of the results we focus on the three narrow waveband spectra.

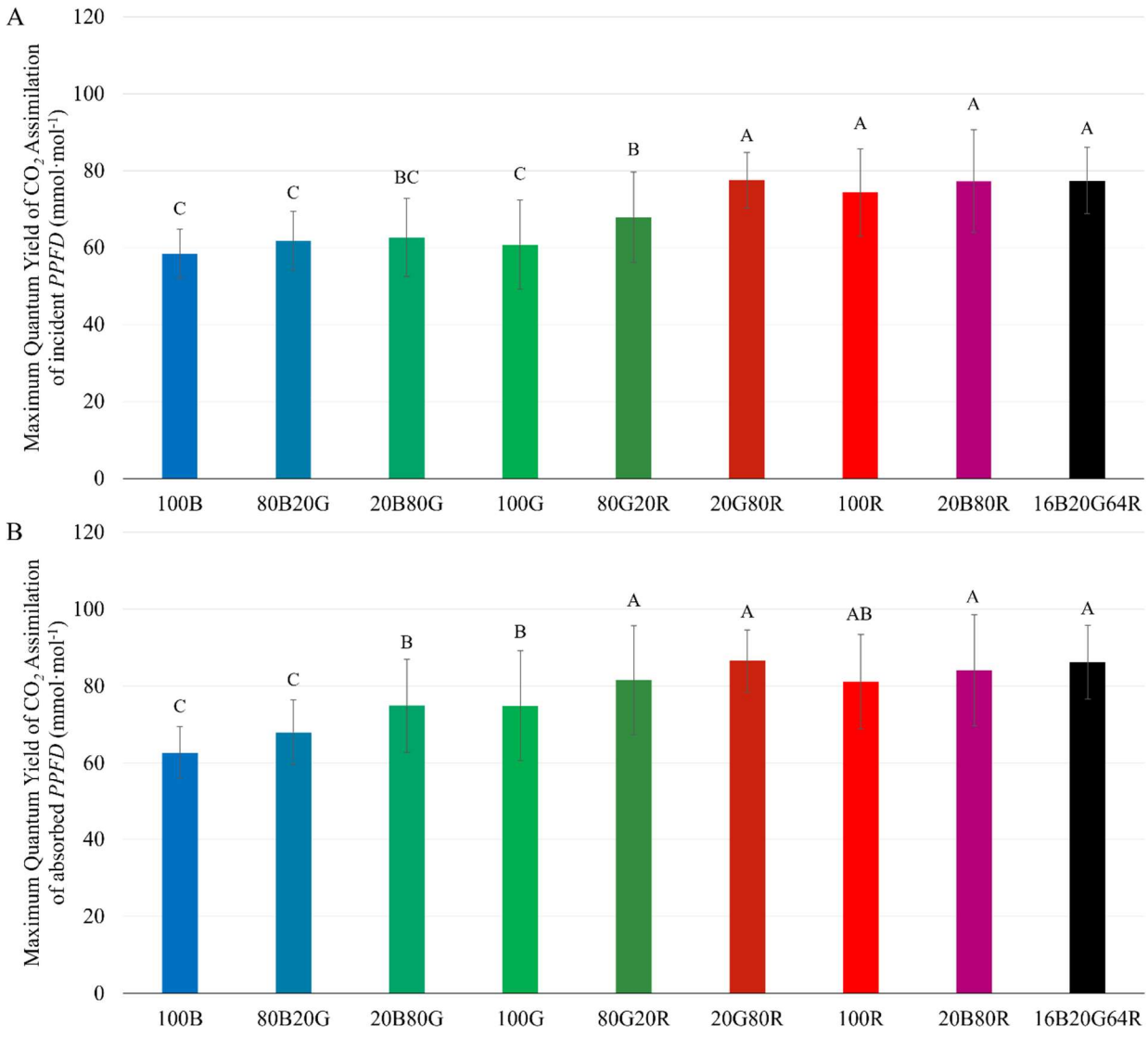

Figure 2.4. Maximum quantum yield of CO_2 assimilation of 'Green Towers' lettuce based on incident ($QY_{m,inc}$) **(A)** and absorbed light ($QY_{m,abs}$) **(B)** under nine different light spectra. Values are calculated as the initial slope of the light response curves of corresponding light spectra (see Fig. 2.3). Bars with the same letter are not statistically different ($p \leq 0.05$). Error bars represent the standard deviation (n=9). The composition of the nine light spectra is shown in Table 2.1.

Among the three narrow waveband lights, 100G resulted in the highest $A_{g,max}$ (20.0 µmol·m^{-2}·s^{-1}), followed by red (18.9 µmol·m^{-2}·s^{-1}), and blue light (17.0 µmol·m^{-2}·s^{-1}) (Fig. 2.5,

Table S2.1). As with $QY_{m,inc}$ and $QY_{m,abs}$, combining two or three colors of light resulted in an $A_{g,max}$ similar to the weighted averages of individual light colors.

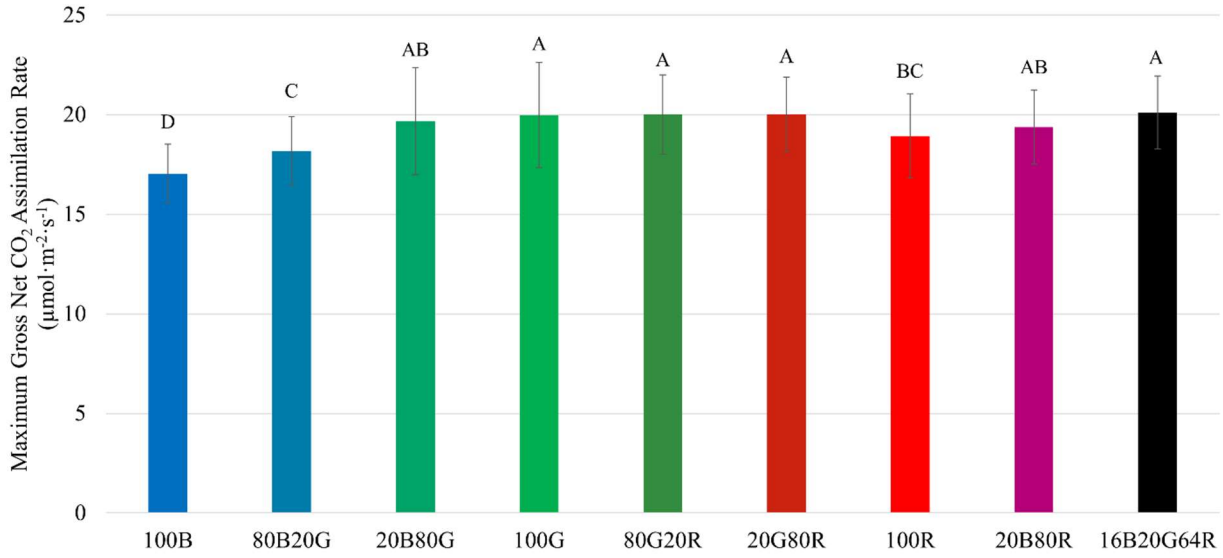

Figure 2.5. Maximum gross assimilation rate ($A_{g,max}$) of 'Green Towers' lettuce under different light spectra, calculated from the light response curves. Bars with the same letter are not statistically different ($p \leq 0.05$). Error bars represent standard deviation (n=9). The composition of the nine light spectra is shown in Table 2.1.

QY_{inc} initially increased with increasing *PPFD* and peaked at 90 - 200 µmol·m^{-2}·s^{-1}, then decreased at higher *PPFDs* (Fig. 2.6A). The QY_{inc} under 100R was higher than under either green or blue light at low *PPFD* (≤ 300 µmol·m^{-2}·s^{-1}). Although 100G resulted in lower QY_{inc} than 100B at low *PPFD* (≤300 µmol·m^{-2}·s^{-1}), the decrease in QY_{inc} under 100G with increasing *PPFD* was slower than that with 100B or 100R. Above 500 µmol·m^{-2}·s^{-1}, the QY_{inc} with 100G was comparable to the QY_{inc} with 100R, and higher than with 100B (Fig. 2.6A). The QY_{abs} with 100R was higher than that with either 100G or 100B at *PPFDs* from 60 to 120 µmol·m^{-2}·s^{-1} ($p <$ 0.05). The QY_{abs} with 100G was similar to 100B at low *PPFD*, but decreased slower than that

with either 100R or 100B as *PPFD* increased. At $PPFD \geq 500$ µmol·m^{-2}·s^{-1}, QY_{abs} was lowest under 100B among the three monochromatic lights ($p < 0.05$) (Fig. 2.6B).

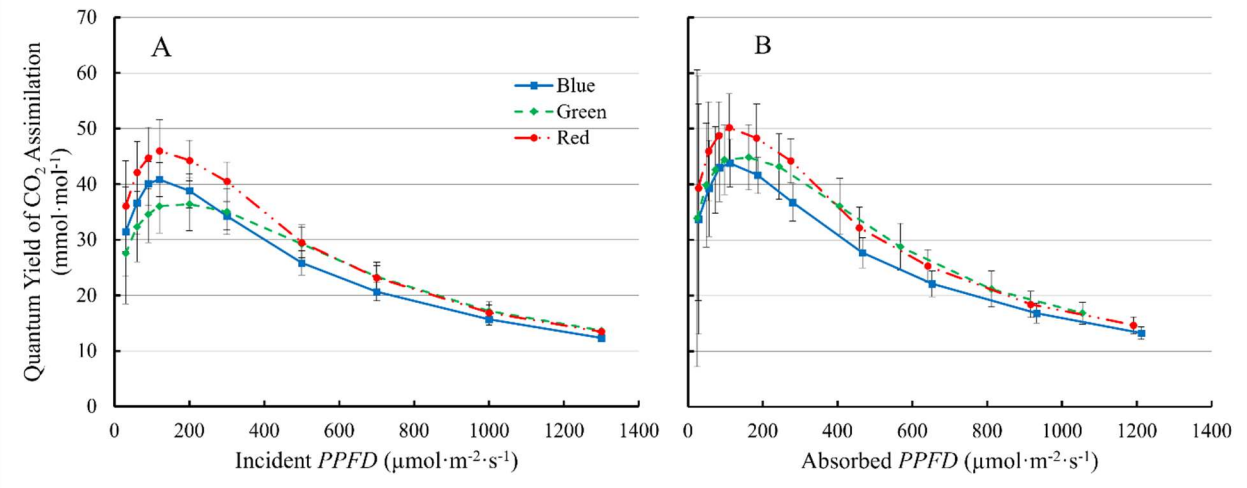

Figure 2.6. The quantum yield of CO_2 assimilation of 'Green Towers' lettuce as a function of incident (QY_{inc}) **(A)** and absorbed *PPFD* (QY_{abs}) **(B)** under blue, green, and red LED light. Error bars represent the standard deviation (n=9).

The differential *QY*, which quantifies the increase in CO_2 assimilation per unit of additional *PPFD*, decreased with increasing *PPFD*. The differential *QY* with 100R was higher than those with 100B and 100G at low *PPFD*. At a *PPFD* of 30 µmol·m^{-2}·s^{-1}, the differential *QY* was 70.5 mmol·mol^{-1} for 100R, 59.4 mmol·mol^{-1} for 100G, and 55.8 mmol·mol^{-1} for 100B (Fig. 2.7). However, the differential *QY* with 100R decreased rapidly with increasing *PPFD* and was lower than the differential *QY* with 100G at high *PPFD* (Fig. 2.7). At high *PPFD*, the differential *QY* with 100G was highest among three monochromatic light (Fig. 2.7). For instance, at a *PPFD* of 1300 µmol·m^{-2}·s^{-1}, the differential *QY* with 100G was 1.09 mmol·mol^{-1}, while those with 100B and 100R were 0.64 mmol·mol^{-1} and 0.46 mmol·mol^{-1}, respectively (Fig. 2.7).

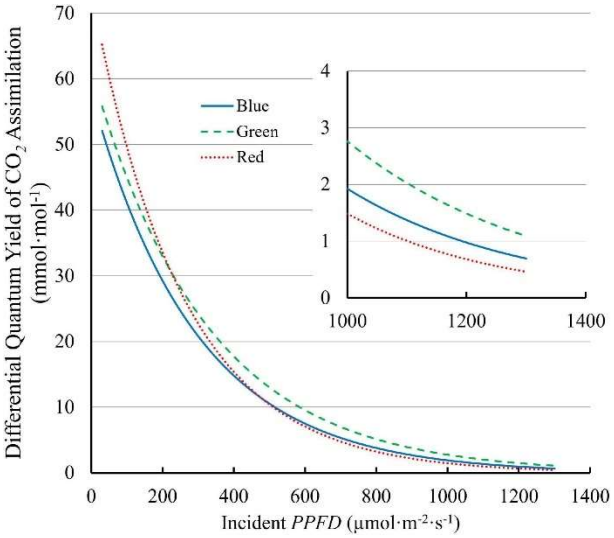

Figure 2.7. The differential quantum yield of CO_2 assimilation (*differential QY*) of 'Green Towers' lettuce under blue, green, and red LED light as a function of the *PPFD*. The *differential QY* is the increase in net assimilation per unit additional *PPFD* and was calculated as the first derivate of the light response curves (Fig. 2.3). The insert shows the differential quantum yield plotted at *PPFDs* of 1000 - 1300 µmol·m^{-2}·s^{-1}s to better show differences at high *PPFD* (note the different y-axis scale).

3.3 Effect of Light Spectrum and Intensity on *J* and $V_{c,max}$

J of lettuce leaves at low *PPFD* was lowest under 100G (47.4 µmol·m^{-2}·s^{-1}), followed by 100B (56.1 µmol·m^{-2}·s^{-1}), and highest under 100R (64.1 µmol·m^{-2}·s^{-1}) (Fig. 2.8A). At high *PPFD*, on the other hand, *J* of leaves exposed to 100G (115.3 µmol·m^{-2}·s^{-1}) and 100R (112.1 µmol·m^{-2}·s^{-1}) were among the highest, while *J* of leaves under 100B was the lowest (97.0 µmol·m^{-2}·s^{-1}) (Fig. 2.8A). At high *PPFD*, $V_{c,max}$ of leaves under blue light (59.3 µmol·m^{-2}·s^{-1}) was lower than $V_{c,max}$ of leaves under 16B20G64R light (72.1 µmol·m^{-2}·s^{-1}), but none of the other treatments differed significantly (Fig. 2.8). When *PPFD* increased from 200 to 1000

µmol·m^{-2}·s^{-1}, *J* under green light increased by 143%, while *J* under blue and red light increased by 73% and 75%, respectively (Fig. 2.8A). *J* and $V_{c,max}$ at high *PPFD* were strongly correlated (R^2 = 0.82) (Fig. S2.3).

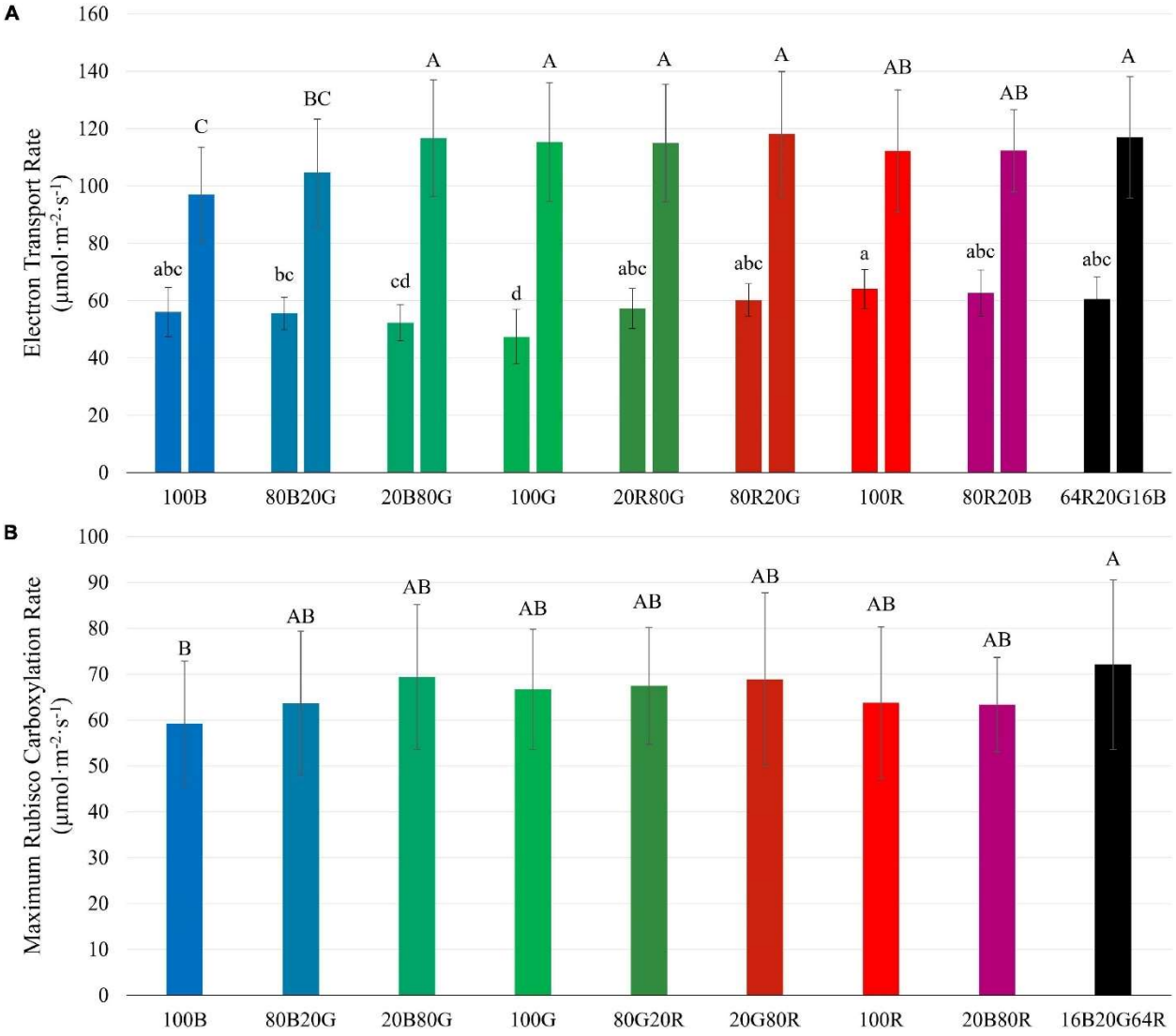

Figure 2.8. Electron transport rate (*J*) at *PPFD*s of 200 (left bars) and 1000 µmol·m^{-2}·s^{-1} (right bars) **(A)** and maximum Rubisco carboxylation rate ($V_{c,max}$) at a *PPFD* of 1000 µmol·m^{-2}·s^{-1} **(B)** of 'Green Towers' lettuce, as estimated from A/C_i curves under different light spectra. Bars with the same letter are not statistically different ($p \leq 0.05$). Error bars represent the standard deviation (n=9). The light composition of the nine light spectra is shown in Table 2.1.

4 Discussion

4.1 Interactive Effect of Light Spectrum and *PPFD* on Photosynthesis

There was an interactive effect of light spectrum and *PPFD* on photosynthetic properties of lettuce. Under low light conditions (≤ 200 μmol·m^{-2}·s^{-1}), the QY_{inc} of lettuce leaves under green light was lowest among blue, green, and red light (Fig. 2.6A), due to its lower absorptance by lettuce leaves. After accounting for absorptance, green photons were used at similar efficiency as blue photons, while red photons were used most efficiently (Fig. 2.6B). The $QY_{m,abs}$ under green and red light were higher than under blue light (Fig. 2.4B). At high *PPFD*, green and red light had similar quantum yield, higher than that of blue light, both on an absorbed and incident light basis (Fig. 2.6A). Multiple factors contributed to the interactive effect of light spectrum and *PPFD* on quantum yield and photosynthesis.

4.1.1 Light Absorptance and Non-Photosynthetic Pigments Determine Assimilation at low *PPFD*

$QY_{m,inc}$ with blue and green light was lower than with red light (Fig. 2.4A), consistent with McCree's action spectrum (McCree, 1971). But when taking leaf absorptance into account, $QY_{m,abs}$ was similar under green and red light and lower under blue light (Fig. 2.4B). Similarly, at low *PPFD* (≤ 200 μmol·m^{-2}·s^{-1}), QY_{inc} of lettuce leaves was highest under red, intermediate under blue, and lowest under green light. When accounting for leaf absorptance, QY_{abs} under red light remained highest and QY_{abs} under both green and blue light were similar at low *PPFD* (Fig. 2.6A). Consistent with our data, previous studies also documented that, once absorbed, green light can drive photosynthesis efficiently at low *PPFD* (Balegh and Biddulph, 1970; McCree, 1971; Evans, 1987; Sun et al., 1998; Nishio, 2000; Terashima et al., 2009; Hogewoning et al., 2012; Vogelmann and Gorton, 2014). For example, the $QY_{m,abs}$ of spinach (*Spinacia oleracea*)

and cabbage (*Brassica oleracea L.*) was highest under red light, followed by that under green light and lowest with blue light. But on incident light basis, $QY_{m,inc}$ of under green light was lower than under red or blue light (Sun et al., 1998).

Both our data (Fig. 2.4B) and those of Sun et al. (1998) show that $QY_{m,abs}$ with blue light is lower than that with red and green light, indicating that blue light is used intrinsically less efficiently by lettuce. Blue light, and, to a lesser extent, green light is absorbed not just by chlorophyll, but also by flavonoids and carotenoids (Sun et al., 1998). Those pigments can divert energy away from photochemistry and thus reduce the QY_{abs} under blue light. Flavonoids (e.g. anthocyanins) are primarily located in the vacuole and cannot transfer absorbed light energy to photosynthetic pigments (Sun et al., 1998). Likewise, free carotenoids do not contribute to photochemistry (Hogewoning et al., 2012). Carotenoids in light-harvesting antennae and reaction centers channel light energy to photochemistry, but with lower transfer efficiency than chlorophylls (Croce et al., 2001; de Weerd et al., 2003a; de Weerd et al., 2003b; Wientjes et al., 2011; Hogewoning et al., 2012). Therefore, absorption of blue light by flavonoids and carotenoids reduces the quantum yield of CO_2 assimilation. Thus, even with the high absorptance of blue light by green leaves, $QY_{m,abs}$ of leaves under blue light was the lowest among the three monochromatic lights (Fig. 2.4B). It is likely that the lower QY_{abs} under green light than that under red light was also due to absorption of green light by carotenoids and flavonoids. (Hogewoning et al., 2012). At high *PPFD*, absorption of blue light by flavonoids and carotenoids still occurs, but this is less of a limiting factor for photosynthesis, since light availability is not limiting under high *PPFD*.

4.1.2 Light Dependence of Respiration and Rubisco Activity May Reduce the Quantum Yield at Low *PPFD*

At *PPFD*s below 200 μmol·m^{-2}·s^{-1}, the QY_{inc} and QY_{abs} of lettuce showed an unexpected pattern in response to *PPFD* (Fig. 2.6). Unlike the quantum yield of PSII, which decreases exponentially with increasing *PPFD* (Weaver and van Iersel, 2019), QY_{inc} and QY_{abs} increased initially with increasing *PPFD* (Fig. 2.6). A similar pattern was previously observed by Craver et al. (2020) in petunia (*Petunia ×hybrida*) seedlings. This pattern could result from light-dependent regulation of respiration (Croce et al., 2001), alternative electron sinks such as nitrate reduction (Skillman, 2008; Nunes-Nesi et al., 2010), or Rubisco activity (Campbell and Ogren, 1992; Zhang and Portis, 1999). In our calculations, we assumed that the leaf respiration in the light was the same as R_d. However, leaf respiration in the light is lower than in the dark, in a *PPFD*-dependent manner (Brooks and Farquhar, 1985; Atkin et al., 1997), which can lead to overestimation of A_g with increasing *PPFD*. When we accounted for this down-regulation of respiration, using the model by Müller et al. (2005) to correct A_g, $QY_{inc,}$ and QY_{abs}, we found that depression of respiration by light did not explain the initial increase in QY_{inc} and QY_{abs} we observed (Fig. S2.4). Alternative electron sinks in the chloroplasts that are upregulated in response to light can explain the low $QY_{inc,}$ and QY_{abs} at low *PPFD*, because they compete with the Calvin cycle for reducing power (ferredoxin/NADPH). Such processes include photorespiration (Krall and Edwards, 1992), nitrate assimilation (Nunes-Nesi et al., 2010), sulfate assimilation (Takahashi et al., 2011) and the Mehler reaction (Badger et al., 2000) and their effect on $QY_{inc,}$ and QY_{abs} would be especially notable under low *PPFD* (Fig. S2.5).

Upregulation of Rubisco activity by Rubisco activase in the light may also have contributed to the increase in QY_{inc} and QY_{abs} at low *PPFD* (Campbell and Ogren, 1992; Zhang and Portis, 1999). In the dark, 2-carboxy-D-arabinitol-1-phosphate (CA1P) or RuBP binds

strongly to the active sites of Rubisco, preventing carboxylation activity. In the light, Rubisco activase releases the inhibitory CA1P or RuBP from the catalytic site of Rubisco, in a light-dependent manner (Campbell and Ogren, 1992; Zhang and Portis, 1999; Parry et al., 2008). At $PPFD < 120$ μmol·m^{-2}·s^{-1}, low Rubisco activity may have limited photosynthesis.

4.1.3 Light Distribution within Leaves Affects *QY* at High *PPFD*

Except for the initial increase at low *PPFD*, both QY_{inc} and QY_{abs} decreased with increasing *PPFD*. QY_{inc} decreased slower under green than under red or blue light (Fig. 2.6A). At a $PPFD \geq 500$ μmol·m^{-2}·s^{-1}, QY_{inc} under green light was higher than that under blue light (Fig. 2.6A). Accordingly, A_n under blue light was lower than under green and red light at *PPFD*s above 500 μmol·m^{-2}·s^{-1} (Fig. 2.3A). The lower QY_{inc} under blue light than under green and red light at high *PPFD* can be explained by disparities in the light distribution within leaves.

Blue and red light were strongly absorbed by lettuce leaves (93.2 and 91.6%, respectively), while green light was absorbed less (81.1%) (Table 2.2). Similar low green absorptance was found in sunflower (*Helianthus annuus* L.), snapdragon (*Antirrhínum majus* L.) (Brodersen and Vogelmann, 2010), and spinach (Vogelmann and Han, 2000). In leaves of those species, absorption of red and blue light peaked in the upper 20% of leaves, and declined sharply further into the leaf. Absorption of red light decreased slower with increasing depth than that of blue light (Vogelmann and Han, 2000; Brodersen and Vogelmann, 2010). Green light absorption peaked deeper into leaves, and was more evenly distributed throughout leaves, because of low absorption of green light by chlorophyll (Vogelmann and Han, 2000; Brodersen and Vogelmann, 2010). The more even distribution of green light within leaves, as compared to red and blue light, can explain the interactive effects between *PPFD* and light spectrum on leaf photosynthesis. It was estimated that less than 10% of blue light traveled through the palisade mesophyll and reached the spongy mesophyll in spinach, while about 35% of green light and 25% of red light

did so (Vogelmann and Evans, 2002). It was also estimated that chlorophyll in the lowermost chloroplasts of spinach leaves absorbed about 10% of green and < 2% of blue light, compared to chlorophyll in the uppermost chloroplasts (Vogelmann and Evans, 2002; Terashima et al., 2009).

The more uniform green light distribution within leaves may be a key contributor to higher leaf level QY_{inc} under high *PPFD* because less heat dissipation of excess light energy is needed (Nishio, 2000; Terashima et al., 2009). Reaction centers near the adaxial leaf surface receive more excitation energy under blue, and to a lesser extent under red light, than under green light, because of the differences in absorptance. Consequently, under high intensity blue light, NPQ is up-regulated in the chloroplasts near the adaxial leaf surface to dissipate some of the excitation energy (Sun et al., 1998; Nishio, 2000), lowering the QY_{inc} under blue light. Since less green light is absorbed near the adaxial surface, less heat dissipation is required. When incident light increased from 150 to 600 $\mu mol \cdot m^{-2} \cdot s^{-1}$, the fraction of whole leaf CO_2 assimilation that occurred in the top half of spinach leaves remained the same under green light (58%), but decreased from 87% to 73% under blue light. This indicates more upregulation of heat dissipation in the top of the leaves under blue, than under green light (Evans and Vogelmann, 2003). On the other hand, the bottom half of the leaves can still utilize the available light with relatively high QY_{inc}, since the amount of light reaching the bottom half is relatively low, even under high *PPFD* (Nishio, 2000). By channeling more light to the under-utilized bottom part of leaves, leaves could achieve higher QY_{inc} even under high intensity green light. In our study, high QY_{inc} under green light and low QY_{inc} under blue light at high *PPFD* (Fig. 2.6) can be thus explained by the large disparities in the light environment in chloroplasts from the adaxial to the abaxial side of leaves due to differences in leaf absorptance. Similarly, differential *QY* of lettuce leaves was highest under green light and lower under blue and red light at high

PPFD (> 300 μmol·m^{-2}·s^{-1}) (Fig. 2.7), also potentially because of the more uniform distribution of green light and the uneven distribution of blue and red light in leaves.

Along the same line, A_n of lettuce leaves was the lowest under blue light at *PPFD* > 500 μmol·m^{-2}·s^{-1} (Fig. 2.3). Also, A_n of lettuce leaves approached light saturation at lower *PPFD*s under blue and red light, than under green light (Fig. 2.3A). Under blue, green, and red light, lettuce leaves reached 95% of $A_{n,max}$ at *PPFD*s of 954, 1110 and 856 μmol·m^{-2}·s^{-1}, respectively. This can be seen more clearly in the differential *QY* at high *PPFD* (Fig. 2.7). At a *PPFD* of 1300 μmol·m^{-2}·s^{-1}, green light had a differential *QY* of 1.09 mmol·mol^{-1}, while that of red and blue light was only 0.46 and 0.69 mmol·mol^{-1}, respectively (Fig. 2.7). Green light also resulted in a higher $A_{g,max}$ (22.9 μmol·m^{-2}·s^{-1}) than red and blue light (21.8 and 19.3 μmol·m^{-2}·s^{-1}, respectively) (Fig. 2.5). As discussed before, the high $A_{g,max}$ under green light resulted from the more uniform light distribution under green light, allowing deeper cell layers to photosynthesize more. Previous research similarly found that at high *PPFD* (>500 μmol·m^{-2}·s^{-1}), A_n of both spinach and cabbage were lower under blue light than under white, red and green light (Sun et al., 1998). Overall, under high *PPFD*, the differences in light distribution throughout a leaf are important to quantum yield and assimilation rate, since it affects NPQ up-regulation (Sun et al., 1998; Nishio, 2000). However, light distribution within a leaf is less important at low than at high *PPFD*, because upregulation of NPQ increases with increasing *PPFD* (Zhen and van Iersel, 2017).

4.2 Light spectrum affects *J*, but not $V_{c,max}$

We examined the effect of light quality and intensity on *J* and $V_{c,max}$ (Fig. 2.8). For the light-dependent reactions, the interactive effect between light spectra and *PPFD* found for CO_2 assimilation and quantum yield was also observed for *J* (Fig. 2.8A). At low *PPFD* (200 μmol·m^{-}

$^{2}\cdot s^{-1}$), green light resulted in the lowest *J* and red light in the highest *J* among single waveband spectra. But at a *PPFD* of 1000 $\mu mol\cdot m^{-2}\cdot s^{-1}$, red and green light resulted in the highest *J* and blue light in the lowest *J* (Fig. 2.8A), similar to the differences in A_g.

There was no clear evidence of Rubisco limitations to photosynthesis at a *PPFD* of 200 $\mu mol\cdot m^{-2}\cdot s^{-1}$, so the rate of the light-dependent reactions likely limited photosynthesis. This is corroborated by the strong correlation between A_g and *J* at a *PPFD* of 200 $\mu mol\cdot m^{-2}\cdot s^{-1}$. Although Rubisco limitations to photosynthesis were observed at a *PPFD* of 1000 $\mu mol\cdot m^{-2}\cdot s^{-1}$, there were no meaningful differences in $V_{c,max}$ in response to light spectrum, in contrast to *J* (Fig. 2.8).

When *PPFD* increased 5×, from 200 to 1000 $\mu mol\cdot m^{-2}\cdot s^{-1}$, there was only a 1.7 to 2.4× increase in *J*, indicating a lower $QY(J)_{inc}$ at higher *PPFD*. This matches the lower QY_{inc} and the asymptotic increase in A_n in response to increasing *PPFD* (Fig. 2.3). The relative increase of *J* under green light (143%) was greater than that under both blue and red light (73% and 75%, respectively) as *PPFD* increased. This similarly can be attributed to a more uniform energy distribution of green light among reaction centers throughout a leaf and weaker upregulation of non-photochemical quenching with increasing green light intensity (Sun et al., 1998; Nishio, 2000; Evans and Vogelmann, 2003), as discussed before.

There was a strong correlation between *J* and A_g under the nine light spectra at both *PPFD* levels (Fig. 2.9A). QY_{abs} and $QY(J)_{abs}$ are similarly strongly correlated (Fig. 2.9B). Unlike *J*, $V_{c,max}$ was largely unaffected by light spectra (Fig. 2.8B) and was not correlated with A_g (data not shown). There was, however, a strong correlation between *J* and $V_{c,max}$ at a *PPFD* of 1000 $\mu mol\cdot m^{-2}\cdot s^{-1}$, ($R^2$ = 0.82, Fig. S2.3), suggesting that *J* and $V_{c,max}$ are co-regulated. Similarly, Wullschleger (1993) noted a strong linear relationship between *J* and $V_{c,max}$ across 109 C_3

species. The ratio between J and $V_{c,max}$ in our study (1.5 – 2.0) similar to the ratio found by Wullschleger (1993). These results suggest that the interactive effect of light spectra and *PPFD* resulted from effects on J, which is associated with light energy harvesting by reaction centers, rather than from $V_{c,max}$.

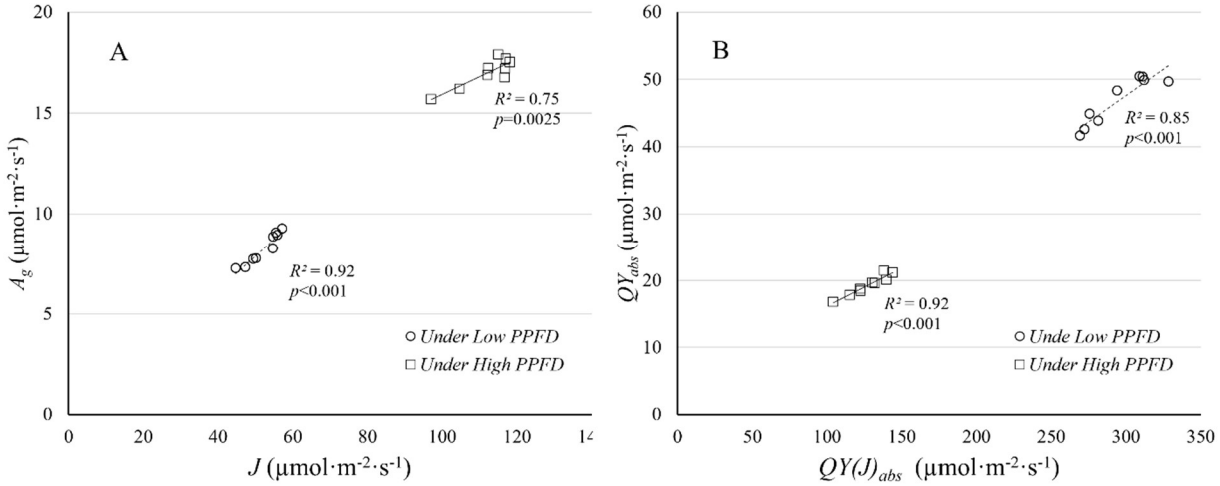

Figure 2.9. The correlation between gross CO_2 assimilation rate (A_g) estimated from light response curves and electron transport rate (J) estimated from A/C_i curves **(A)**, and between the quantum yield of CO_2 assimilation (QY_{abs}) and the quantum yield of electron transport on an absorbed light basis [$QY(J)_{abs}$] **(B)**, under low *PPFD* (200 μmol·m^{-2}·s^{-1}) and high *PPFD* (1000 μmol·m^{-2}·s^{-1}) under nine light spectra averaged over nine 'Green Towers' lettuce plants. The color scheme representing the nine spectra is the same as Fig. 2.8.

4.3 No Interactive Effects among Blue, Green and Red Light

The Emerson enhancement effect describes a synergistic effect between lights of different wavebands (red and far-red) on photosynthesis (Emerson, 1957). McCree (1971) attempted to account for interactions between light with different spectra when developing photosynthetic action spectra and applied low intensity monochromatic lights from 350 nm to 725 nm with white background light to plants. His results showed no interactive effect between

those monochromatic lights and white light (McCree, 1971). We tested different ratios of blue, green, and red light and different *PPFD*s, and similarly did not find any synergistic or antagonistic effect of different wavebands on any physiological parameters measured or calculated.

4.4 Importance of Interactions between *PPFD* and Light Quality and Its Applications

The interactive effect between *PPFD* and light quality demonstrates a remarkable adaptation of plants to different light intensities. By not absorbing green light strongly, plants open up a 'green window', as Terashima et al. (2009) called it, to excite chloroplasts deeper into leaves, and thus facilitating CO_2 assimilation throughout the leaf. While red light resulted in relatively high QY_{inc}, QY_{abs} and A_n at both high and low *PPFD* (Fig. 2.3, Fig. 2.6), it is still mainly absorbed in the upper part of leaves (Sun et al., 1998; Brodersen and Vogelmann, 2010). Green light can penetrate deeper into leaves (Brodersen and Vogelmann, 2010) and help plants drive efficient CO_2 assimilation at high *PPFD* (Fig. 2.3, Fig. 2.5).

Many early photosynthesis studies investigated the absorptance and action spectrum of photosynthesis of green algae, e.g. Haxo and Blinks (1950) or chlorophyll or chloroplasts extracts, e.g. Chen (1952). Extrapolating light absorptance of green algae and suspension of chlorophyll or chloroplast to whole leaves from can lead to an underestimation of absorptance of green light by whole leaves and the belief that green light has little photosynthetic activity (Moss and Loomis, 1952; Smith et al., 2017). Photosynthetic action spectra developed on whole leaves of higher plants, however, have long shown that green light effectively contributes to CO_2 assimilation, although with lower QY_{inc} than red light (Hoover, 1937; McCree, 1971; Inada, 1976; Evans, 1987). The importance of green light for photosynthesis was clearly established in more recent studies, emphasizing its role in more uniformly exciting all chloroplasts, which

especially important under high *PPFD* (Sun et al., 1998; Nishio, 2000; Terashima et al., 2009; Hogewoning et al., 2012; Smith et al., 2017). The idea that red and blue light are more efficient at driving photosynthesis, unfortunately, still lingers, e.g. Singh et al. (2015).

Light-emitting diodes (LEDs) have received wide attention in recent years for use in controlled environment agriculture, as they now have superior efficacy over traditional lighting technologies (Pattison et al., 2018). LEDs can have a narrow spectrum and great controllability. This provides unprecedented opportunities to fine tune light spectra and *PPFD* to manipulate crop growth and development. Blue and red LEDs have higher efficacy than white and green LEDs (Kusuma et al., 2020). By coincidence, McCree's action spectrum (Fig. 2.1) (McCree, 1971) also has peaks in the red and blue region, although the peak in the blue region is substantially lower than the one in the red region. Therefore, red and blue LEDs are sometimes considered optimal for driving photosynthesis. This claim holds true only under low *PPFD*. Green light plays an important role in photosynthesis, as it helps plants to adapt to different light intensities. The wavelength-dependent absorptance of chlorophylls channels green light deeper into leaves, resulting in more uniform light absorption throughout leaves and providing excitation energy to cells further from the adaxial surface. Under high *PPFD*, this can increase leaf photosynthesis. Plant evolved under sunlight for hundreds of millions of years, and it seems likely that the relatively low absorptance of green light contributes to the overall photosynthetic efficiency of plants (Nishio, 2000).

4.5 Conclusions

There was an interactive effect of light spectrum and *PPFD* on leaf photosynthesis. Under low *PPFD*, QY_{inc} was lowest under green and highest under red light. The low QY_{inc} under green light at low *PPFD* was due to low absorptance. In contrast, at high *PPFD*, green and red

light achieved similar QY_{inc}, higher than that of blue light. The strong absorption of blue light by chlorophyll creates a large light gradient from the top to the bottom of leaves. The large amount of excitation energy near the adaxial side of a leaf results in upregulation of nonphotochemical quenching, while chloroplasts near the bottom of a leaf receive little excitation energy under blue light. The more uniform distribution of green light absorption within leaves reduces the need for nonphotochemical quenching near the top of the leaf, while providing more excitation energy to cells near the bottom of the leaf. We also found that the interactive effect of light spectrum and *PPFD* on photosynthesis was a result of the light-dependent reactions; gross assimilation and *J* were strongly correlated. We detected no synergistic or antagonistic interactions between blue, green, and red light.

References:

Atkin, O.K., Westbeek, M., Cambridge, M.L., Lambers, H., and Pons, T.L. (1997). Leaf Respiration in Light and Darkness (A Comparison of Slow- and Fast-Growing Poa Species). *Plant Physiology* 113(3)**,** 961-965. doi: 10.1104/pp.113.3.961.

Badger, M.R., von Caemmerer, S., Ruuska, S., and Nakano, H. (2000). Electron flow to oxygen in higher plants and algae: rates and control of direct photoreduction (Mehler reaction) and rubisco oxygenase. *Philosophical transactions of the Royal Society of London. Series B, Biological sciences* 355(1402)**,** 1433-1446. doi: 10.1098/rstb.2000.0704.

Balegh, S.E., and Biddulph, O. (1970). The Photosynthetic Action Spectrum of the Bean Plant. *Plant Physiology* 46(1)**,** 1-5. doi: 10.1104/pp.46.1.1.

Brodersen, C.R., and Vogelmann, T.C. (2010). Do changes in light direction affect absorption profiles in leaves? *Functional Plant Biology* 37(5)**,** 403-412. doi: 10.1071/fp09262.

Brooks, A., and Farquhar, G.D. (1985). Effect of temperature on the CO2/O2 specificity of ribulose-1,5-bisphosphate carboxylase/oxygenase and the rate of respiration in the light. *Planta* 165(3)**,** 397-406. doi: 10.1007/BF00392238.

Campbell, W.J., and Ogren, W.L. (1992). Light Activation of Rubisco by Rubisco Activase and Thylakoid Membranes. *Plant and Cell Physiology* 33(6)**,** 751-756. doi: 10.1093/oxfordjournals.pcp.a078314.

Chen, S.L. (1952). The Action Spectrum for the Photochemical Evolution of Oxygen by Isolated Chloroplasts. *Plant physiology* 27(1)**,** 35-48. doi: 10.1104/pp.27.1.35.

Craver, J.K., Nemali, K.S., and Lopez, R.G. (2020). Acclimation of Growth and Photosynthesis in Petunia Seedlings Exposed to High-intensity Blue Radiation. 1. doi: 10.21273/jashs04799-19.

Croce, R., Müller, M.G., Bassi, R., and Holzwarth, A.R. (2001). Carotenoid-to-chlorophyll energy transfer in recombinant major light-harvesting complex (LHCII) of higher plants. I. Femtosecond transient absorption measurements. *Biophysical Journal* 80(2)**,** 901-915. doi: 10.1016/S0006-3495(01)76069-9.

de Weerd, F.L., Dekker, J.P., and van Grondelle, R. (2003a). Dynamics of β-carotene-to-chlorophyll singlet energy transfer in the core of photosystem II. *The Journal of Physical Chemistry B* 107(25)**,** 6214-6220. doi: 10.1021/jp027737q.

de Weerd, F.L., Kennis, J.T., Dekker, J.P., and van Grondelle, R. (2003b). β-Carotene to Chlorophyll Singlet Energy Transfer in the Photosystem I Core of Synechococcus e longatus Proceeds via the β-Carotene S2 and S1 States. *The Journal of Physical Chemistry B* 107(24)**,** 5995-6002. doi: 10.1021/jp027758k.

Emerson, R. (1957). Dependence of yield of photosynthesis in long-wave red on wavelength and intensity of supplementary light. *Science* 125(3251)**,** 746-746. doi: 10.1126/science.125.3251.746.

Evans, J. (1987). The dependence of quantum yield on wavelength and growth irradiance. *Functional Plant Biology* 14(1)**,** 69-79. doi: 10.1071/PP9870069.

Evans, J., and Vogelmann, T.C. (2003). Profiles of 14C fixation through spinach leaves in relation to light absorption and photosynthetic capacity. *Plant, Cell & Environment* 26(4)**,** 547-560. doi: 10.1046/j.1365-3040.2003.00985.x.

Haxo, F.T., and Blinks, L. (1950). Photosynthetic action spectra of marine algae. *The Journal of general physiology* 33(4)**,** 389-422. doi: 10.1085/jgp.33.4.389.

Hogewoning, S.W., Wientjes, E., Douwstra, P., Trouwborst, G., Van Ieperen, W., Croce, R., et al. (2012). Photosynthetic quantum yield dynamics: from photosystems to leaves. *The plant*

cell 24(5)**,** 1921-1935. doi: 10.1105/tpc.112.097972.

Hoover, W.H. (1937). The dependence of carbon dioxide assimilation in a higher plant on wave length of radiation. *Smithsonian Miscellaneous Collections*.

Inada, K. (1976). Action spectra for photosynthesis in higher plants. *Plant and Cell Physiology* 17(2)**,** 355-365. doi: 10.1093/oxfordjournals.pcp.a075288.

Krall, J.P., and Edwards, G.E. (1992). Relationship between photosystem II activity and CO2 fixation in leaves. *Physiologia Plantarum* 86(1)**,** 180-187. doi: 10.1111/j.1399-3054.1992.tb01328.x.

Kusuma, P., Pattison, P.M., and Bugbee, B. (2020). From physics to fixtures to food: current and potential LED efficacy. *Horticulture Research* 7(1)**,** 56. doi: 10.1038/s41438-020-0283-7.

McCree, K.J. (1971). The action spectrum, absorptance and quantum yield of photosynthesis in crop plants. *Agricultural Meteorology* 9(Supplement C)**,** 191-216. doi: 10.1016/0002-1571(71)90022-7.

McCree, K.J. (1972). Test of current definitions of photosynthetically active radiation against leaf photosynthesis data. *Agricultural Meteorology* 10**,** 443-453. doi: 10.1016/0002-1571(72)90045-3.

Moss, R.A., and Loomis, W.E. (1952). Absorption Spectra of Leaves. I. The Visible Spectrum. *Plant Physiology* 27(2)**,** 370-391. doi: 10.1104/pp.27.2.370.

Nishio, J. (2000). Why are higher plants green? Evolution of the higher plant photosynthetic pigment complement. *Plant, Cell & Environment* 23(6)**,** 539-548. doi: 10.1046/j.1365-3040.2000.00563.x.

Nunes-Nesi, A., Fernie, A.R., and Stitt, M. (2010). Metabolic and signaling aspects underpinning the regulation of plant carbon nitrogen interactions. *Molecular plant* 3(6)**,** 973-996.

Parry, M.A., Keys, A.J., Madgwick, P.J., Carmo-Silva, A.E., and Andralojc, P.J. (2008). Rubisco regulation: a role for inhibitors. *Journal of experimental botany* 59(7)**,** 1569-1580. doi: 10.1093/jxb/ern084.

Pattison, P., Lee, K., stober, k., and Yamada, M. (2018). *Energy Savings Potential of SSL in Horticultural Applications.*

Sharkey, T.D., Bernacchi, C.J., Farquhar, G.D., and Singsaas, E.L. (2007). Fitting photosynthetic carbon dioxide response curves for C3 leaves. *Plant, cell & environment* 30(9)**,** 1035-1040. doi: 10.1111/j.1365-3040.2007.01710.x.

Singh, D., Basu, C., Meinhardt-Wollweber, M., and Roth, B. (2015). LEDs for energy efficient greenhouse lighting. *Renewable and Sustainable Energy Reviews* 49**,** 139-147.

Skillman, J.B. (2008). Quantum yield variation across the three pathways of photosynthesis: not yet out of the dark. *Journal of Experimental Botany* 59(7)**,** 1647-1661. doi: 10.1093/jxb/ern029.

Smith, H.L., McAusland, L., and Murchie, E.H. (2017). Don't ignore the green light: exploring diverse roles in plant processes. *Journal of experimental botany* 68(9)**,** 2099-2110. doi: 10.1093/jxb/erx098.

Stinziano, J.R., Morgan, P.B., Lynch, D.J., Saathoff, A.J., McDermitt, D.K., and Hanson, D.T. (2017). The rapid A–Ci response: photosynthesis in the phenomic era. *Plant, cell & environment* 40(8)**,** 1256-1262. doi: 10.1111/pce.12911.

Sun, J., Nishio, J.N., and Vogelmann, T.C. (1998). Green light drives CO2 fixation deep within leaves. *Plant and Cell Physiology* 39(10)**,** 1020-1026. doi: 10.1093/oxfordjournals.pcp.a029298.

Takahashi, H., Kopriva, S., Giordano, M., Saito, K., and Hell, R. (2011). Sulfur Assimilation in

Photosynthetic Organisms: Molecular Functions and Regulations of Transporters and Assimilatory Enzymes. *Annual Review of Plant Biology* 62(1)**,** 157-184. doi: 10.1146/annurev-arplant-042110-103921.

Terashima, I., Fujita, T., Inoue, T., Chow, W.S., and Oguchi, R. (2009). Green light drives leaf photosynthesis more efficiently than red light in strong white light: revisiting the enigmatic question of why leaves are green. *Plant and cell physiology* 50(4)**,** 684-697. doi: 10.1093/pcp/pcp034.

Vogelmann, T., and Han, T. (2000). Measurement of gradients of absorbed light in spinach leaves from chlorophyll fluorescence profiles. *Plant, Cell & Environment* 23(12)**,** 1303-1311. doi: 10.1046/j.1365-3040.2000.00649.x.

Vogelmann, T.C., and Evans, J. (2002). Profiles of light absorption and chlorophyll within spinach leaves from chlorophyll fluorescence. *Plant, Cell & Environment* 25(10)**,** 1313-1323. doi: 10.1046/j.1365-3040.2002.00910.x.

Vogelmann, T.C., and Gorton, H.L. (2014). "Leaf: Light Capture in the Photosynthetic Organ," in *The Structural Basis of Biological Energy Generation,* ed. M.F. Hohmann-Marriott. (Dordrecht: Springer Netherlands), 363-377.

Weaver, G., and van Iersel, M.W. (2019). Photochemical Characterization of Greenhouse-grown Lettuce (Lactuca sativa L. 'Green Towers') with Applications for Supplemental Lighting Control. 54(2)**,** 317. doi: 10.21273/hortsci13553-18.

Wientjes, E., van Stokkum, I.H., van Amerongen, H., and Croce, R. (2011). The role of the individual Lhcas in photosystem I excitation energy trapping. *Biophysical Journal* 101(3)**,** 745-754. doi: 10.1016/j.bpj.2011.06.045.

Wullschleger, S.D. (1993). Biochemical Limitations to Carbon Assimilation in C3 Plants—A

Retrospective Analysis of the A/Ci Curves from 109 Species. *Journal of Experimental Botany* 44(5)**,** 907-920. doi: 10.1093/jxb/44.5.907.

Zhang, N., and Portis, A.R. (1999). Mechanism of light regulation of Rubisco: A specific role for the larger Rubisco activase isoform involving reductive activation by thioredoxin-f. *Proceedings of the National Academy of Sciences* 96(16)**,** 9438-9443. doi: 10.1073/pnas.96.16.9438.

Zhen, S., Haidekker, M., and van Iersel, M.W. (2019). Far‐red light enhances photochemical efficiency in a wavelength‐dependent manner. *Physiologia plantarum* 167(1)**,** 21-33. doi: 10.1111/ppl.12834.

Zhen, S., and van Iersel, M.W. (2017). Photochemical Acclimation of Three Contrasting Species to Different Light Levels: Implications for Optimizing Supplemental Lighting. *Journal of the American Society for Horticultural Science* 142(5)**,** 346-354. doi: 10.21273/jashs04188-17.

Supplementary Table 2.1. Dark respiration rate (R_d), maximum quantum yield of CO_2 assimilation ($QY_{m,inc}$) and maximum gross assimilation rate ($A_{g,max}$) of 'Green towers' lettuce derived from the light response curves for nine different spectra using equation 1. The light response curves are shown in Fig. 2.3.

Light spectrum*	R_d (µmol·m^{-2}·s^{-1})	$QY_{m,inc}$ (mol·mol^{-1})	$A_{g,max}$ (µmol·m^{-2}·s^{-1})
100B	2.30	0.058 c	17.0 d
80B20G	2.73	0.061 c	18.1 c

20B80G	2.96	0.062	c	19.5	ab
100G	2.89	0.061	c	19.8	a
80G20R	2.59	0.067	b	19.8	a
20G80R	3.32	0.078	a	19.9	ab
100R	2.81	0.073	ab	18.8	bc
20B80R	2.88	0.077	a	19.2	ab
16B20G64R	3.21	0.078	a	20.0	a

[*]See light composition of nine lights presented here in Table 2.1

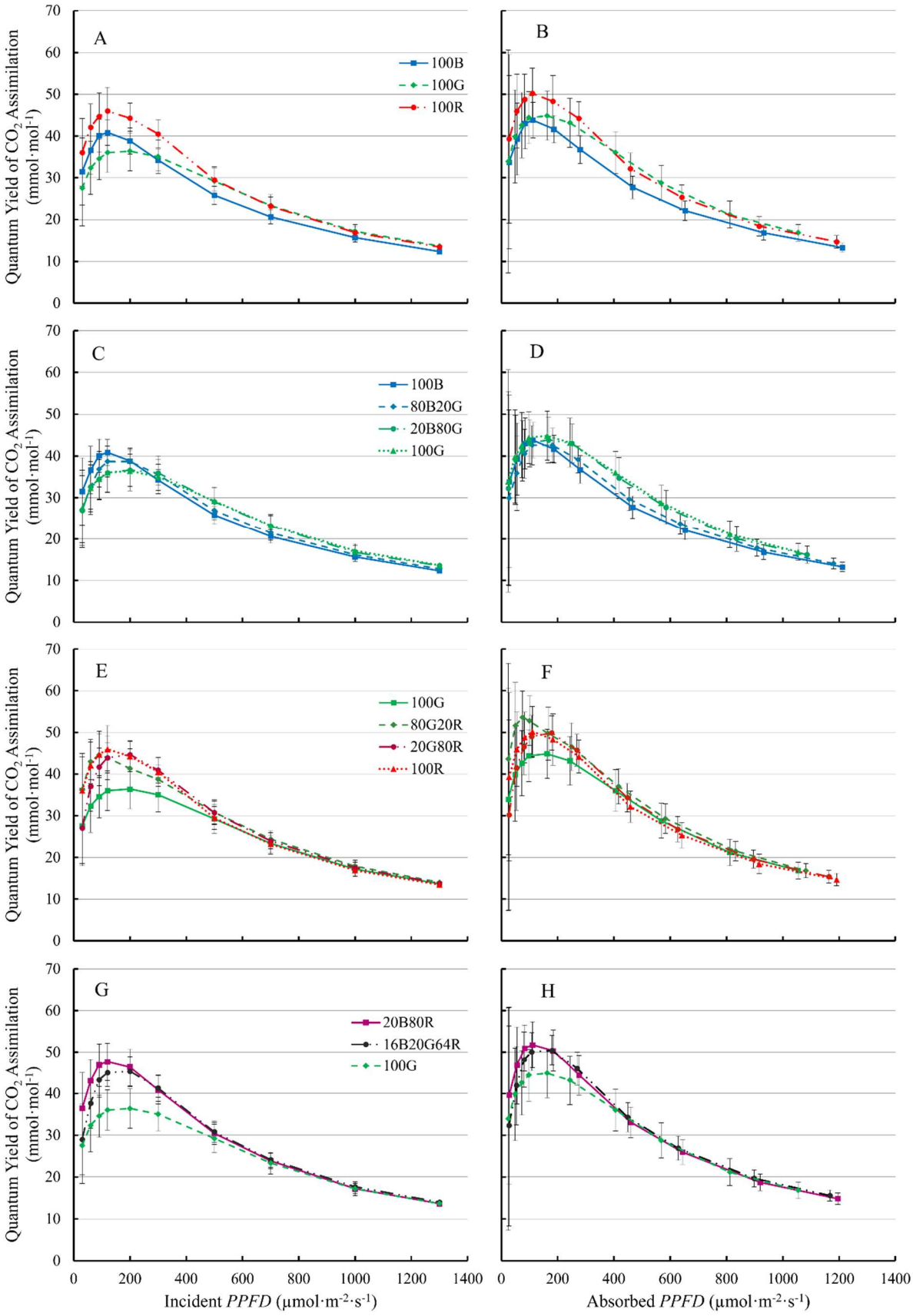
A
100B
100G
100R
B
C
100B
80B20G
20B80G
100G
D
E
100G
80G20R
20G80R
100R
F
G
20B80R
16B20G64R
100G
H
Quantum Yield of CO_2 Assimilation (mmol·mol^{-1})
0
10
20
30
40
50
60
70
0
200
400
600
800
1000
1200
1400
Incident *PPFD* (μmol·m^{-2}·s^{-1})
Absorbed *PPFD* (μmol·m^{-2}·s^{-1})

Supplementary Figure 2.1. (Related to Fig. 2.6) Quantum yield of CO_2 assimilation of 'Green Towers' lettuce as a function of incident (QY_{inc}) (**A**, **C**, **E** and **G**) and absorbed *PPFD* (QY_{abs}) (**B**, **D**, **F** and **H**) under nine light spectra (see Table 2.1). Error bars represent standard deviation (n=9).

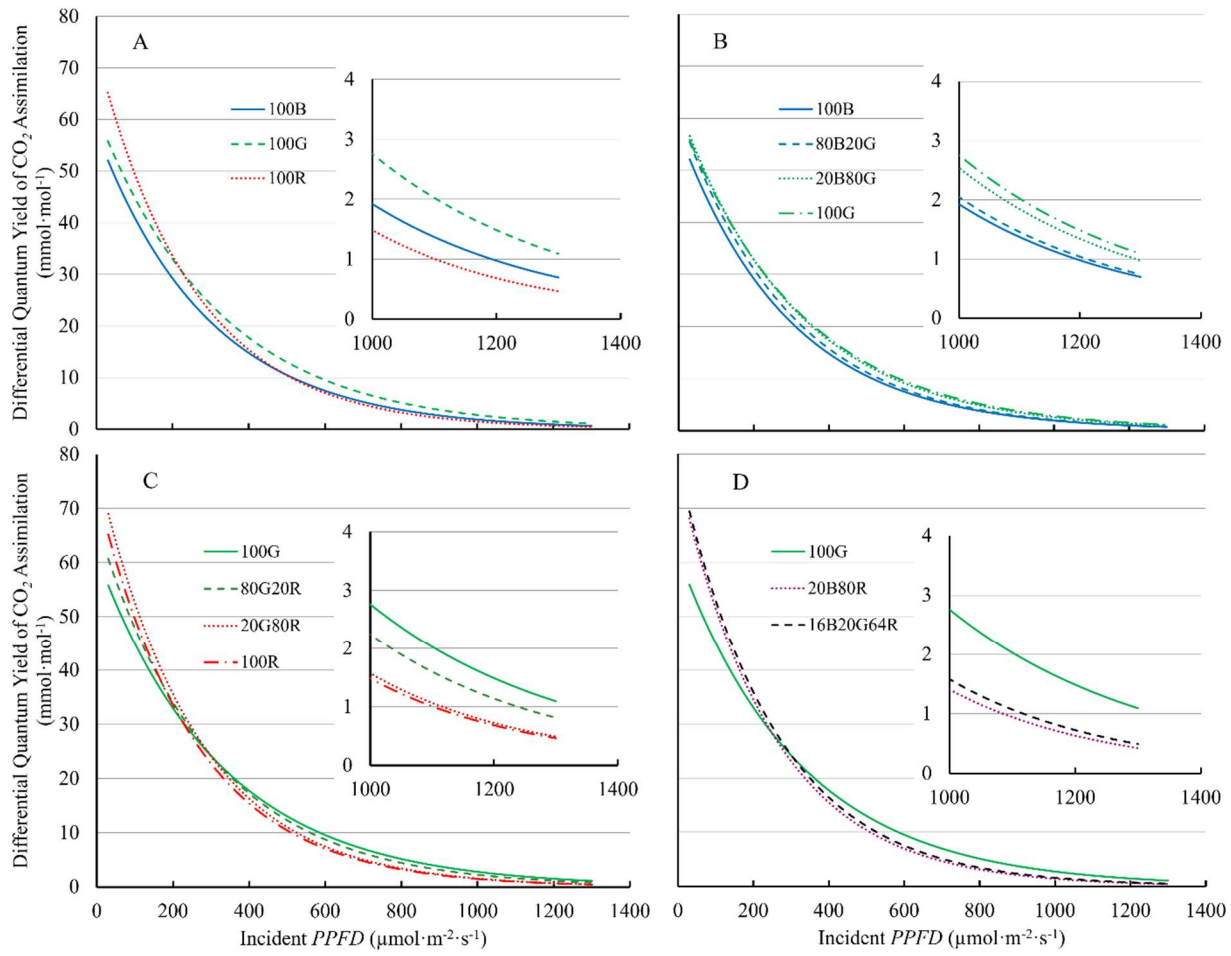

Supplementary Figure 2.2. (Related to Fig. 2.7) Differential quantum yield of CO_2 assimilation (*differential QY*) of 'Green Towers' lettuce under nine light spectra as a function of the *PPFD*. Inserts show *differential QY* at *PPFD*s of 1000 - 1300 µmol·m^{-2}·s^{-1}s to better show differences at high *PPFD* (note the different y-axis scale). The composition of the nine light spectra is shown in Table 2.1.

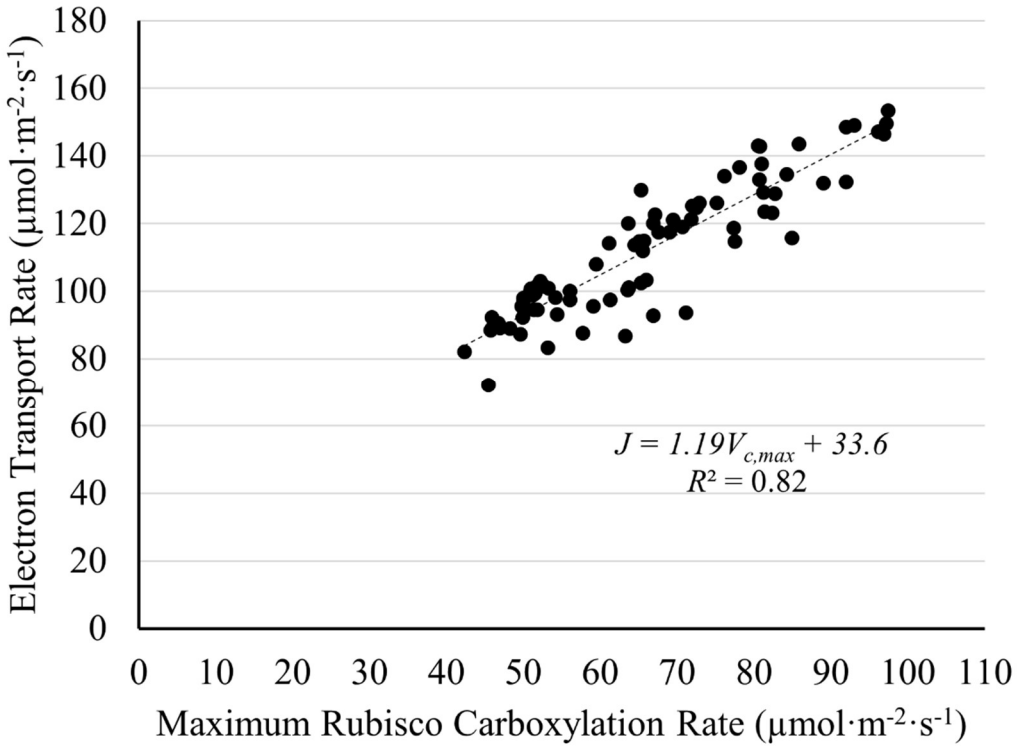

Supplementary Figure 2.3. (Related to Fig. 2.6) The correlation between electron transport (*J*) and maximum Rubisco carboxylation rate ($V_{c,max}$) of 'Green Towers' lettuce estimated from A/C_i curves under *PPFD* (1000 µmol·m^{-2}·s^{-1}) under nine light spectra ($p < 0.001$).

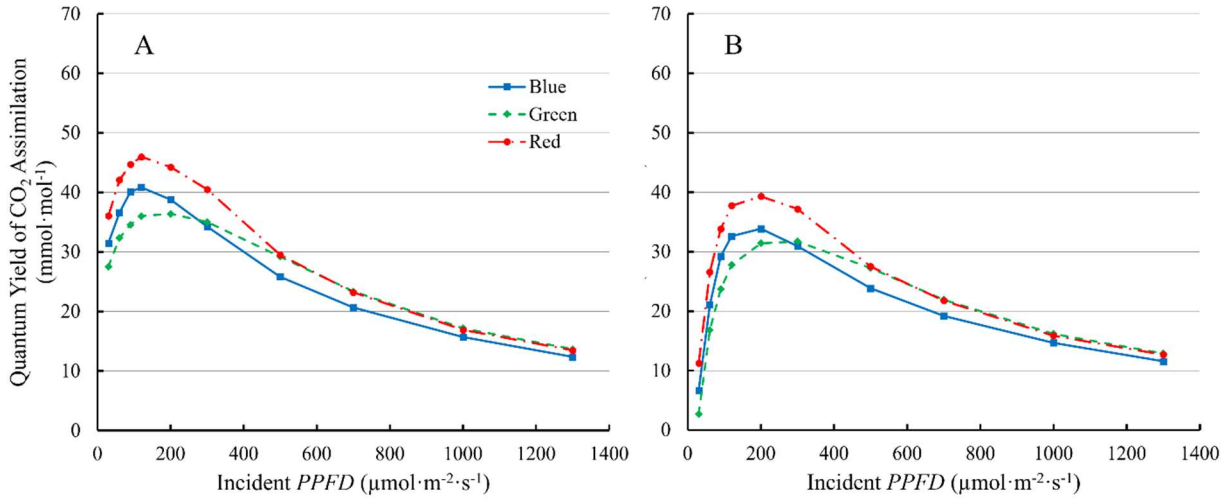

Supplementary Figure 2.4. (Related to Fig. 2.6) The comparison between QY_{inc} before (A) and after (B) correcting for light-suppression of respiration under blue, green, and red LED light. Note that the initial increase in QY_{inc} became more pronounced after correction of light suppressed respiration.

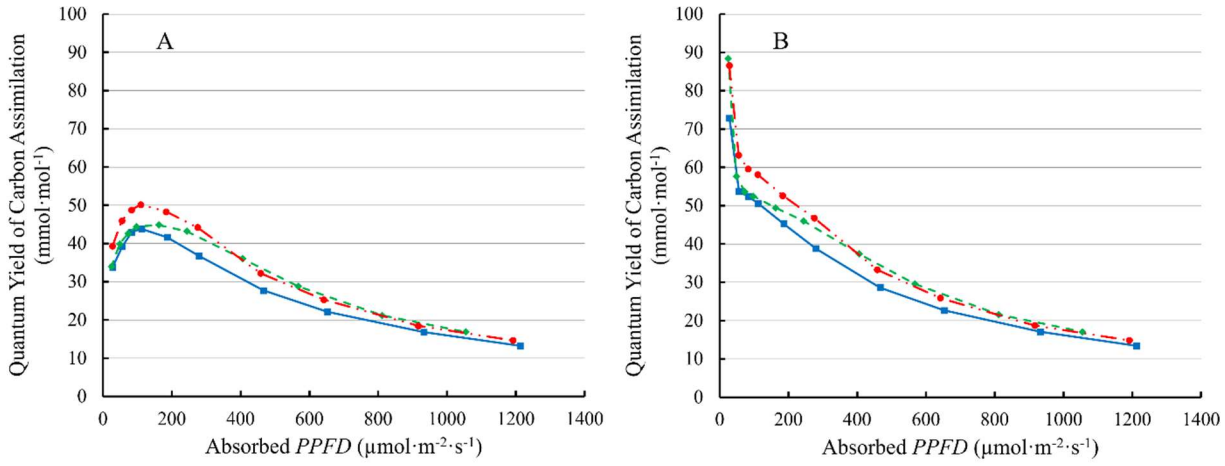

Supplementary Figure 2.5. The comparison between QY_{abs} before (A) and after (B) correcting for alternative electron sinks under blue, green, and red LED light. Assuming a simplified electron sink that diverts energy of 15 µmol·m^{-2}·s^{-1} of absorbed photons (an arbitrary value used for illustrative purposes only) away from the Calvin cycle under all *PPFD*s, the corrected QY_{abs} was calculated based on remaining photons available to support Calvin cycle processes (B). Note that the pattern of QY_{inc} after correcting of alternative electron sink (B) is similar to quantum yield of PSII measured by chlorophyll fluorescence by Weaver and van Iersel (2019).

CHAPTER 3

FAR-RED LIGHT EFFECTS ON LETTUCE GROWTH AND MORPHOLOGY IN INDOOR PRODUCTION ARE CULTIVAR-SPECIFIC[2]

[2]Liu, J. and M.W. van Iersel. To be submitted to *Plants*.

Abstract

Understanding crop responses to light spectrum is critical for optimal indoor crop production. Far-red light is of particular interest, because it can accelerate crop growth through both physiological and morphological mechanisms. Far-red light can increase photosynthetic efficiency when combined with light of shorter wavelengths. It also can induce leaf expansion, possibly increasing light interception and growth. However, the optimal amount of supplemental far-red light for crop growth and yield in indoor lettuce production is yet to be quantified. Lettuce 'Cherokee', 'Green Salad Bowl', and 'Little Gem' were grown under 204 $\mu mol \cdot m^{-2} \cdot s^{-1}$ warm-white light-emitting diode (LED) light with 16 levels of supplemental far-red light, with far-red photon flux densities (*PFD*) ranging from 5.3 to 75.9 $\mu mol \cdot m^{-2} \cdot s^{-1}$. Supplemental far-red light increased canopy light interception 5 days after the start of far-red light treatment (DAT) for 'Green Salad Bowl' and 'Little Gem' and after 7 days for 'Cherokee'. The increase in light interception was no longer evident after 12 and 16 DAT for 'Green Salad Bowl' and 'Little Gem', respectively. The increased light interception was likely a result of increased leaf expansion, as the length of the longest leaf of all three cultivars increased linearly with increasing far-red *PFD* at 20 DAT, consistent with a shade acclimation response to far-red light. We did not find evidence that supplemental far-red photons increased leaf-level photosynthesis. Final dry weight of 'Cherokee' and 'Little Gem' increased linearly with far-red *PFD* when harvested at 20 and 35 DAT, but the dry weight of 'Green Salad Bowl' was not affected. In conclusion, adding far-red light in indoor production increased light interception during the early growth stage and likely increased whole plant carbon assimilation and thus growth, but those effects were cultivar-specific; the enhancement in dry weight was linear, with 75.9 $\mu mol \cdot m^{-2} \cdot s^{-1}$ supplemental far-red *PFD* resulting in 38% and 31% higher dry weight of 'Cherokee' and 'Little Gem' lettuce, respectively.

1. Introduction

Far-red light is defined here as light with wavelengths of 700-750 nm. Depending on location and weather conditions, sunlight has about 19% far-red relative to photosynthetically active radiation (PAR, 400-700 nm) (Zhen and Bugbee, 2020a). Green leaves efficiently absorb UV light and PAR, with a small reduction in absorptance in the green region (400 – 500 nm). Leaves reflect and transmit more light in the far-red part of the spectrum (McCree, 1971; Holmes and Smith, 1977). Under plant canopies, therefore, light is relatively rich in far-red light and has a lower red/far-red ratio. Plants perceive a far-red enriched light environment as a signal of being shaded by other plant canopies. Responses of plants to shading can be classified into two categories: shade avoidance and shade tolerance. Shade-avoiding plants elongate more and branch less in response to a high far-red light environment, in an attempt to outgrow their neighbors and escape the shade (Ruberti et al., 2012). Shade-tolerant plants acclimate to shade by increasing interception of available light and optimizing the light use efficiency of absorbed light, known as the 'carbon gain hypothesis' (Valladares and Niinemets, 2008; Gommers et al., 2013). Shade-tolerant plants exhibit increased leaf expansion to increase light interception. They also tend to have low dark respiration, a low light compensation point, and a high quantum yield of CO_2 assimilation, which together increase carbon gain per unit leaf area or unit soluble leaf protein and minimize maintenance carbon cost (Valladares and Niinemets, 2008; Gommers et al., 2013). Plants in both categories share some common shade responses, like increased specific leaf area (SLA, leaf area / shoot dry weight), reduced chlorophyll a:b ratio, and increased shoot:root ratio to boost light interception and utilization (Valladares and Niinemets, 2008; Ruberti et al., 2012; Gommers et al., 2013).

Regardless of avoidance or tolerance, shade responses of plants can be used to manipulate plant growth and morphology in controlled environment agriculture (CEA) production, where supplemental or sole-source lighting is used. A moderate shade avoidance response of plants improves light interception and efficiency of utilizing absorbed light (Gommers et al., 2013). CEA growers can enrich the light environment with far-red light to induce shade avoidance responses of crops, without reducing the light intensity and photosynthetic rate. For many vegetable and ornamental crops, such as lettuce, basil (*Ocimum basilicum*), coreopsis (*Coreopsis grandiflora*), geranium (*Pelargonium* × *hortorum*), pansy (*Viola* ×*wittrockiana*), petunia (*Petunia* ×*hybrida*), and snapdragon (*Antirrhinum majus*), inclusion of far-red light in CEA increases leaf area, canopy size and thus light interception, resulted in greater biomass (Li and Kubota, 2009; Kubota et al., 2011; Park and Runkle, 2017; Craver et al., 2018; Hernandez and Spalholz, 2019; Meng and Runkle, 2019a; Zou et al., 2019; Legendre and van Iersel, 2021).

In addition to morphological effects, far-red photons also have photosynthetic activity when combined with photons with shorter wavelengths. Traditionally, light with wavelengths of 400– 700 nm is considered to be photosynthetically active and is designated as PAR. However, higher plants have two photosystems, photosystem I and photosystem II (PSI and PSII), that operate in a linear fashion to drive linear photosynthetic electron transport. PSII utilizes photons with wavelengths shorter than 685 nm (Emerson and Lewis, 1943; Zhen and van Iersel, 2017). Far-red photons have lower energy than PAR photons and cannot excite PSII. Thus, far-red photons have minimal photosynthetic activity when applied alone. PSI, on the other hand, can be excited by far-red photons. When applied along with PAR, far-red light can excite PSI and increase the quantum yield of photosystem II and photosynthesis (Evans, 1987; Zhen and van Iersel, 2017). Furthermore, light within the PAR region tends to over excite PSII compared to PSI, with the

exception of light between 570 – 620 nm and > 690 nm, resulting in a sub-optimal quantum yield of oxygen evolution, a measure of PSII activity (Evans, 1987). Since PSII and PSI work linearly, these two photosystems must work at matching rates to achieve high linear electron transport rates. Far-red photons can balance the excitation energy between the two photosystems and increase quantum yield of PSII (Zhen and van Iersel, 2017).

This concept is not unfamiliar to plant scientists. Over 60 years ago, far-red photons were shown to synergistically enhance photosynthesis when added to red photons, known as the 'Emerson enhancement effect' (Emerson, 1957; Myers, 1971). This synergistic effect has been long overlooked, partially due to influential work by McCree (1971; 1972) defining PAR. In recent years, the addition of far-red light to PAR to improve quantum efficiency has gotten renewed attention. The synergistic photosynthetic enhancement from adding far-red light to PAR is well-documented for lettuce (Zhen and van Iersel, 2017; Zhen and Bugbee, 2020b; a). At the leaf level, adding far-red light to warm white or red/blue light significantly increased the quantum yield of PSII (Φ_{PSII}) and net photosynthetic rate (P_n) of lettuce across a wide PAR range, from 50 – 750 $\mu mol \cdot m^{-2} \cdot s^{-1}$ (Zhen and van Iersel, 2017). At the canopy level, far-red photons, when combined with light of shorter wavelength, were shown to have equal photosynthetic efficiency as PAR photons (Zhen and Bugbee, 2020b; a). This relationship held true across 14 different crops, including C3 plants and C4 species (Zhen and Bugbee, 2020a).

Another benefit of far-red inclusion in CEA lighting is the high efficacy (μmoles photon output per joule energy input) of far-red LEDs, which is greater than that of blue, red, and white LEDs (Kusuma et al., 2020). Adding far-red LEDs to CEA has the potential to not only improve the crop's light use efficiency by increasing photon capture and photosynthetic efficiency, far-red LEDs also can reduce energy cost by replacing LEDs with lower efficacy.

In summary, inclusion of far-red light in sole-source lighting can increase crop yield in two ways: 1) by inducing shade responses such as leaf expansion, which increases light interception by the plant canopy and 2) by enhancing photosynthetic efficiency through the Emerson enhancement effect. Because far-red photons can have long-term effects on both plant morphology and physiology, the overall response of crop growth to far-red light is complicated.

A previous study on lettuce under sole-source lighting found that plants grown with additional far-red light had higher SLA (specific leaf area, $m^2 \cdot g^{-1}$), lower chlorophyll and nitrogen content per unit area, and subsequently lower leaf light absorptance and lower quantum yield of CO_2 assimilation at *PPFD*s above 300 $\mu mol \cdot m^{-2} \cdot s^{-1}$ (Zou et al., 2019). The negative effects of far-red light supplementation on leaf light absorptance and quantum yield of CO_2 assimilation did not negate the beneficial effect of far-red light on growth, as both shoot fresh and dry weight increased under supplemental far-red light (Zou et al., 2019). Another study similarly found that lettuce plants grown under a high far-red environment had greater biomass than lettuce plants adapted to a low far-red light environment at the same total *PFD* (integrating over a wavelength of 400 – 750 nm), despite lower chlorophyll content and leaf-level light absorptance (Zhen and Bugbee, 2020b). At the whole plant level, lettuce plants in a far-red enriched environment had a similar quantum yield of CO_2 assimilation as lettuce plants in a low far-red environment (Zhen and Bugbee, 2020b). Although more far-red light can increase growth, excessive far-red light also can lead to undesirable stem elongation in lettuce (Hernandez and Spalholz, 2019). Other undesirable traits were also observed in lettuce with far-red photon inclusion, such as reduced red coloration for red-leaf lettuce (Meng and Runkle, 2019a; b; Zou et al., 2019).

Although numerous studies showed the benefit of far-red photon inclusion in CEA light fixtures, there is a lack of studies that quantify the extent of benefit from far-red light inclusion

and the optimal amount of far-red light to supply. We hypothesize that both the negative effect on leaf-level quantum yield of CO_2 assimilation and the positive effect on canopy light interception of far-red light inclusion depend on far-red light intensity. This study aimed to examine the effect of a wide range of intensities of supplemental far-red light on lettuce plants in indoor production to identify the optimal *PFD* and the magnitude of benefit of supplemental far-red light, which would allow us to make recommendations for lettuce production under sole-source lighting.

2. Results

Three lettuce cultivars, 'Cherokee', 'Green Saladbowl' and 'Little Gem', were grown in a walk-in growth chamber. All plants received white LED light (Fig. S3.1) at 204 ± 11 $\mu mol \cdot m^{-2} \cdot s^{-1}$, which included 5.6 ± 0.3 $\mu mol \cdot m^{-2} \cdot s^{-1}$ far-red photons. Supplemental far-red light (peak at 724 nm, with a full width at half maximum of 18 nm) was provided ranging from 0 to 70.4 $\mu mol \cdot m^{-2} \cdot s^{-1}$, starting 6 days after seeding. Fifteen plants of each cultivar were grown in each of the 18 growing areas. We harvested seven plants at the first harvest (20 DAT) when canopies were closed, and another seven plants at the second harvest at 29 DAT ('Green Saladbowl') and 35 DAT ('Cherokee' and 'Little Gem') after the canopy had closed again.

2.1. Morphological responses to far-red light

At 7 DAT, far-red *PFD* linearly increased seedling height (Fig. 3.1). Far-red photons increased 'Cherokee' height by 0.47 mm per $\mu mol \cdot m^{-2} \cdot s^{-1}$ of far-red photons (Fig. 3.1A). Similarly, for both 'Green Saladbowl' and 'Little Gem', far-red light increased plant height by 0.22 and 0.75 mm per $\mu mol \cdot m^{-2} \cdot s^{-1}$ of far-red photons, respectively (Fig. 3.1A). The relative increase in plant height was calculated as the ratio of increase in plant height induced by supplemental far-red light to average plant height without supplement far-red light (Fig. 3.1B). The height of 'Little Gem' increased 229% when grown under the highest far-red light intensity compared to plants grown

without supplemental far-red light, while the height of 'Green Saladbowl' increased by only 55% (Fig. 3.1B). Similarly, at the first harvest at 20 DAT, far-red photons increased plant height of 'Cherokee', 'Green Saladbowl' and 'Little Gem' by 0.72, 0.71, and 1.25 mm per $\mu mol \cdot m^{-2} \cdot s^{-1}$ of far-red photons (Fig. S3.2A). Plant height of 'Little Gem' more than doubled under the highest far-red *PFD*, while the plant height of 'Green Saladbowl' and 'Cherokee' increased about 70% under the highest far-red *PFD* (Fig. S3.2B).

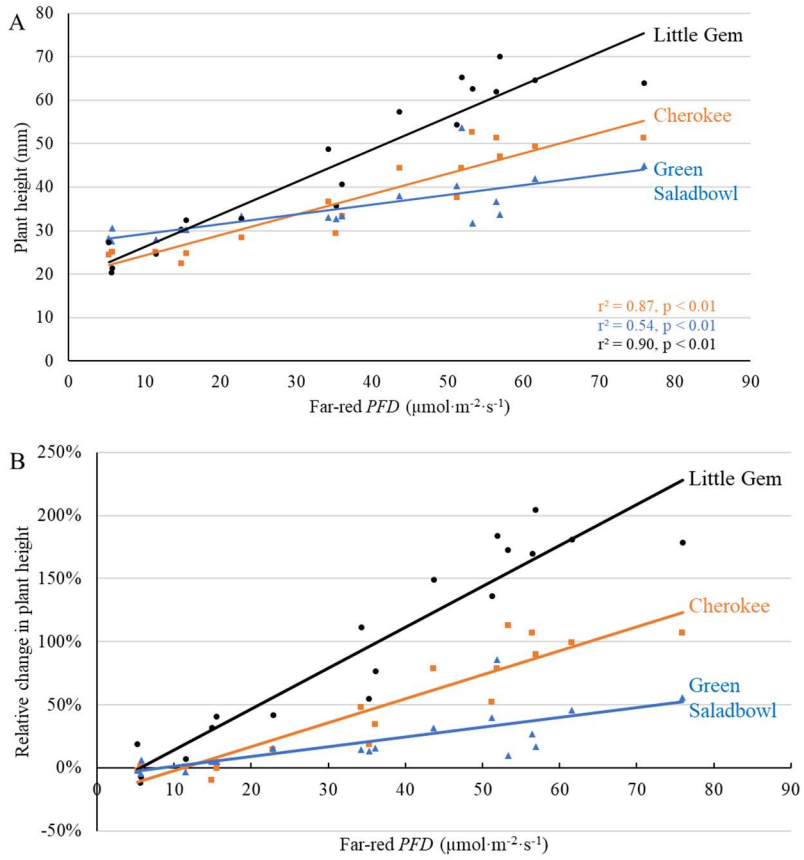

Figure 3.1. With a background of 204 $\mu mol \cdot m^{-2} \cdot s^{-1}$ white LED light, supplemental far-red photons linearly increased plant height (A) and the relative change in plant height (B, compared to plants under no supplemental far-red light) 7 days after the start of far-red light treatment for 'Cherokee', 'Green Saladbowl', and 'Little Gem' lettuce. The r^2 and p values for regression of each cultivar apply to both graphs and are shown with the respective color.

Other morphological changes induced by far-red photons were evident at the first harvest as well. The length of the longest leaf increased linearly with increasing far-red *PFD* for all three cultivars (Fig. 3.2), consistent with a shade acclimation response to a high far-red light environment. At the first harvest (20 DAT), far-red photons increased the length of the longest leaf of 'Cherokee', 'Green Saladbowl' and 'Little Gem' by 0.69, 1.15, and 1.12 mm per $\mu mol \cdot m^{-2} \cdot s^{-1}$, respectively (Fig. 3.2A). There was also a significant interactive effect between far-red *PFD* and cultivar: the increase in longest leaf length with far-red *PFD* was larger for 'Green Saladbowl' and 'Little Gem' than for 'Cherokee' lettuce ($p = 0.023$). The relative increase in the longest leaf length was highest for 'Little Gem', which was 1.14% per $\mu mol \cdot m^{-2} \cdot s^{-1}$ of far-red photons, compared to 0.66% and 0.78% per $\mu mol \cdot m^{-2} \cdot s^{-1}$ increase in longest leaf length for 'Cherokee' and 'Green Saladbowl' (Fig. 3.2B).

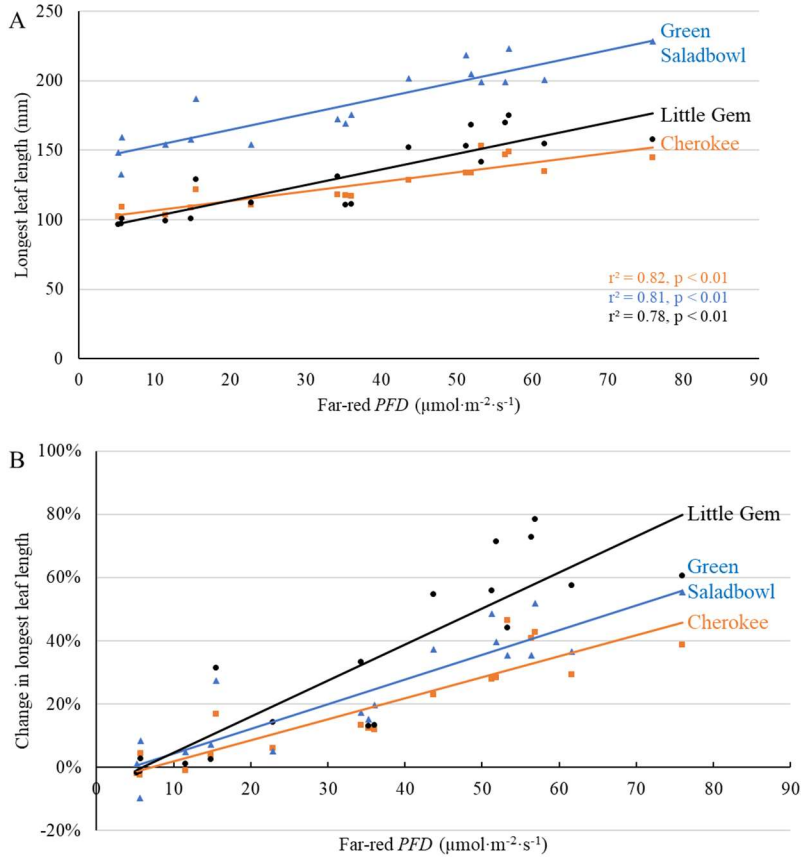

Figure 3.2. With a background of 204 μmol·m^{-2}·s^{-1} white LED light, supplemental far-red photons linearly increased length of the longest leaf (A) and the relative change in length of the longest leaf (B, compared to plants under no supplemental far-red light) 20 days after the start of far-red light treatment for 'Cherokee', 'Green Saladbowl', and 'Little Gem' lettuce. The r^2 and p values for regression of each cultivar apply to both graphs and are shown with the respective color.

Canopy light interception was measured and also served as an indicator of canopy size. Light interception was calculated based on light measurements above and below the canopy. Canopy light interception increased with time in a sigmoidal pattern for all three cultivars. The effect of supplemental far-red photons on canopy light interception started to show at 7 DAT for 'Cherokee' and persisted until the first harvest (Fig. S3.3, S3.4, S3.5, S3.6 and S3.7). The canopy light interception of 'Green Saladbowl' and 'Little Gem' was increased by far-red photons starting at 5 DAT (Fig. S3.8), but this increase in light interception in response to far-red photons was no longer evident by 12 and 16 DAT for 'Green Saladbowl' and 'Little Gem', respectively (Fig. S3.5 and S3.6). At 9 DAT (Fig. 3.3), there was a positive correlation between light interception and far-red *PFD* for all three cultivars. At 9 DAT, 'Cherokee', 'Green Saladbowl' and 'Little Gem' lettuce grown without supplemental far-red intercepted 6.2, 8.8 and 4.8% photons of total incident photons, respectively (Fig. 3.3A). With 70.4 μmol·m^{-2}·s^{-1} of supplemental far-red photons, light interception of 'Cherokee', 'Green Saladbowl' and 'Little Gem' increased to 12.8, 16.5% and 12.5%, respectively (Fig. 3.3A). Although light interception was low, the relative increase in light interception of 'Cherokee', 'Green Saladbowl' and 'Little Gem' plants grown under the highest far-red *PFD* were 120, 78, and 153%, respectively, compared to plants grown without supplemental far-red light (Fig. 3.3B).

Lettuce cultivar affected light interception ($p < 0.01$), but there was no interactive effect of cultivar and far-red *PFD* on light interception ($p = 0.52$), indicating that light interception of all

three cultivars changed in a similar manner with far-red *PFD* (e.g., similar slopes in Fig. 3.3A). Light interception of 'Green Saladbowl' lettuce increased faster over time than light interception of 'Cherokee' and 'Little Gem' (Fig. S3.8) during the seedling stage. Starting at 7 DAT, light interception of 'Green Saladbowl' was higher than light interception of 'Cherokee' and 'Little Gem', averaged across different far-red *PFD*s (Fig. S3.8). At 12 DAT, light interception of 'Cherokee' lettuce caught up with 'Green Saladbowl', and light interception of 'Green Saladbowl' was no longer the highest among the three cultivars (Fig. S3.8). The light interception of 'Little Gem' was consistently lowest among three cultivars (Fig. S3.8).

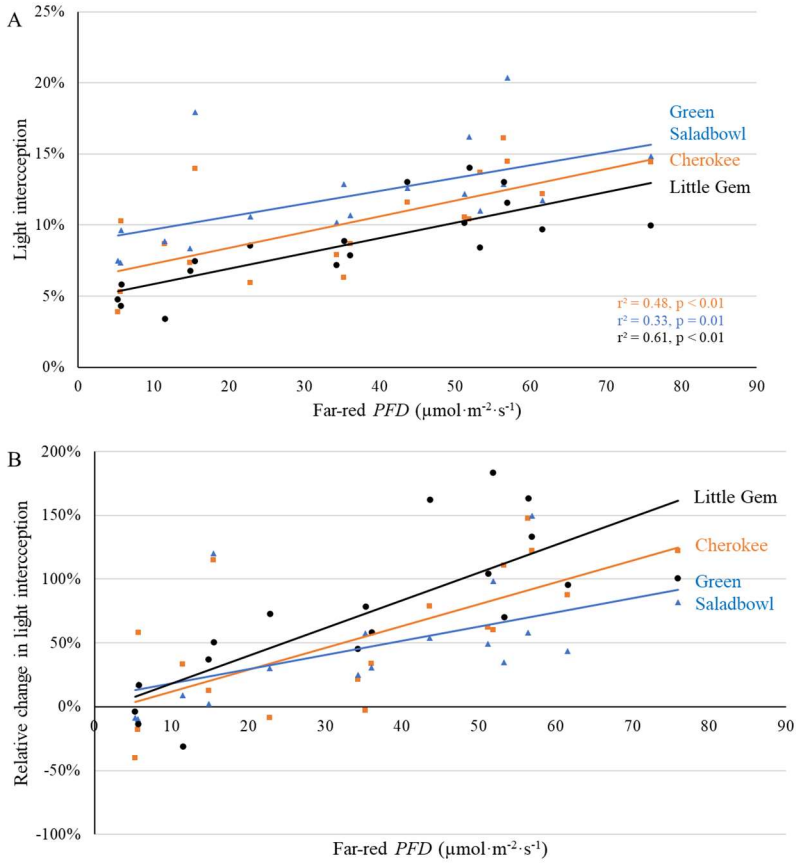

Figure 3.3. With a background of 204 µmol·m^{-2}·s^{-1} white LED light, supplemental far-red photons linearly increased canopy light interception (A) and the relative change in canopy light interception (B, comparing to plants under no supplemental far-red light) 9 days after the start of far-red light treatment for 'Cherokee', 'Green Saladbowl', and 'Little Gem' lettuce. The r^2 and p values for regression of each cultivar apply to both graphs and are shown with the respective color.

Leaf area at the first harvest also increased in response to supplemental far-red *PFD* in 'Cherokee' and 'Little Gem', but not in 'Green Saladbowl' (Fig. 3.4). 'Cherokee' and 'Little Gem' plants under the highest far-red *PFD* had 131 and 166 $cm^2 \cdot plant^{-1}$ greater leaf area than plants grown without supplemental far-red photons (Fig. 3.4A), which represented a 52.1% and 38.0% increase of leaf area, compared to plants without supplemental far-red light (Fig. 3.4B). At the second harvest, leaf area of 'Green Saladbowl' increased with higher far-red *PFD*, but this was not the case for 'Cherokee' and 'Little Gem' (Fig. 3.5). 70.4 $\mu mol \cdot m^{-2} \cdot s^{-1}$ supplemental far-red *PFD* resulted in 333 $cm^2 \cdot plant^{-1}$ larger leaf area for 'Green Saladbowl' (Fig. 3.5A), which represented a 20.8% increase compared to plants without supplemental far-red light (Fig. 3.5B).

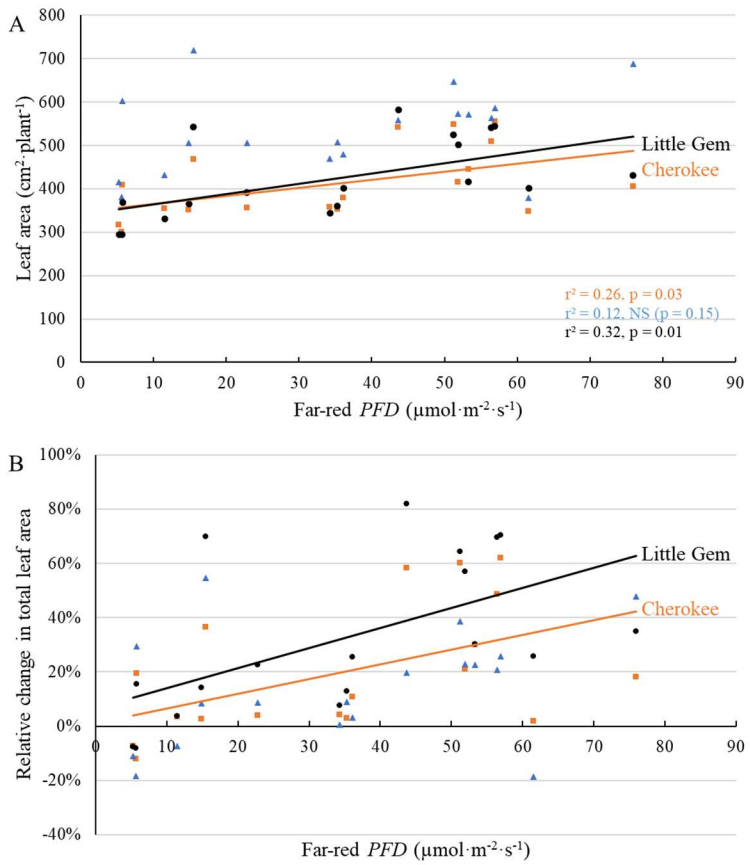

Figure 3.4. With a background of 204 µmol·m^{-2}·s^{-1} white LED light, supplemental far-red photons linearly increased leaf area (A) and the relative change in leaf area (B, compared to plants without supplemental far-red light) at 21 days after the start of far-red light treatment for 'Cherokee' and 'Little Gem' lettuce, but not for 'Green Saladbowl' (blue triangles). The r^2 and p values for regression of each cultivar apply to both graphs and are shown with the respective color.

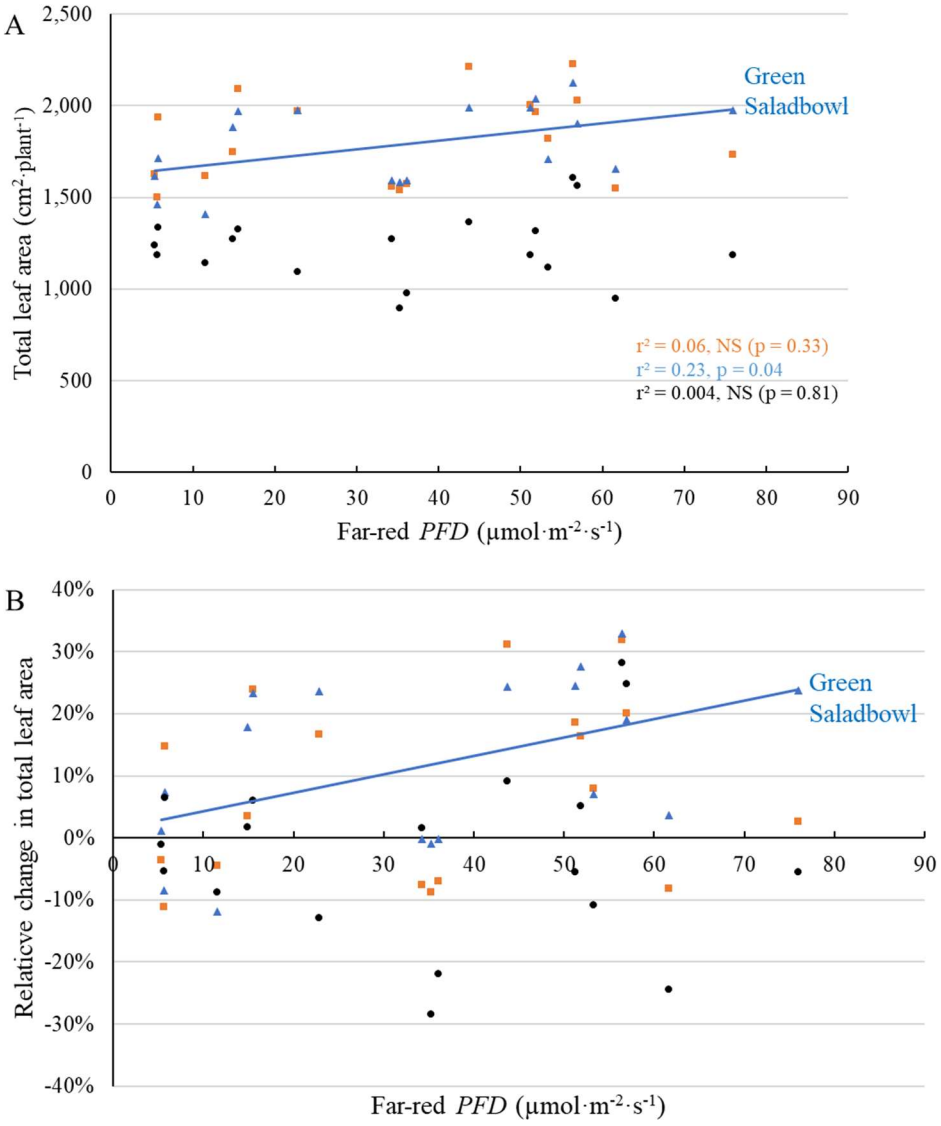

Figure 3.5. With a background of 204 µmol·m^{-2}·s^{-1} white LED light, supplemental far-red photons linearly increased total leaf area (A) and the relative change in total leaf area (B, compared to plants without supplemental far-red light) 35 days after the start of far-red light treatment for 'Green Saladbowl' lettuce, but not for 'Cherokee' (orange squares) and 'Little Gem' (black dots). The r^2 and p values for regression of each cultivar apply to both graphs and are shown with the respective color.

We did not find a consistent trend in specific leaf weight (shoot dry weight divided by total leaf area) at the two harvests. At the first harvest, specific leaf weight decreased with far-red *PFD* for 'Little Gem', but not for 'Cherokee' and 'Green Saladbowl' (Fig. S3.9). For 'Green Saladbowl', the correlation between far-red *PFD* and specific leaf weight was borderline significant ($p = 0.075$). Contrary to results from the first harvest, specific leaf weight of 'Cherokee' increased with increasing far-red *PFD* at the second harvest (Fig. S3.10). No effect of far-red *PFD* on specific leaf weight of 'Little Gem' and 'Green Saladbowl' was observed at the second harvest (Fig. S3.10).

Leaf pigments were also affected by the addition of far-red photons (Fig. 3.6 and 3.10). Leaf chlorophyll content index (CCI) and anthocyanin content index (ACI) were measured twice before the first harvest: at 12 (data not shown) and at 16 DAT (Fig. 3.6). Far-red photons decreased CCI for all three lettuce cultivars at both dates. The ACI was only measured for 'Cherokee', a red lettuce cultivar, and was negatively correlated with far-red *PFD* at 16 DAT (Fig. 3.7). No effect of far-red photons on ACI was detected at 12 DAT (data not shown).

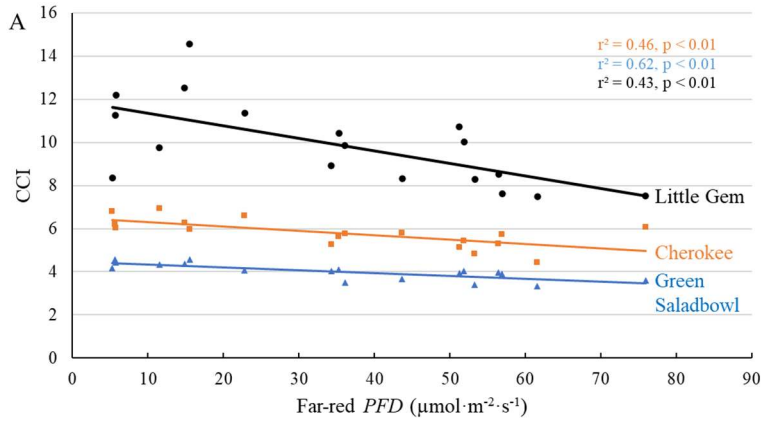

Figure 3.6. With a background of 204 µmol·m^{-2}·s^{-1} white LED light, supplemental far-red photons linearly decreased chlorophyll content index at 16 days after the start of far-red light treatment for 'Cherokee', 'Green Saladbowl' and 'Little Gem' lettuce. The r^2 and p values for regression of each cultivar are shown with the respective color.

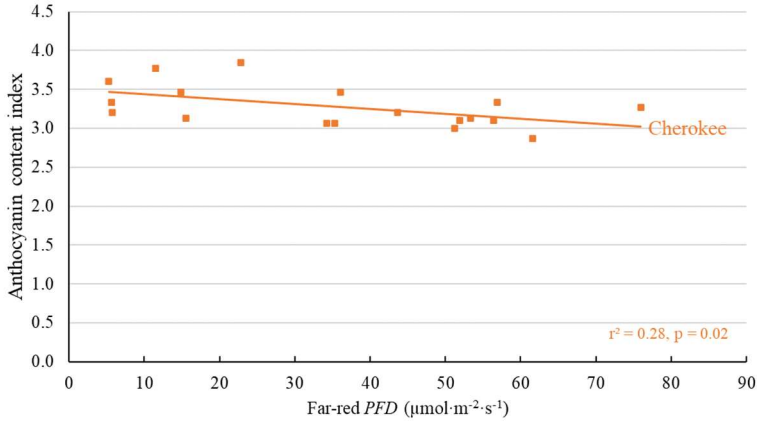

Figure 3.7. With a background of 204 µmol·m^{-2}·s^{-1} white LED light, supplemental far-red photons linearly decreased anthocyanin content index of 'Cherokee' lettuce at 16 days after the start of far-red light treatment. The r^2 and p value are shown in the graph.

Excessive stem elongation of lettuce is undesirable. At the second harvest, we observed elongated stems for 'Cherokee' and 'Green Saladbowl' under supplemental far-red photons, but not for 'Little Gem' (Fig. 3.8). Stems of 'Cherokee' and 'Green Saladbowl' lettuce under the highest far-red *PFD* were 97% and 179% longer than those without supplemental far-red light (Fig. 3.8B). But since the stems were short to start with, the stem length of 'Cherokee' and 'Green Saladbowl' increased by only 1.0 and 1.8 cm (Fig. 3.8A). These increases in stem length were statistically significant, but not horticulturally meaningful.

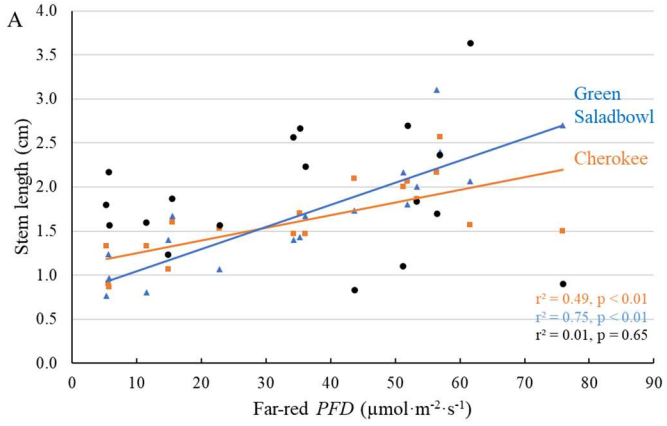

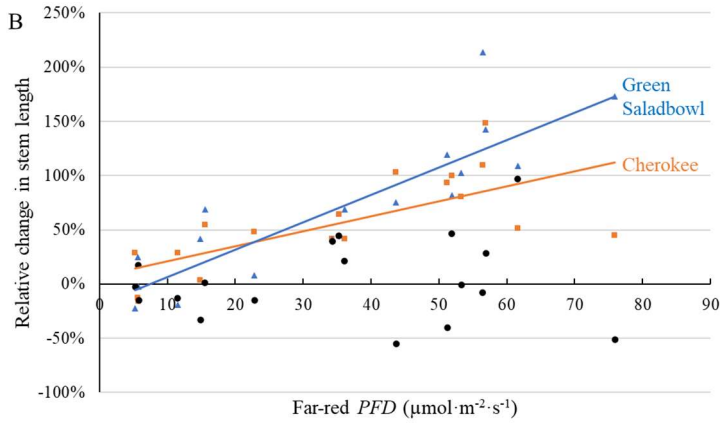

Figure 3.8. With a background of 204 µmol·m^{-2}·s^{-1} white LED light, supplemental far-red photons linearly increased stem length 35 days after the start of far-red light treatment for 'Cherokee' and 'Green Saladbowl', but not for 'Little Gem' (black dots) lettuce. The r^2 and p values for regression of each cultivar apply to both graphs and are shown with the respective color.

2.2. Leaf-level photosynthetic response to supplemental far-red light

We found no significant effect of far-red *PFD* on Φ_{PSII} or P_n of all three cultivars. The Φ_{PSII} at 27 DAT of 'Cherokee', 'Green Saladbowl' and 'Little Gem' lettuce averaged 0.706, 0.682, and 0.682, respectively, and were not significantly affected by far-red *PFD* (Fig. 3.9). Similarly, the leaf level P_n of all three cultivars was not affected by far-red *PFD*. The P_n of 'Cherokee', 'Green Saladbowl' and 'Little Gem' at 28 DAT averaged 6.25, 5.18, and 7.25 µmol·m^{-2}·s^{-1}, respectively, regardless of far-red *PFD* (data not shown).

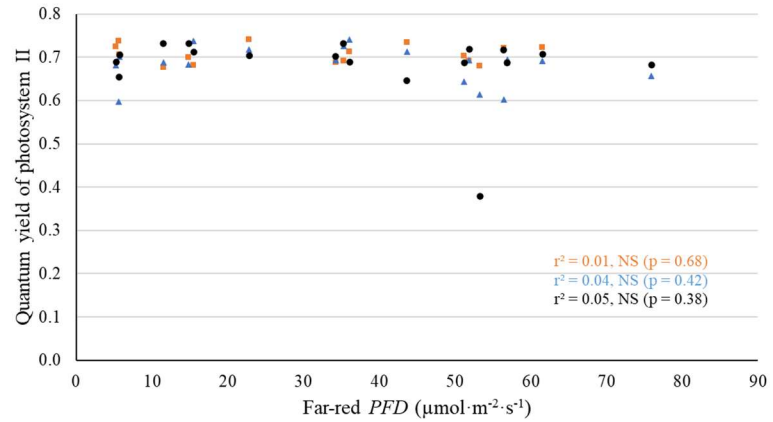

Figure 3.9. With a background of 204 µmol·m^{-2}·s^{-1} white LED light, supplemental far-red photons had no effect on quantum yield of photosystem II at 27 days after the start of far-red light treatment for 'Cherokee' (orange squares), 'Green Saladbowl' (blue triangles), and 'Little Gem' (black dots) lettuce.

In addition, we measured leaf-level Φ_{PSII} and P_n under their growing spectrum, then turned off the supplemental far-red light and measured Φ_{PSII} and P_n under white light only at 28 DAT. The effect of supplemental far-red photons on electron transport and leaf photosynthesis was expressed as the ratio of Φ_{PSII} or P_n under white light with supplemental far-red light to Φ_{PSII} or P_n under white LED light only (Fig. 3.10 and Fig. S3.11), referred to as $\Phi_{PSII,FRon}$ to $\Phi_{PSII,FRoff}$ ratio and $P_{net,FRon}$ to $P_{net,FRoff}$ ratio. We did not find any significant differences in Φ_{PSII} and P_n under white LED light with and without supplemental far-red light (Fig. 3.10).

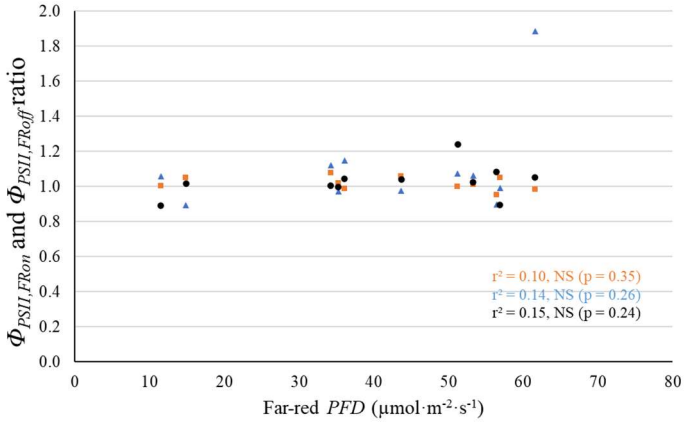

Figure 3.10. With a background of 204 µmol·m^{-2}·s^{-1} white LED light, turning off supplemental far-red lights had no effect on quantum yield of photosystem II for 'Cherokee' (orange squares), 'Green Saladbowl' (blue triangles) and 'Little Gem' (black dots) lettuce 28 days after the start of far-red light treatment. The r^2 and p values for regression of each cultivar apply to both graphs and are shown with the respective color.

2.3. Final yield

Shoot dry weight of 'Cherokee' and 'Little Gem' were positively correlated with far-red *PFD* at both 20 DAT and 35 DAT, but dry weight of 'Green Salad Bowl' was not affected at either

harvest (Fig. 3.11 and Fig. 3.12). At the first harvest, the highest supplemental far-red PFD (70.4 $\mu mol \cdot m^{-2} \cdot s^{-1}$) resulted in 0.264 $g \cdot plant^{-1}$ (38.1%) and 0.267 $g \cdot plant^{-1}$ (31.0%) higher shoot dry weight for 'Cherokee' and 'Little Gem' (Fig. 3.11), compared to plants without supplemental far-red. At the second harvest, shoot dry weights of 'Cherokee' and 'Little Gem' plants were similar without supplemental far-red light (3.81 and 3.92 $g \cdot plant^{-1}$, respectively) (Fig. 3.12A), but responded differently to far-red *PFD*. Supplemental far-red light increased shoot dry weight of 'Cherokee' and 'Little Gem' by 0.023 g and 0.011 g per plant per $\mu mol \cdot m^{-2} \cdot s^{-1}$ far-red photons (Fig. 3.12A). The relative increase in shoot dry weight in response to 70.4 $\mu mol \cdot m^{-2} \cdot s^{-1}$ supplemental far-red *PFD* was thus higher for 'Cherokee' (39.4%) than for 'Little Gem' (19.0%) (Fig. 3.12B).

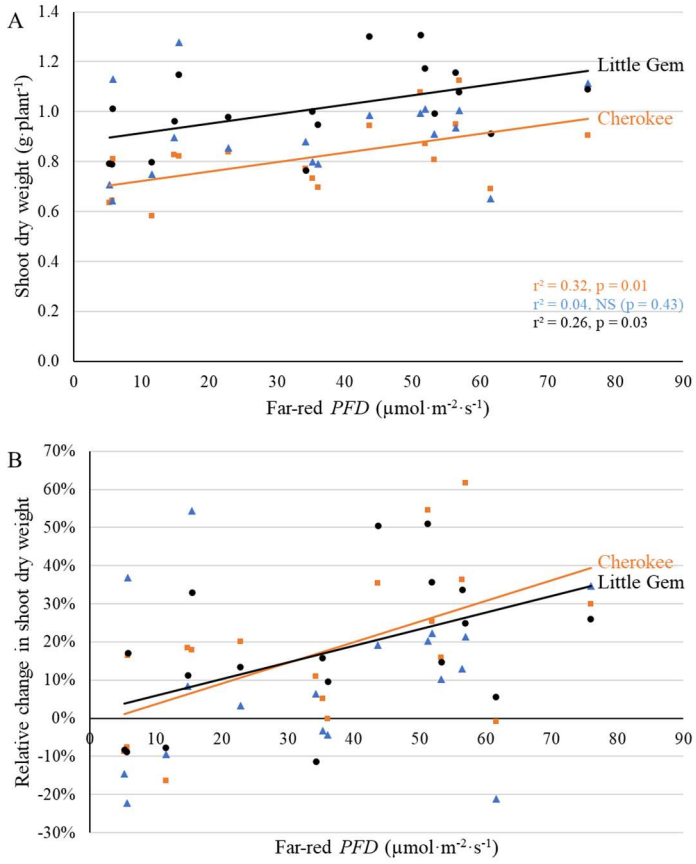

Figure 3.11. With a background of 204 $\mu mol \cdot m^{-2} \cdot s^{-1}$ white LED light, supplemental far-red photons linearly increased shoot dry weight at 20 days after the start of far-red light

treatment for ‘Cherokee’ and ‘Little Gem’, but not for ‘Green Saladbowl’ (blue triangles) lettuce. The r^2 and p values for regression of each cultivar apply to both graphs and are shown with the respective color.

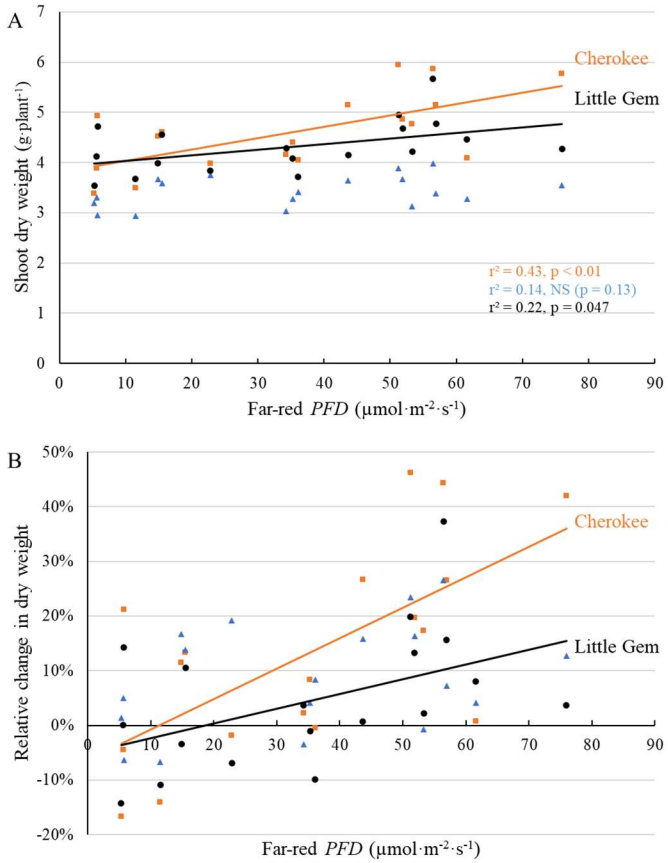

Figure 3.12. With a background of 204 µmol·m^{-2}·s^{-1} white LED light, supplemental far-red photons linearly increased shoot dry weight at 35 days after the start of far-red light treatment for ‘Cherokee’ and ‘Little Gem’, but not for ‘Green Saladbowl’ (blue triangles) lettuce at 29 DAT. The r^2 and p values for regression of each cultivar apply to both graphs and are shown with the respective color.

For 'Little Gem' and 'Green Saladbowl', the effect of far-red *PFD* on total shoot fresh weight was not statistically significant at either harvest (Fig. S3.12 and Fig. S3.13). At the 1st harvest, shoot fresh weight of ‘Cherokee’ lettuce increased 6.94 g·plant^{-1} with the highest supplemental far-red *PFD* (Fig. S3.12A), representing a 38.0% increase in shoot fresh weight compared to plants grown without supplemental far-red light (Fig. S3.12B). At the 2nd harvest, the highest (70.4 µmol·m^{-2}·s^{-1}) supplemental far-red *PFD* resulted in 27.5 g·plant^{-1} more shoot fresh

weight compared to plants without supplemental far-red photons for 'Cherokee' (Fig. S3.13B), a 26.8% increase in shoot fresh weight compared to plants without far-red light (Fig. S3.13B).

3. Discussion

3.1. Morphological changes induced by adding far-red light

Adding far-red light resulted in longer leaves (Fig. 3.2) and longer stems (Fig. 3.8), as well as an upward growing habit (hyponasty) (Fig. 3.1 and Fig. S3.2), which is consistent with shade responses (Ruberti et al., 2012). The mechanism of plants' morphological responses to far-red light is well understood. Red light and far-red light shift the balance between two photo-reversible isoforms of phytochrome: red photons convert Pr to Pfr and far-red photons convert Pfr to Pr. Changes in the phytochrome photo-equilibrium (PPE; ratio of Pfr to total phytochrome) induce downstream morphological responses (Valladares and Niinemets, 2008; Li and Kubota, 2009; Ruberti et al., 2012; Casal, 2013; Gommers et al., 2013). A low PPE induces shade response in lettuce, such as leaf expansion, stem elongation and hyponasty (Casal, 2013).

A positive correlation between leaf expansion and supplemental far-red *PFD* was observed for all three cultivars (Fig. 3.2). Leaf expansion as a result of supplemental far-red light was previously observed in various lettuce cultivars (Li and Kubota, 2009; Meng and Runkle, 2019b; Legendre and van Iersel, 2021), but the extent of leaf expansion varied among cultivars. A 1.1 mm per $\mu mol \cdot m^{-2} \cdot s^{-1}$ increase in leaf length in response to supplemental far-red *PFD* was previously observed for 'Green Saladbowl' under white LED light of similar intensity (Legendre and van Iersel, 2021), similar to the 1.12 mm per $\mu mol \cdot m^{-2} \cdot s^{-1}$ increase in leaf length observed in our study (Fig. 3.2).

Supplemental far-red *PFD* linearly increased plant height in the seedling stage (Fig. 3.1) and after canopy closure at the first harvest (Fig. S3.2). This was the combined result of longer

leaf length and hyponasty; leaves under higher far-red *PFD* grew at a steeper, upward angle. This is consistent with a shade avoidance response (Ruberti et al., 2012; Gommers et al., 2013). Hyponasty, resulting from increased far-red *PFD*, can create a more open canopy structure, allowing for a more uniform light distribution throughout the canopy, which in turn increases canopy photosynthesis (Zou et al., 2019).

Greater total leaf area, because of leaf expansion induced by supplemental far-red, was observed for 'Cherokee' and 'Little Gem', but not for 'Green Saladbowl' at the first harvest (Fig. 3.4). Supplemental far-red photons did promote leaf expansion of 'Green Saladbowl' lettuce at an early stage, as is evident from the higher light interception from 5 DAT to 9 DAT induced by supplemental far-red photons (Fig. 3.3, S3,1 and S3.2) and larger longest leaf length at 20 DAT (Fig. 3.2). But later on, the rapid growth of 'Green Saladbowl' lettuce created a denser canopy and more self-shading in the canopy, compared to 'Cherokee' and 'Little Gem' lettuce, which may have diminished the effect of supplemental far-red *PFD* on total leaf area. 'Green Saladbowl' lettuce had the highest light interception among the three lettuce cultivars from 5 DAT to 9 DAT (Fig. 3.3, S3.4 and S3.8). It can also be seen at the 1st harvest that 'Green Saladbowl' lettuce had higher total leaf area than 'Cherokee' and 'Little Gem' lettuce ($p = 0.02$) (Fig. 3.4A), which suggests more leaf overlap and self-shading. The stronger self-shading might mask the effect of supplemental far-red photons on leaf area of 'Green Saladbowl' at the 1st harvest.

A previous study found that supplemental far-red photons increased lettuce biomass production mainly through leaf expansion and higher light interception. The effect of supplemental far-red photons on lettuce was stronger at low planting density than at high planting density (Jin et al., 2021). They argued that for lettuce at high planting density, the light interception was already high; thus, supplemental far-red photons had limited effect on plant growth (Jin et al., 2021). This

theory applies to our study as well. It is possible that light interception was already high and the red:far-red ratio was low within the dense canopy of 'Green Saladbowl' lettuce after the early stage. Thus, supplemental far-red photons did not increase leaf area of 'Green Saladbowl' but increased the leaf area of 'Cherokee' and 'Little Gem' at the first harvest (Fig. 3.4). After the 1st harvest, when eight of the 15 plants were removed, 'Green Saladbowl' plants quickly closed the canopy gaps created by the harvest. Therefore 'Green Saladbowl' lettuce was harvested nine days after the 1st harvest, whereas 'Cherokee' and 'Little Gem' were harvested 15 days after the 1st harvest. At this time, supplemental far-red photons increased leaf area of 'Green Saladbowl' but did not increase leaf area of 'Cherokee' and 'Little Gem' (Fig. 3.5).

Chlorophyll and anthocyanin biosynthesis are affected by PPE (Oelze-Karow and Mohr, 1982; Yanovsky et al., 1998; Li and Kubota, 2009). In lettuce, lower chlorophyll and lower anthocyanin for red-leaf cultivars were previously observed under higher far-red *PFD* (Li and Kubota, 2009; Meng and Runkle, 2019a; Zou et al., 2019). In our study, CCI of all three cultivars decreased with increasing far-red *PFD* (Fig. 3.6). ACI of the red-leaf 'Cherokee' also decreased with increasing far-red *PFD* (Fig. 3.7). These are likely results of lower pigment synthesis under high far-red *PFD*, rather than lower specific leaf weight (SLW) (as seen in Fig. S3.9), as we found no correlation between CCI and SLW at the 1st harvest ($p = 0.86$ for 'Cherokee', $p = 0.07$ for 'Green Saladbowl' and $p = 0.30$ for 'Little Gem'). For the red cultivar 'Cherokee', ACI also was not correlated with SLW ($p = 0.84$). Previous studies found that light with a high red:far-red ratio converts the PPE towards Pfr, which stimulates both chlorophyll synthesis and anthocyanin synthesis (Lange et al., 1971; Oelze-Karow and Mohr, 1982; Mancinelli, 1985). Our results agree with the previous observation that the reduction in chlorophyll and anthocyanin content was a result of decreased biosynthesis rather than decreased SLW.

Other parameters related to crop quality were also affected by supplemental far-red *PFD*. Stem length (Fig. 3.8) and internode length (data not shown) of 'Cherokee' and 'Green Saladbowl' increased linearly with increasing far-red *PFD*. Stem elongation was previously also observed for other lettuce cultivars (Hernandez and Spalholz, 2019; Legendre and van Iersel, 2021). In our study, 'Cherokee' and 'Green Saladbowl' plants grown under the highest far-red *PFD* had an 84.5% and 187.9% increase, respectively, in stem length compared to plants without supplemental far-red light (Fig. 3.8B). But the absolute increase was small, only 1.0 and 1.8 cm for 'Cherokee' and 'Green Saladbowl', respectively. The supplemental far-red light did not affect stem length of 'Little Gem' plants (Fig. 3.8). A shade avoidance response may reduce the productivity of field crops, as plants allocate more resources to the stem, in competition with leaf and root (Ruberti et al., 2012). However, in our study, with up to 70.4 $\mu mol \cdot m^{-2} \cdot s^{-1}$ supplemental far-red light added to 204 $\mu mol \cdot m^{-2} \cdot s^{-1}$ white light, the length of lettuce stems was still small.

3.2. No evidence that far-red photons affected leaf-level photosynthesis

We found no difference in leaf-level P_n and Φ_{PSII} among plants grown under different supplemental far-red *PFDs* (Fig. 3.9). A previous study found that lettuce plants that grew in a far-red supplemented environment had similar Φ_{PSII} but lower P_n, than plants under only white LED light, particularly at high *PPFD* (Zou et al., 2019). Lettuce leaves from a far-red supplemented environment had lower leaf nitrogen concentration per unit area, chlorophyll concentration per unit area, light absorptance, and stomatal conductance, which resulted in lower P_n at high *PPFD* (Zou et al., 2019). In our study, lettuce leaves responded to supplemental far-red *PFD* by lowering CCI (Fig. 3.6). Lower CCI correlates with lower chlorophyll concentration in leaves and could lead to lower leaf level light absorptance (Bauerle et al., 2004; Parry et al., 2014; Zhen and

Kusuma, 2020). It may explain our observation that the leaf-level P_n and Φ_{PSII} was not affected by far-red *PFD* (Fig. 3.9).

Leaf-level P_n and Φ_{PSII} did not significantly change either when supplemental far-red light was turned off (Fig. 3.10 and Fig. S3.11). Far-red photons have been shown to efficiently drive photosynthesis of lettuce at both leaf and canopy level (Zhen and van Iersel, 2017; Zou et al., 2019; Zhen and Bugbee, 2020a; b). Previous studies also showed that temporarily turning on or off far-red lights affected both leaf level and canopy level photosynthetic rates of lettuce whether developed under supplemental far-red light or not (Zou et al., 2019; Zhen and Bugbee, 2020a; b). In our study, however, we did not find any changes in P_n and Φ_{PSII} of lettuce leaves when turning off supplemental far-red lights. This is likely because our photosynthetic measurements with and without far-red light was not taken on the same spot of leaves. The cuvette of the leaf gas exchange system was removed and re-clamped on the leaves before and after far-red lights were turned off. Therefore, our data may have failed to capture the change in leaf level P_n and Φ_{PSII} after far-red lights were turned off. In the case of 'Cherokee', a red-leaf lettuce cultivar, the ACI decreased linearly with increasing far-red *PFD* (Fig. 3.7). Anthocyanins may competitively absorb light energy and divert absorbed energy away from photosynthesis (Sun et al., 1998). Nevertheless, in our study, the anthocyanins in 'Cherokee' leaves had no significant effect on leaf-level P_n ($p = 0.53$). In summary, we did not find evidence that supplemental far-red photons increased leaf photosynthesis, likely due to noise in our photosynthetic data.

3.3. Supplemental far-red light increased final yield in a cultivar-specific manner

At both harvests, shoot dry weight of 'Cherokee' and 'Little Gem', but not that of 'Green Saladbowl', increased with increasing far-red *PFD* (Fig. 3.11 and Fig. 3.12). Higher light

interception, resulting from increased leaf elongation in response to supplemental far-red light, increased the amount of light energy available for photosynthesis and would thus be expected to increase whole-canopy photosynthetic rates and plant growth. This would be especially important for young plants, since their canopy size and light interception are small. Higher light interception in response to supplemental far-red photons during the seedling stage increases seedlings' light energy capture and carbon assimilation, thus promoting canopy enlargement and light capture.

In our study, supplemental far-red light increased the final dry weight of "Little Gem' and 'Cherokee' lettuce through increasing light interception, but not that of 'Green Saladbowl'. The importance of light interception for crop growth is evident from the correlations between light interception and shoot dry weight. Shoot dry weight at the 1st harvest correlated with light interception of 'Cherokee' (at 12 and 16 DAT), 'Green Saladbowl' (12 to 19 DAT) and 'Little Gem' (9 DAT till the 1st harvest). Light interception starting from 7 DAT until the 1st harvest also strongly correlated with the final shoot dry weight of all three cultivars at the 2nd harvest, except for the light interception of 'Green Saladbowl' at 9 DAT. For example, light interception by 'Cherokee', 'Green Saladbowl' and 'Little Gem' at 12 DAT was strongly correlated with shoot dry weight at both the 1st and 2nd harvest (Fig. 3.13). The dry weight at the 1st harvest did not correlate with the quantum yield of photosystem II for any of the cultivars ($p \geq 0.44$, $r \leq 0.19$). Leaf-level photosynthesis often does not correlate with crop yield since it is a short-term measurement, limited to a small section of a single leaf and thus not representative of the entire canopy during the growing cycle (Zelitch, 1982). These results suggest that the changes in dry weight induced by supplemental far-red *PFD* were due mainly to changes in light interception rather than leaf-level photosynthesis.

Far-red inclusion has been shown to increase canopy size and light interception, thus resulting in greater biomass for a wide range of vegetable and ornamental crops, including lettuce (Li and Kubota, 2009; Kubota et al., 2011; Park and Runkle, 2017; Craver et al., 2018; Hernandez and Spalholz, 2019; Meng and Runkle, 2019a; Zou et al., 2019; Legendre and van Iersel, 2021). Throughout this study, 'Cherokee' plants grown under high far-red *PFD* consistently intercepted more light than plants grown under low far-red *PFD*, which resulted in higher shoot dry weight and fresh weight at both harvests (Fig. 3.11, Fig. 3.12, Fig. S3.12 and Fig. S3.13). With the inclusion of far-red photons, plants enter a 'self-re-enforcing' cycle: larger leaves and better light interception boost plant growth, further enhancing light interception and resulting in higher dry weight (Legendre and van Iersel, 2021). Light interception of 'Green Saladbowl' plants was increased by supplemental far-red photons only from 5 to 9 DAT (Fig. 3.3, S3.3, S3.4, and S3.5). It is possible that the rapid growth of 'Green Saladbowl' lettuce created self-shading within their canopies, which masked the effect of supplemental far-red photons. In contrast, for 'Little Gem', where supplemental far-red *PFD* only increased light interception during a short window of the seedling stage (5-12 DAT) (Fig. 3.3, S3.3, S3.4, S3.5 and S3.6), the benefit of the increased light interception nevertheless carried over to final dry weight (Fig. 3.11 and Fig. 3.12). In short, this self-re-enforcing cycle appears to be cultivar-dependent.

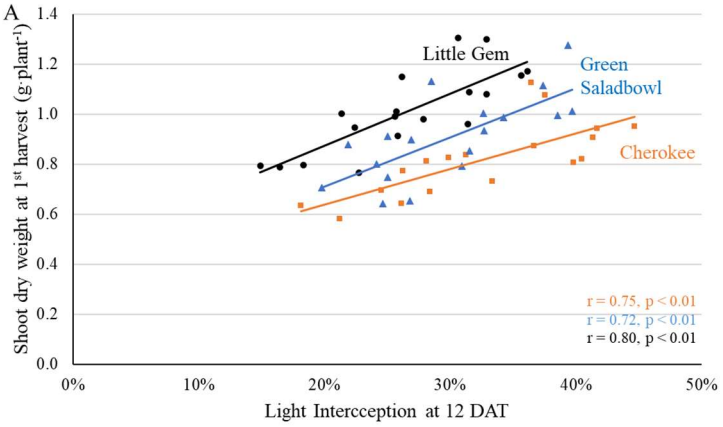

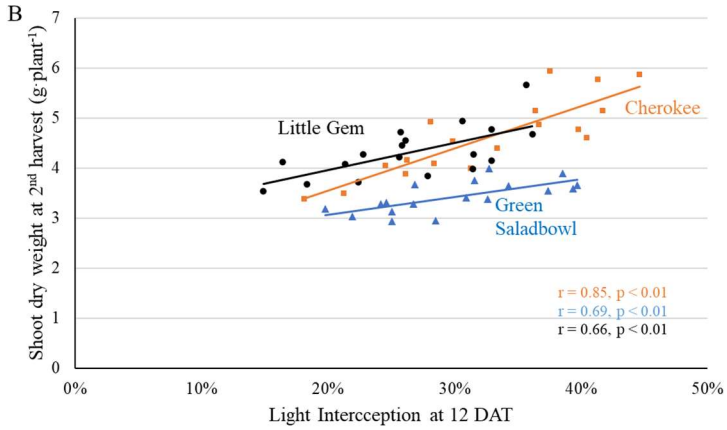

Figure 3.13. Canopy light interception at 12 DAT strongly correlated with shoot dry weight at both harvests for 'Cherokee', 'Green Saladbowl' and 'Little Gem' lettuce. The *r* and *p* values for regression of each cultivar are shown with the respective color.

Previous research suggested that plants grown with supplemental far-red light had an open canopy structure, facilitating more uniform light distribution within the canopy, and increased light use efficiency and whole canopy photosynthesis (Zou et al., 2019). We observed a similar change in canopy structure as a consequence of change in leaf angle (hyponasty) and taller plants (Fig. 3.1 and S3.2). It is possible that better light penetration into canopy similarly increased canopy level photosynthesis in our study. Better light penetration possibly benefits growth of 'Cherokee' and 'Little Gem' lettuces more than 'Green Saladbowl' lettuces, as 'Green Saladbowl' is a loose-leaf lettuce cultivar, which lacks a tight canopy architecture.

3.4. Conclusions

Increasing far-red *PFD* linearly increased leaf expansion with a background of 204 $\mu mol \cdot m^{-2} \cdot s^{-1}$ white LED light. The increase in light interception resulting from this leaf expansion was cultivar-dependent. Supplemental far-red photons increased light interception of 'Cherokee' throughout the whole production cycle and resulted in higher shoot fresh and dry weight. The

increase in light interception caused by supplemental far-red photons was transient for ‘Green Saladbowl’ and ‘Little Gem’, and the transient benefits of increased light interception translated to higher shoot dry weight for ‘Little Gem’, but not for ‘Green Saladbowl’. Supplemental far-red light resulted in lower chlorophyll content for all three cultivars and lower anthocyanin content for the red lettuce ‘Cherokee’. Those changes in pigmentation did not significantly affect Φ_{PSII}. In summary, adding far-red light in indoor production increased light interception of lettuce seedlings, but did not significantly affect leaf photosynthesis, and resulted in linear increases of biomass, up to 70.4 $\mu mol \cdot m^{-2} \cdot s^{-1}$ in two of the three cultivars tested.

4. Materials and Methods

Walk-in cooler setup

Three metal shelves were installed inside a walk-in growth chamber. Each shelving unit had 3 levels, and each level was divided into two 1.2 x 0.6 m units, resulting in 18 separate growing areas. During the study, the temperature in the growth chamber was 20.4 ± 0.2 °C (average ± standard deviation), vapor pressure deficit was 0.74 ± 0.13 kPa, and the CO_2 concentration was 819 ± 44 $\mu mol \cdot mol^{-1}$.

Plant material

Three lettuce cultivars were used in this study: 'Green Saladbowl', 'Little Gem", and 'Cherokee' (Johnny's seeds, Winslow, ME, USA). Plants were grown from seed in 10-cm square pots filled with a peat-based soilless substrate (Fafard 4P, Sun Gro Horticulture, Agawam, MA, USA). One tray with 15 plants of each cultivar was placed in each section of the shelving units, totaling 54 trays of lettuce, 18 for each cultivar. Plants were sub-irrigated with nutrient solution once a day. The nutrient solution contained 100 $mg \cdot L^{-1}$ N (Peters Excel 15-5-15 Cal-Mag water-soluble fertilizer; 15N-2.2P-12.5K, Everris, Dublin, OH, USA). During germination, trays on the

metal shelves were rotated periodically within the same section to minimize the impact of any environmental gradients.

Far-red light treatments

Seeds were germinated under white LED light (Fig. S3.1) of 204 ± 11.0 $\mu mol \cdot m^{-2} \cdot s^{-1}$ with a 16 h photoperiod. After germination (6 days after sowing), far-red LED lights were turned on. Plants in three of the 18 units were grown under white LED light only as a control, while plants in the remaining 15 units were grown with supplemental far-red *PFD*s ranging from 6.0 to 70.3 $\mu mol \cdot m^{-2} \cdot s^{-1}$ (Table S3.1). Far-red light had the same photoperiod as the white LED light.

Physiological and morphological measurements

Light interception of the crops was measured using a ceptometer (ACCUPAR LP-80, METER Group, Pullman, WA, USA) twice a week. Plant height was measured for three lettuce plants per experimental unit at 7 and 20 DAT (at first harvest). Chlorophyll content index (CCI) and anthocyanin content index (ACI) were measured with a CCM-200+ chlorophyll content meter and ACM-200+ anthocyanin content meter (Opti-Sciences, Hudson, NH, USA), respectively, at 12 DAT and 16 DAT.

At 27 DAT, Φ_{PSII} of a newly fully-expanded leaf of each cultivar was measured under the light environment plants were grown under using a fluorometer (Junior-PAM, Heinz Walz GmbH, Effeltrich, Germany). At 28 DAT, P_n and Φ_{PSII} of a recently fully expanded leaf were measured on one plant of each cultivar in 11 of the 18 experimental units, using the same fluorometer and a leaf gas exchange system (CIRAS-3, PP system, Amesbury, MA, USA). We then turned off the supplemental far-red light, waited for 20 min, and measured P_n and Φ_{PSII} on the same leaf (but not the same location) under only white LED light to quantify the effect of supplemental far-red light

on photochemistry and photosynthesis. All P_n and Φ_{PSII} measurements were taken under a *PPFD* of about 200 $\mu mol \cdot m^{-2} \cdot s^{-1}$.

The first harvest occurred at 20 DAT. Seven plants from each experimental unit were harvested at the first harvest. During the first harvest, canopy height and length of the longest leaf from three plants of each experimental unit were measured. Total leaf area, shoot fresh weight, and shoot dry weight were measured on all seven plants combined. The second harvest of 'Cherokee' and 'Little Gem' occurred at 35 DAT and that of 'Green Saladbowl' at 29 DAT. 'Green Saladbowl' was harvested earlier due to its rapid growth. During the second harvest, stem length of three plants in each experimental unit was measured in addition total leaf area, shoot fresh weight, and shoot dry weight of seven plants. Total leaf area was measured using a leaf area meter (Li-3100, Li-Cor Biosciences, Lincoln, NE, USA). The dry weight was measured after shoot tissue was dried at 80˚C for at least 72 hours. Specific leaf weight was calculated as shoot dry weight divided by total leaf area. One extra plant was discarded before canopy closure after the 1st harvest.

Data analysis

This study used a completely randomized design with a split-plot for the three cultivars, with far-red *PFD* randomly assigned to the 18 growing spaces. Data were analyzed using regression analysis in Microsoft Excel (Microsoft, Seattle, WA, USA) to detect effect of far-red *PFD* on physiological and morphological parameters. Correlations were tested with multivariate analysis of JMP Pro 15 to detect correlations between leaf area and light interception, specific leaf area and CCI, as well as light interception and lettuce dry weight (SAS Institute, Cary, NC, United States). ANOVA was also performed in JMP Pro 15.

References:

Bauerle, W.L., Weston, D.J., Bowden, J.D., Dudley, J.B., and Toler, J.E. (2004). Leaf absorptance of photosynthetically active radiation in relation to chlorophyll meter estimates among woody plant species. *Scientia Horticulturae* 101(1)**,** 169-178. doi: https://doi.org/10.1016/j.scienta.2003.09.010.

Casal, J.J. (2013). Photoreceptor signaling networks in plant responses to shade. *Annual review of plant biology* 64**,** 403-427.

Craver, J.K., Boldt, J.K., and Lopez, R.G. (2018). Radiation Intensity and Quality from Sole-source Light-emitting Diodes Affect Seedling Quality and Subsequent Flowering of Long-day Bedding Plant Species. *HortScience* 53(10)**,** 1407-1415.

Emerson, R. (1957). Dependence of yield of photosynthesis in long-wave red on wavelength and intensity of supplementary light. *Science* 125(3251)**,** 746-746. doi: 10.1126/science.125.3251.746.

Emerson, R., and Lewis, C.M. (1943). The dependence of the quantum yield of Chlorella photosynthesis on wave length of light. *American Journal of Botany* 30(3)**,** 165-178.

Evans, J. (1987). The dependence of quantum yield on wavelength and growth irradiance. *Functional Plant Biology* 14(1)**,** 69-79. doi: 10.1071/PP9870069.

Gommers, C.M.M., Visser, E.J.W., Onge, K.R.S., Voesenek, L.A.C.J., and Pierik, R. (2013). Shade tolerance: when growing tall is not an option. *Trends in Plant Science* 18(2)**,** 65-71. doi: 10.1016/j.tplants.2012.09.008.

Hernandez, R., and Spalholz, H. (Year). "Characterization of Solar Radiation Spectral Contribution in Lettuce Bolting and Flowering Using LEDs in an Indoor Setting", in: *2019 ASHS Annual Conference*: ASHS).

Holmes, M., and Smith, H. (1977). The function of phytochrome in the natural environment—II. The influence of vegetation canopies on the spectral energy distribution of natural daylight. *Photochemistry and Photobiology* 25(6)**,** 539-545.

Jin, W., Urbina, J.L., Heuvelink, E., and Marcelis, L.F.M. (2021). Adding Far-Red to Red-Blue Light-Emitting Diode Light Promotes Yield of Lettuce at Different Planting Densities. *Frontiers in Plant Science* 11(2219). doi: 10.3389/fpls.2020.609977.

Kubota, C., Chia, P., Yang, Z., and Li, Q. (Year). "Applications of far-red light emitting diodes in plant production under controlled environments", in: *International Symposium on Advanced Technologies and Management Towards Sustainable Greenhouse Ecosystems: Greensys2011 952*), 59-66.

Kusuma, P., Pattison, P.M., and Bugbee, B. (2020). From physics to fixtures to food: current and potential LED efficacy. *Horticulture Research* 7(1)**,** 56. doi: 10.1038/s41438-020-0283-7.

Lange, H., Shropshire, W., Jr., and Mohr, H. (1971). An Analysis of Phytochrome-mediated Anthocyanin Synthesis. *Plant Physiology* 47(5)**,** 649-655. doi: 10.1104/pp.47.5.649.

Legendre, R., and van Iersel, M.W. (2021). Supplemental Far-Red Light Stimulates Lettuce Growth: Disentangling Morphological and Physiological Effects. *Plants* 10(1)**,** 166.

Li, Q., and Kubota, C. (2009). Effects of supplemental light quality on growth and phytochemicals of baby leaf lettuce. *Environmental and Experimental Botany* 67(1)**,** 59-64.

Mancinelli, A.L. (1985). Light-dependent anthocyanin synthesis: a model system for the study of plant photomorphogenesis. *The Botanical Review* 51(1)**,** 107-157.

McCree, K.J. (1971). The action spectrum, absorptance and quantum yield of photosynthesis in crop plants. *Agricultural Meteorology* 9(Supplement C)**,** 191-216. doi: 10.1016/0002-

1571(71)90022-7.

McCree, K.J. (1972). Test of current definitions of photosynthetically active radiation against leaf photosynthesis data. *Agricultural Meteorology* 10**,** 443-453. doi: 10.1016/0002-1571(72)90045-3.

Meng, Q., and Runkle, E.S. (2019a). Far-red radiation interacts with relative and absolute blue and red photon flux densities to regulate growth, morphology, and pigmentation of lettuce and basil seedlings. *Scientia Horticulturae* 255**,** 269-280. doi: 10.1016/j.scienta.2019.05.030.

Meng, Q., and Runkle, E.S. (2019b). Regulation of flowering by green light depends on its photon flux density and involves cryptochromes. *Physiologia Plantarum* 166(3)**,** 762-771. doi: 10.1111/ppl.12832.

Myers, J. (1971). Enhancement studies in photosynthesis. *Annual Review of Plant Physiology* 22(1)**,** 289-312.

Oelze-Karow, H., and Mohr, H. (1982). Phytochrome Action on Chlorophyll Synthesis—A Study of the Escape from Photoreversibility. *Plant Physiology* 70(3)**,** 863-866. doi: 10.1104/pp.70.3.863.

Park, Y., and Runkle, E.S. (2017). Far-red radiation promotes growth of seedlings by increasing leaf expansion and whole-plant net assimilation. *Environmental and experimental botany* 136**,** 41-49. doi: 10.1016/j.envexpbot.2016.12.013.

Parry, C., Blonquist Jr, J.M., and Bugbee, B. (2014). In situ measurement of leaf chlorophyll concentration: analysis of the optical/absolute relationship. *Plant, cell & environment* 37(11)**,** 2508-2520.

Ruberti, I., Sessa, G., Ciolfi, A., Possenti, M., Carabelli, M., and Morelli, G. (2012). Plant

adaptation to dynamically changing environment: the shade avoidance response. *Biotechnology advances* 30(5)**,** 1047-1058.

Sun, J., Nishio, J.N., and Vogelmann, T.C. (1998). Green light drives CO2 fixation deep within leaves. *Plant and Cell Physiology* 39(10)**,** 1020-1026. doi: 10.1093/oxfordjournals.pcp.a029298.

Valladares, F., and Niinemets, Ü. (2008). Shade Tolerance, a Key Plant Feature of Complex Nature and Consequences. *Annual Review of Ecology, Evolution, and Systematics* 39(1)**,** 237-257. doi: 10.1146/annurev.ecolsys.39.110707.173506.

Yanovsky, M.J., Alconada-Magliano, T.M., Mazzella, M.A., Gatz, C., Thomas, B., and Casal, J.J. (1998). Phytochrome A affects stem growth, anthocyanin synthesis, sucrose-phosphate-synthase activity and neighbour detection in sunlight-grown potato. *Planta* 205(2)**,** 235-241. doi: 10.1007/s004250050316.

Zelitch, I. (1982). The close relationship between net photosynthesis and crop yield. *Bioscience* 32(10)**,** 796-802.

Zhen, S., and Bugbee, B. (2020a). Far‐red photons have equivalent efficiency to traditional photosynthetic photons: implications for redefining photosynthetically active radiation. *Plant, Cell & Environment*.

Zhen, S., and Bugbee, B. (2020b). Substituting Far-Red for Traditionally Defined Photosynthetic Photons Results in Equal Canopy Quantum Yield for CO2 Fixation and Increased Photon Capture During Long-Term Studies: Implications for Re-Defining PAR. *Frontiers in Plant Science* 11(1433). doi: 10.3389/fpls.2020.581156.

Zhen, S., and Kusuma, P. (2020). Accuracy of the Generic Equation to Convert CCI to Chlorophyll Concentration in the Apogee Model MC-100 Chlorophyll Concentration

Meter.

Zhen, S., and van Iersel, M.W. (2017). Far-red light is needed for efficient photochemistry and photosynthesis. *Journal of Plant Physiology* 209**,** 115-122. doi: http://dx.doi.org/10.1016/j.jplph.2016.12.004.

Zou, J., Zhang, Y., Zhang, Y., Bian, Z., Fanourakis, D., Yang, Q., et al. (2019). Morphological and physiological properties of indoor cultivated lettuce in response to additional far-red light. *Scientia Horticulturae* 257**,** 108725. doi: 10.1016/j.scienta.2019.108725.

Supplementary Materials:

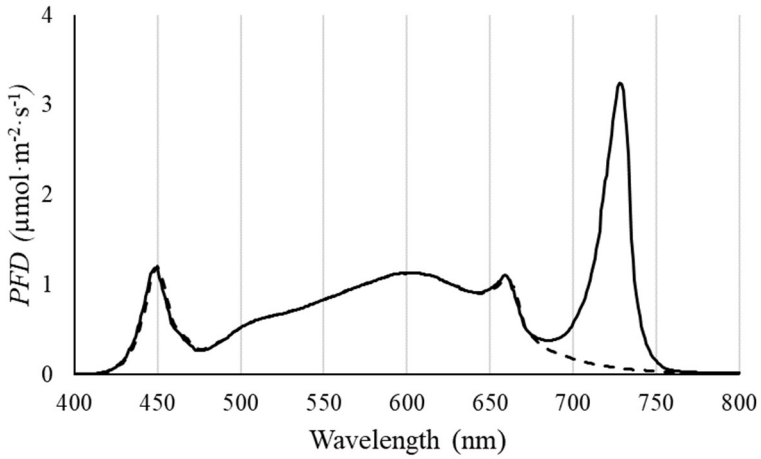

Figure S3.1. Light spectrum of white LED light (dashed line) and the light spectrum of highest far-red *PFD* (solid line).

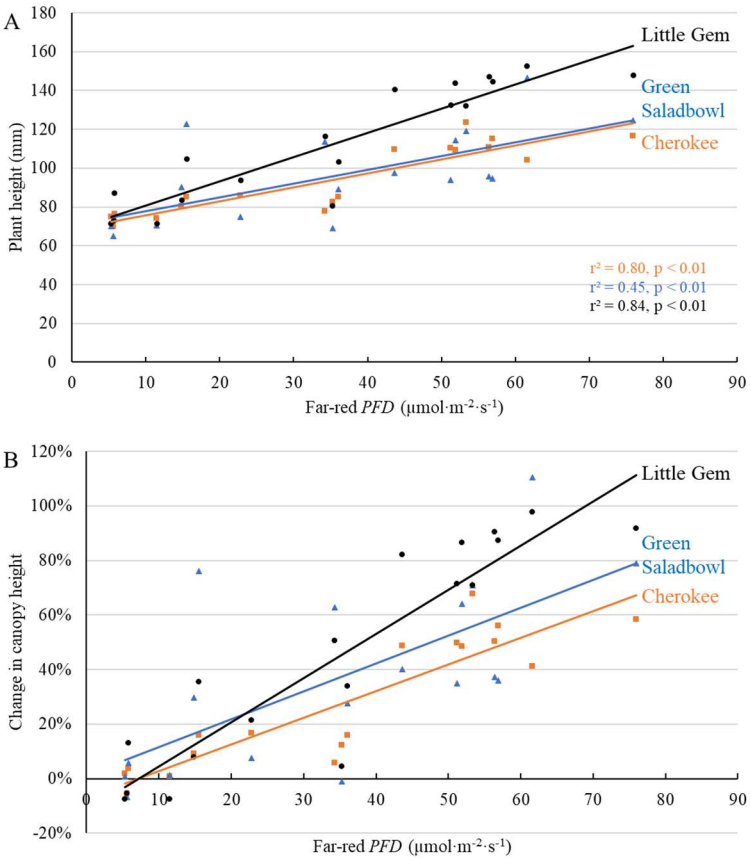

Figure S3.2. With a background of 204 µmol·m^{-2}·s^{-1} white LED light, supplemental far-red photons linearly increased plant height (A) and the relative change in plant height (B, compared to plants under no supplemental far-red light) at 20 days after the start of far-red light treatment for 'Cherokee', 'Green Saladbowl', and 'Little Gem' lettuce. The r^2 and p values for regression of each cultivar apply to both graphs and are shown with the respective color.

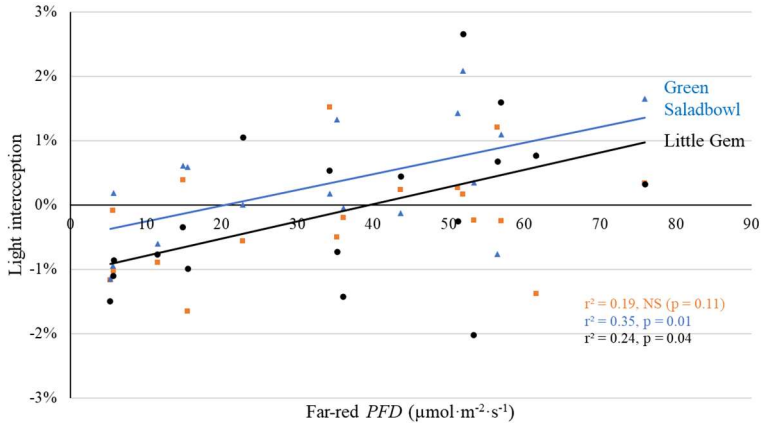

Figure S3.3. With a background of 204 µmol·m^{-2}·s^{-1} white LED light, supplemental far-red photons linearly increased canopy light interception 5 days after the start of far-red

light treatment for ‘Green Saladbowl’ and ‘Little Gem’ lettuce, but not for ‘Cherokee’ (orange squares) lettuce.

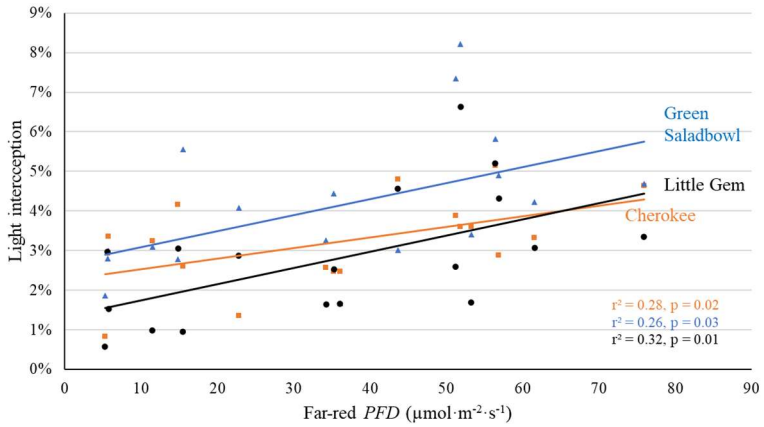

Figure S3.4. With a background of 204 µmol·m^{-2}·s^{-1} white LED light, supplemental far-red photons linearly increased canopy light interception 7 days after the start of far-red light treatment for ‘Cherokee’, ‘Green Saladbowl’ and ‘Little Gem’ lettuce.

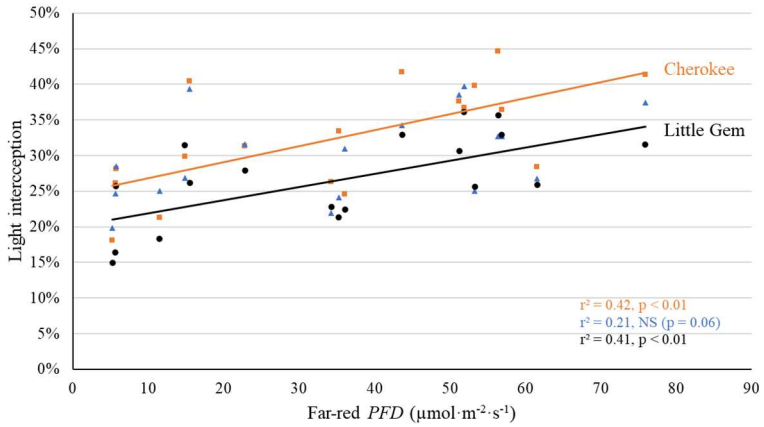

Figure S3.5. With a background of 204 µmol·m^{-2}·s^{-1} white LED light, supplemental far-red photons linearly increased canopy light interception 12 days after the start of far-red light treatment for ‘Cherokee’ and ‘Little Gem’ lettuce, but not for ‘Green Saladbowl’ (blue triangles) lettuce.

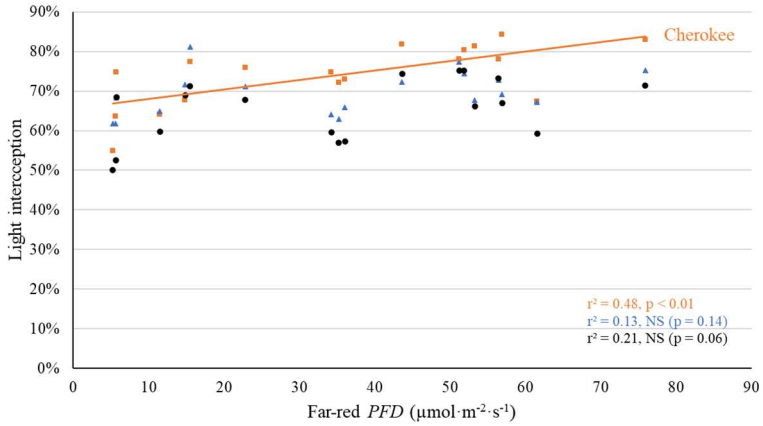

Figure S3.6. With a background of 204 µmol·m^{-2}·s^{-1} white LED light, supplemental far-red photons linearly increased canopy light interception 16 days after the start of far-red light treatment for 'Cherokee' lettuce, but not for 'Green Saladbowl' (blue triangles) and 'Little Gem' (black dots) lettuce.

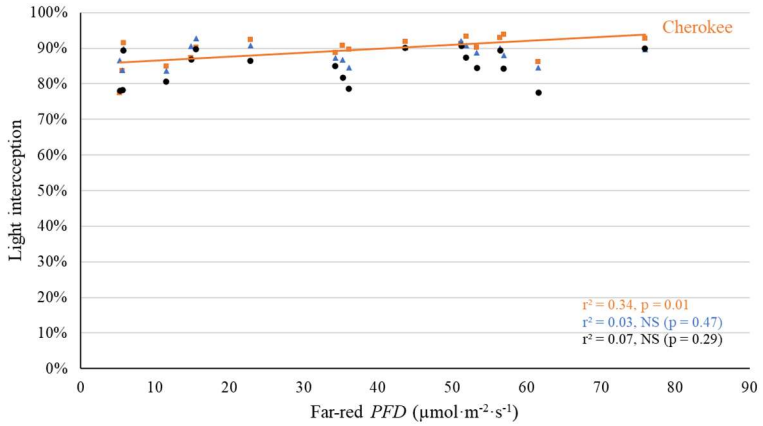

Figure S3.7. With a background of 204 µmol·m^{-2}·s^{-1} white LED light, supplemental far-red photons linearly increased canopy light interception 19 days after the start of far-red light treatment for 'Cherokee' lettuce, but not for 'Green Saladbowl' (blue triangles) and 'Little Gem' (black dots) lettuce.

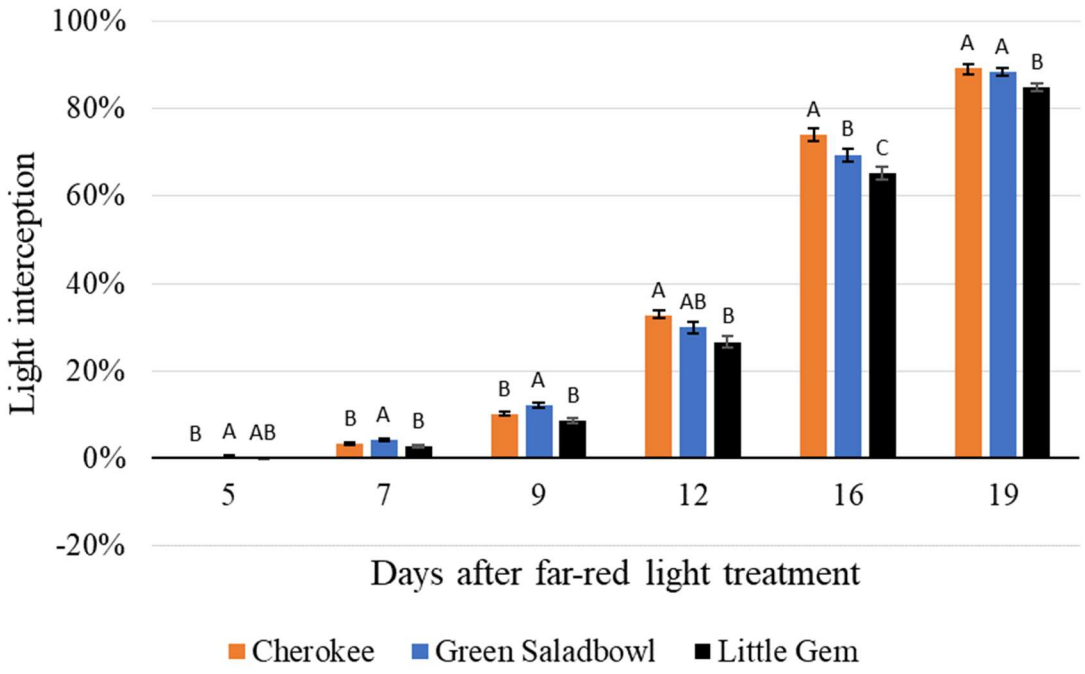

Figure S3.8 Light interception of 'Cherokee', 'Green Saladbowl' and 'Little Gem' lettuce plotted against time. Bars with the same letter, within a day, are not statistically different (p = 0.05). Error bars represent the standard error (n = 18).

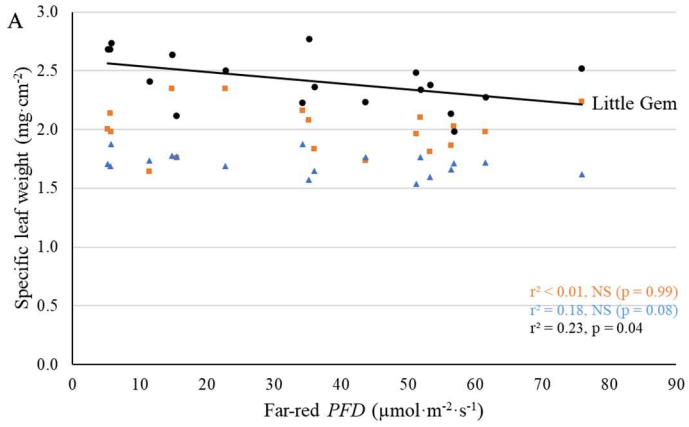

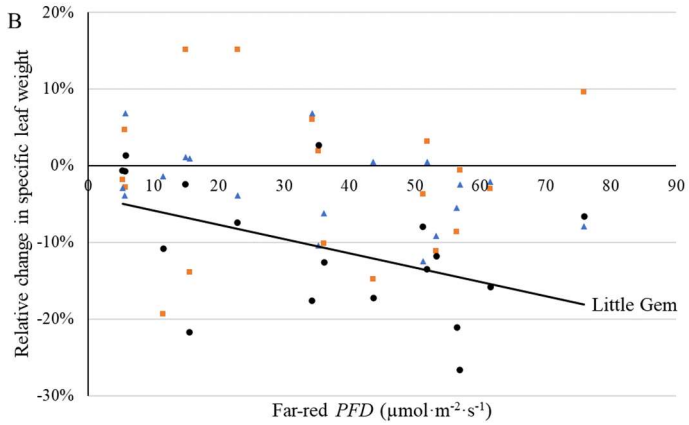

Figure S3.9. With a background of 204 µmol·m^{-2}·s^{-1} white LED light, supplemental far-red photons linearly decreased specific leaf weight (A) and the relative change in specific leaf weight (B, compared to plants without supplemental far-red light) at 20 days after the start of far-red light treatment only for 'Little Gem' lettuces, not for 'Cherokee' (orange squares) and 'Green Saladbowl' (blue triangles). The r^2 and p values for regression of each cultivar apply to both graphs and are shown with the respective color.

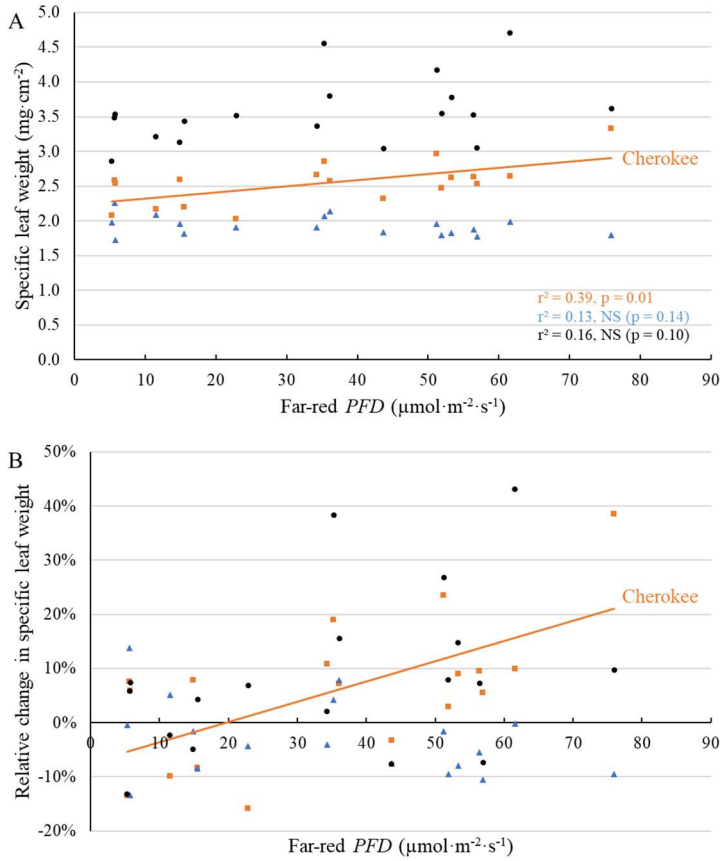

Figure S3.10. With a background of 204 µmol·m^{-2}·s^{-1} white LED light, supplemental far-red photons linearly increased specific leaf weight (A) and the relative change in specific leaf weight (B, compared to plants without supplemental far-red light) at 35 days after the

start of far-red light treatment only for ‘Cherokee’, but not for ‘Green Saladbowl’ (blue triangles) and ‘Little Gem’ (black dots) lettuce. The r^2 and p values for regression of each cultivar apply to both graphs and are shown with the respective color.

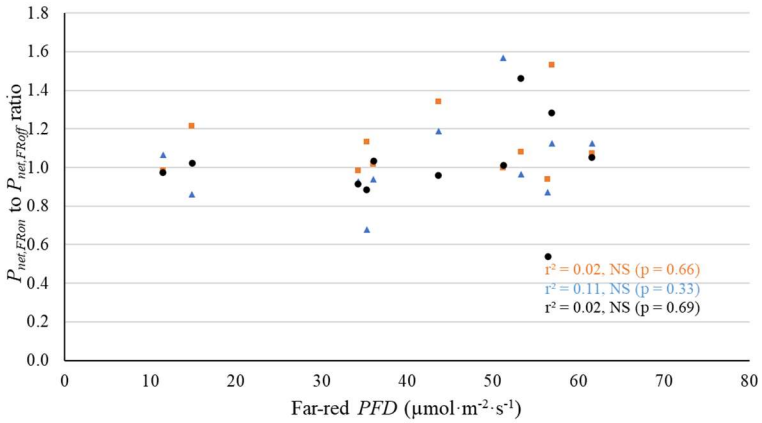

Figure S3.11. With a background of 204 µmol·m^{-2}·s^{-1} white LED light, turning off supplemental far-red lights did not affect net photosynthetic rates for ‘Cherokee’ (orange squares), ‘Green Saladbowl’ (blue triangles) and ‘Little Gem’ (black dots) lettuces 28 days after the start of far-red light treatment. The r^2 and p values for regression of each cultivar apply to both graphs and are shown with the respective color.

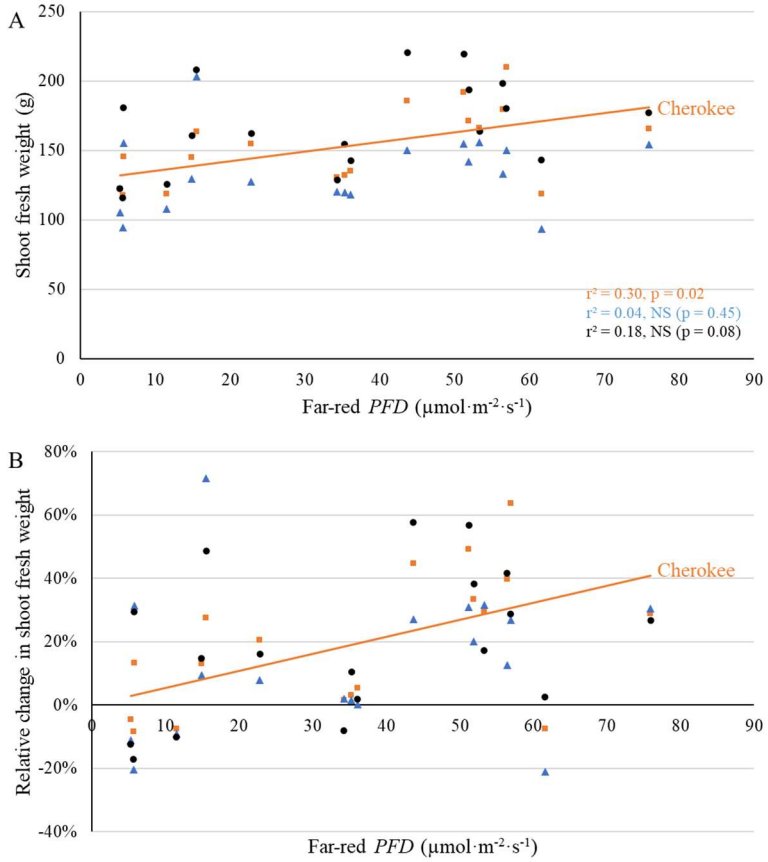

Figure S3.12. With a background of 204 µmol·m^{-2}·s^{-1} white LED light, supplemental far-red photons linearly increased shoot fresh weight at 20 days after the start of far-red light treatment for 'Cherokee', but not for 'Green Saladbowl' (blue triangles) and 'Little Gem' (black dots) lettuce. The r^2 and p values for regression of each cultivar apply to both graphs and are shown with the respective color.

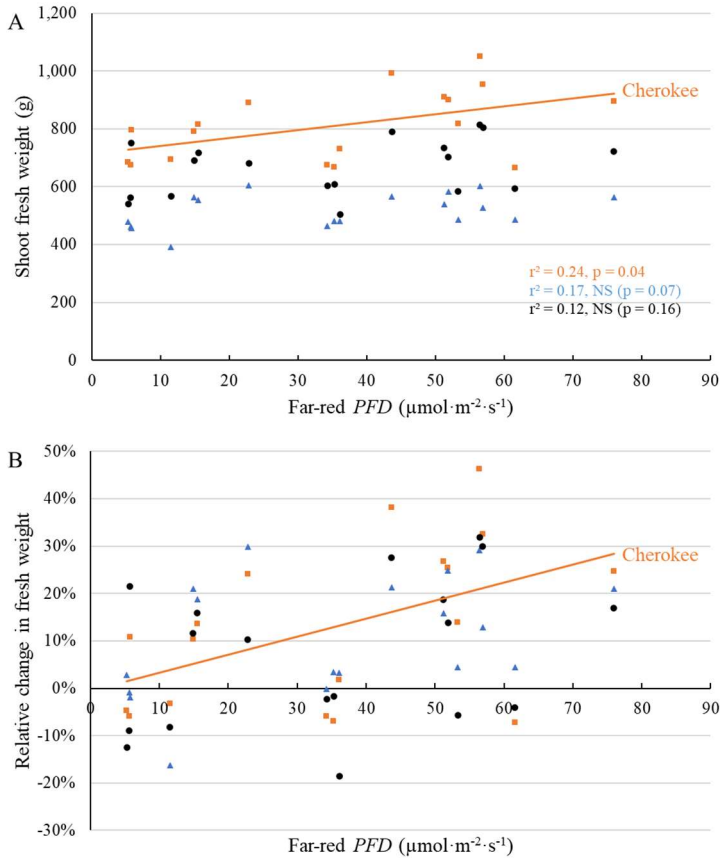

Figure S3.13. With a background of 204 µmol·m^{-2}·s^{-1} white LED light, supplemental far-red photons linearly increased shoot fresh weight 35 days after the start of far-red light treatment for 'Cherokee', but not for 'Green Saladbowl' (blue triangles) and 'Little Gem' (black dots) lettuce. The r^2 and p values for regression of each cultivar apply to both graphs and are shown with the respective color.

Table S3.1. Details of light spectrums used in this study, including different metrics that quantify far-red light in spectrum.

Far-red *PFD* (700-750 nm) ($\mu mol \cdot m^{-2} \cdot s^{-1}$)	*PPFD* (400-700 nm) ($\mu mol \cdot m^{-2} \cdot s^{-1}$)	Total *PFD* (400-750 nm) ($\mu mol \cdot m^{-2} \cdot s^{-1}$)	R:FR ratio ($\frac{600-700\ nm}{700-750\ nm}$)	FR fraction ($\frac{700-750\ nm}{400-750\ nm}$)
5.3	193.0	198.3	14.4	2.7%
5.6	197.2	202.9	13.8	2.8%
5.8	204.1	209.9	14.0	2.7%
11.5	194.0	205.5	6.7	5.6%
14.9	207.0	221.9	5.5	6.7%
15.5	204.9	220.4	5.2	7.0%
22.8	226.0	248.8	3.9	9.2%
34.3	195.9	230.2	2.3	14.9%
35.3	211.4	246.7	2.4	14.3%
36.1	219.7	255.8	2.4	14.1%
43.7	209.5	253.1	1.9	17.3%
51.2	207.8	259.1	1.6	19.8%
51.9	213.0	264.9	1.6	19.6%
53.3	194.0	247.3	1.4	21.6%
56.4	207.3	263.7	1.5	21.4%
56.9	205.0	262.0	1.4	21.7%
61.6	178.5	240.1	1.1	25.6%
75.9	209.1	285.1	1.1	26.6%

CHAPTER 4

SUBSTITUTING RED PHOTONS WITH FAR-RED PHOTONS: EXPLORING THE EFFECTS ON CANOPY CARBON ASSIMILATION

Introduction

Far-red photons (700 - 750 nm) are rarely used in sole-source lighting for controlled-environment agriculture. However, plants have evolved under sunlight for millions of years and far-red photons make up ~19% of photons relative to photosynthetically active radiation (PAR, 400 – 700 nm) (Zhen and Bugbee, 2020a). Far-red photons are important for efficient photochemistry and photosynthesis (Zhen and van Iersel, 2017; Zhen and Bugbee, 2020a) and can increase light capture and crop yield of numerous vegetable and ornamental crops under sole-source lighting by eliciting leaf elongation (Li and Kubota, 2009; Kubota et al., 2011; Park and Runkle, 2017; Craver et al., 2018; Hernandez and Spalholz, 2019; Meng and Runkle, 2019; Zou et al., 2019; Zhen and Bugbee, 2020a; b; Jin et al., 2021; Legendre and van Iersel, 2021). With its benefits in both morphological and photosynthetic processes, there is increasing interest in far-red applications in controlled environment agriculture.

Far-red photons have photosynthetic activity when combined with photons with shorter wavelengths. But far-red photons are traditionally considered to have very low photosynthetic efficiency because they have too little energy to drive photochemistry (Emerson and Rabinowitch, 1960; McCree, 1971; Evans, 1987). Only photons with wavelengths of 400 – 700 nm are typically considered photosynthetically active and

designated as PAR (McCree, 1971; 1972). Higher plants have two photosystems, photosystem I and photosystem II (PSI and PSII), which operate in series to drive linear photosynthetic electron transport. PSII utilizes photons with wavelengths shorter than 685 nm (Emerson and Lewis, 1943). Far-red photons have less energy than PAR photons and are unable to excite PSII. Thus, far-red photons have minimal photosynthetic activity when applied alone. PSI, on the other hand, can be excited by far-red photons. When applied alongside PAR, far-red photons can excite PSI and increase the quantum yield of photosystem II and photosynthesis (Evans, 1987; Zhen and van Iersel, 2017). Furthermore, photons within the PAR region tend to over-excite PSII compared to PSI, except for light between 570 – 620 nm and > 690 nm, resulting in a sub-optimal quantum yield of photosynthesis (Evans, 1987). Since PSII and PSI work linearly, these two photosystems must work at matching rates to achieve high linear electron transport rates. Far-red photons can balance the excitation energy between the two photosystems and increase quantum yield of PSII (Zhen and van Iersel, 2017). Therefore, leaves exposed to both far-red and PAR photons often have higher photosynthetic rates than the sum of photosynthetic rates when far-red photons and PAR photons are applied separately. This synergistic effect of far-red photons on photosynthesis is known as the 'Emerson enhancement effect' (Emerson, 1957; Myers, 1971). This synergistic effect has been long overlooked, partially due to influential work by McCree (1971; 1972) defining PAR. In recent years, the application of far-red light to PAR to improve both quantum yield of photosystem II and quantum yield of CO_2 assimilation has gotten renewed attention.

For lettuce, the effect of far-red photon inclusion on photosynthesis is well quantified at both the leaf and canopy levels (Zhen and van Iersel, 2017; Zhen and Bugbee, 2020b; a). At the leaf level, adding far-red light to warm white or red/blue light significantly increased the

quantum yield of photosystem II (Φ_{PSII}) and net photosynthetic rate (P_n) of lettuce across a wide *PPFD* range (50 – 750 $\mu mol \cdot m^{-2} \cdot s^{-1}$) (Zhen and van Iersel, 2017). At the canopy level, far-red photons had equal photosynthetic efficiency as PAR photons when combined with PAR photons (Zhen and Bugbee, 2020b; a). This was true across 14 crops, including C3 and C4 species (Zhen and Bugbee, 2020a).

Far-red photons can also increase canopy carbon assimilation by inducing canopy enlargement. Leaves absorb far-red photons less efficiently than UV and PAR photons (McCree, 1971; Holmes and Smith, 1977). Underneath plant canopies, the light environment is thus low in red and rich in far-red photons. Therefore, a low red to far-red ratio (R:FR ratio) is recognized by plants as a shading signal, which is perceived by phytochromes (Sager et al., 1988). Most species share some common responses to shading, including decreased specific leaf weight (SLW), reduced chlorophyll a:b ratio, and increased shoot:root ratio to boost light capture and utilization (Valladares and Niinemets, 2008; Ruberti et al., 2012; Gommers et al., 2013).

Extensive research has been conducted to explore the possibility of manipulating shading responses of crops to increase growth and yield in controlled environment agriculture (CEA). Growers can enrich the light environment with far-red photons to induce shade responses of crops without reducing light intensity and photosynthetic rate. For many vegetable and ornamental crops, such as lettuce, basil (*Ocimum basilicum*), coreopsis (*Coreopsis grandiflora*), geranium (*Pelargonium ×hortorum*), pansy (*Viola ×wittrockiana*), petunia (*Petunia ×hybrida*), and snapdragon (*Antirrhinum majus*), inclusion of far-red light under sole-source lighting increased leaf area and canopy size, thus light capture, and resulted in faster growth and greater biomass (Li and Kubota,

2009; Kubota et al., 2011; Park and Runkle, 2017; Craver et al., 2018; Hernandez and Spalholz, 2019; Meng and Runkle, 2019; Zou et al., 2019; Legendre and van Iersel, 2021). In the case of lettuce, for example, replacing 50 $\mu mol \cdot m^{-2} \cdot s^{-1}$ of white or red/blue light with far-red light increased dry weight by 31% and 29% at the same extended PAR (ePAR, photons from 400 – 750 nm) at 350 $\mu mol \cdot m^{-2} \cdot s^{-1}$ (Zhen and Bugbee, 2020b). Far-red-photon inclusion benefited crop growth under sole-source lighting, but not in a greenhouse (Kubota et al., 2011). It is likely that sunlight contains enough far-red to mask the effect of far-red photons provided by supplemental lighting in the greenhouse.

Other aspects of far-red photon inclusion, however, potentially reduce carbon assimilation. Lettuce plants grown under sole-source lighting with additional far-red light had lower SLW, lower chlorophyll and nitrogen concentrations per unit area, and consequentially lower leaf light absorptance (Zou et al., 2019). Leaves grown under supplemental far-red light also had lower efficiency at using absorbed photons for photosynthesis at *PPFD*s above 300 $\mu mol \cdot m^{-2} \cdot s^{-1}$ (Zou et al., 2019). The negative effects of far-red light supplementation on leaf light absorptance and quantum yield of photosynthesis did not negate the beneficial effect of far-red light on growth, as both shoot fresh and dry weight increased with supplemental far-red light (Zou et al., 2019).

Plant growth depends not only on canopy carbon assimilation, but also on how efficiently the carbohydrates are used to produce biomass. Carbon use efficiency (CUE) is the fraction of assimilated carbon that gets incorporated into in their biomass (Bugbee and Monje, 1992). CUE is fairly consistent (0.4-0.6 $mol \cdot mol^{-1}$) among plants (Gifford, 1994; Reich et al., 1998; Cannell and Thornley, 2000). In studies on wheat and lettuce grown in a controlled environment, the CUE of mature plants was about 0.6 $mol \cdot mol^{-1}$ (Monje and Bugbee, 1998; Frantz et al., 2004;

Zhen and Bugbee, 2020b). Varying the PPFD does not dramatically change the CUE, since the ratio between carbon assimilation and carbon export from leaves remains constant (Dewar et al., 1998). A previous study on the effect of far-red photon inclusion in CEA showed that CUE is unaffected by the far-red photon flux density (*PFD*) (Zhen and Bugbee, 2020b).

In addition to the effects of far-red photons on crop physiology and growth, there is an added benefit to including far-red in the light of LED fixtures for sole-source lighting: far-red LEDs have higher efficacy (μmol photon output per joule energy consumed) than blue, red, and white LEDs (Kusuma et al., 2020). Thus, replacing LEDs that provide PAR with far-red LEDs can reduce power consumption, without decreasing the overall photon flux. Unfortunately, the efficacy of LED grow lights typically is calculated as PAR photons/energy use, which discourages the use of far-red LEDs in grow light (Engineers, 2017; Zhen et al., 2021).

Although numerous studies have shown the benefit of far-red photon inclusion for indoor production, there is little information on the effects on whole-plant photosynthesis, respiration, and carbon use efficiency. Specifically, there is a lack of studies that quantify and distinguish the contributions from the Emerson enhancement effect versus increased leaf elongation and light capture on the growth and yield resulting from far-red photon inclusion. A previous study quantified the long-term effects of far-red substitution on light capture and whole-plant photosynthesis of lettuce (Zhen and Bugbee, 2020b). They reported higher biomass of lettuce grown under 300 $\mu mol \cdot m^{-2} \cdot s^{-1}$ PAR photons with 50 $\mu mol \cdot m^{-2} \cdot s^{-1}$ far-red photons than lettuce grown under 350 $\mu mol \cdot m^{-2} \cdot s^{-1}$ PAR photons, despite lower chlorophyll concentration and leaf level

absorptance (Zhen and Bugbee, 2020b). Also, at whole plant level, lettuce grown with far-red photon substitution had similar quantum yield of photosynthesis as lettuce plants grown PAR only (Zhen and Bugbee, 2020b). In that study, the photon flux density across the entire PAR range was decreased when substituting PAR with far-red photons. Effects of substituting photons in the PAR range with far-red on plant morphology are likely greater when only red photons are replaced with PAR-red photons, because of the importance of the red:far-red ratio on phytochrome activity (Sager et al., 1988). We thus quantified the effects of substituting 0 to 51 $\mu mol \cdot m^{-2} \cdot s^{-1}$ red photons with far-red photons on light capture and canopy photosynthesis of lettuce.

Materials and Methods

Plant material

Lettuce ('Little Gem') seeds were sown in 10 cm^2 square pots filled with a peat-based soilless substrate (Fafard 4P, SunGro Horticulture, Agawam, MA). Eighteen pots of lettuce were placed in a 30.5 cm × 61 cm tray. Seeds were then germinated in growth chambers (E15, Conviron, Winnipeg, Canada) under a 16-h photoperiod with a *PPFD* of 236 $\mu mol \cdot m^{-2} \cdot s^{-1}$ from warm-white fluorescent light. Temperature for germination was 23.9 ± 1.1 °C (mean ± standard deviation) and vapor pressure deficit was 0.56 ± 0.14 kPa. CO_2 concentration was maintained at 816 ± 15 $\mu mol \cdot mol^{-1}$. The pots were top-watered with tap water to keep them moist. Seedlings were thinned to one per pot after emergence. Seedlings were selected for uniformity six days after sowing for the 1st run and eight days after sowing for the 2nd run. A total of 144 plants per run were selected and randomly distributed to eight trays with a capillary mat in the bottom. These eight trays of 18 lettuce seedlings were then transferred into a whole-plant gas exchange

system, where they were exposed to different light treatments and whole canopy gas exchange measurements were taken.

The whole-plant gas exchange system consists of ten acrylic gas exchange chambers, eight of which held one tray (18 plants). Those eight gas exchange chambers were placed inside two growth chambers (E15, Conviron, Winnipeg, Manitoba, Canada), with four gas exchange chambers inside each growth chamber. The other two chambers were left empty outside of the growth chambers as controls. The growth chambers were set at 10 °C to remove the heat generated by the LED lights and condense water inside the gas exchange chambers to reduce the VPD. Temperature and relative humidity probes (HMP50, Campbell Scientific, Logan, UT) measured temperature and relative humidity inside each gas exchange chamber. Temperature and relative humidity were recorded by a datalogger (CR10T, Campbell Scientific) every 15 min. Each gas exchange chamber was equipped with a heater which maintained the temperature of each chamber to a setpoint based on the temperature reading of probe. A secondary temperature sensor (type T thermocouple) also measured temperature of each chamber as a secondary temperature reading. The secondary temperature was recorded by a different datalogger (CR23X, Campbell Scientific) every 10 min. Air blowing into the gas exchange chambers was enriched with CO_2 up to ~ 800 $\mu mol \cdot mol^{-1}$. Plants were sub-irrigated when needed with fertilizer solution of 100 $mg \cdot L^{-1}N$ made with a water-soluble fertilizer (Peters Excel 15-5-15 Cal-Mag, Everris, Marysville, OH). For more details about the gas exchange system, see (van Iersel and Bugbee, 2000).

Light treatments

We substituted different amounts of red photons with far-red photons to test the effect of red versus far-red light. PAR was provided by commercial LED grow lights (Pro 650, LumiGrow, Emeryville, CA). Far-red photons were provided by custom-made LED bars (peak @ 738 nm, full width at half maximum: 20 nm). All plants were grown under a 16-h photoperiod with an ePAR of 205 ± 2 (mean ± standard deviation) $\mu mol \cdot m^{-2} \cdot s^{-1}$ for the 1st run and 208 ± 1 $\mu mol \cdot m^{-2} \cdot s^{-1}$ for the 2nd run. The background light consisted of ~150 $\mu mol \cdot m^{-2} \cdot s^{-1}$ of white and blue light from LEDs, to which 51 $\mu mol \cdot m^{-2} \cdot s^{-1}$ of red and far-red photons were added (0/51, 17/34/ 34/17, and 51/0 $\mu mol \cdot m^{-2} \cdot s^{-1}$ of red/ far-red photons) to create four light treatments with different R:FR ratios. The detailed spectral distributions can be found in Table S4.1. The four light treatments with different R:FR ratio will be referred to by the far-red light portion relative to ePAR (%FR) since it was shown to be a better metric than phytochrome photo-equilibrium or R:FR ratio (Kusuma and Bugbee, 2021). Hereafter, the four light treatments will be called 2.5%, 9.2%, 16.5% and 23.6% FR in the 1st run and 3.2%, 11.0%, 19,0% and 27.4% FR in the 2nd run.

A randomized complete block design was used, with the four light treatments randomly assigned to the four gas exchange chambers within each growth chamber. All plants within each gas exchange chamber were exposed to the same light treatment and treated as one experimental unit.

Data collection and statistical analyses:

Photosynthetic measurements

The whole-plant gas exchange system took 10 min in the 1st run and 20 min in the 2nd run to complete one round of gas exchange measurements of all ten chambers. Chamber level net photosynthetic rate (crop P_n, $\mu mol \cdot s^{-1}$) of lettuce plants in each gas exchange chamber was recorded by a datalogger. The average daily P_n, dark respiration (crop R_d, $\mu mol \cdot s^{-1}$), and gross

photosynthetic rate (crop P_g, μmol·s^{-1}) were calculated for each chamber. Crop P_g was calculated as $P_g = P_n + |R_d|$, assuming respiration is the same in the dark and in the light (van Iersel and Bugbee, 2000). We also calculated average daily plant level P_g, P_n, and R_d (μmol·s^{-1}·plant^{-1}) by dividing the crop P_g, P_n, and R_d by number of plants in the gas exchange chambers on each day.

Daily carbon gain per plant (DCG, mol·d^{-1}·plant^{-1}), the net amount of carbon gained, and a measure of growth rate, was calculated as:

$$DCG = (P_n \times 16\ h \times 3600\ s \cdot h^{-1} - |R_d| \times 8\ h \times 3600\ s \cdot h^{-1}) \times 10^{-6}\ mol \cdot \mu mol^{-1}$$

Carbon use efficiency (mol·mol^{-1}) of each group of plants was calculated as:

$$CUE = DCG / (Pg \times 16\ h \times 3600\ s \cdot h^{-1}) \times 10^{-6}\ mol \cdot \mu mol^{-1}$$

The cumulative carbon gain per plant (CCG, mol·plant^{-1}) was calculated as the integral of DCG over time. To test the reliability of our whole-plant gas exchange system, the total CCG was calculated for each run integrating the CCG of all plants in the system throughout the life cycle of plants. We also calculated total dry weight of each run by adding together the shoot dry weight of plants in all harvests. To further quality the photosynthetic activity of far-red photons, at 21 and 29 DAT of the 1st tun and at 9 and 32 DAT of the 2nd run, we briefly turned off the far-red lights and measured the change in photosynthesis in response to the absence of far-red photons. At 32 DAT of the 2nd run, near the end of this study (the last harvest was at 33 DAT), we also turned off the red lights and measured the changes in photosynthesis in response to both red and far-red photons.

Morphology and growth

We took top view canopy images of the plants to quantify projected canopy size (PCS) and estimate canopy light interception. In the 1st run, we photographed the whole tray of lettuce plants *in situ* with a cellphone camera. The images were taken twice a week until the canopies were too large to be captured within the camera's field of view, 20 d after the plants were moved into the whole-plant gas exchange system. The PCS was quantified with Image J (National Institutes of Health, Bethesda, Maryland) by extracting the area of green pixels in the photos. In the 2nd run, the whole tray was imaged by our custom-made chlorophyll fluorescent imaging (CFI) system, similar to that described by Kim and van Iersel (2022). The plants were imaged twice a week throughout the whole growing cycle. Photos from the CFI system was analyzed by a Python program following similar principle as Kim and van Iersel (2022).

In the 1st run, we harvested nine plants at 22 days after light treatment started (DAT) when the canopy was closed. The remaining nine plants were harvested 35 DAT when the canopy was closed again. Plant density was 97 plant·m^{-2} before and 48 plant·m^{-2} after the 1st harvest. In the 2nd run, we harvested nine plants at 12 DAT, five plants at 18 DAT, and the remaining four plants at 33 DAT. We harvested more frequently during the 2nd run to minimize leaf overlap and light competition among plants. Plant density was 97 plant·m^{-2} before the 1st harvest, 48 plant·m^{-2} before the 2nd harvest and 22 plant·m^{-2} before the 3rd harvest. The total leaf area, length of the longest leaf, and dry weight of the harvested plants were measured, and SLW was calculated as leaf dry weight divided by leaf area.

We also measured leaf-level light absorptance at each harvest, except for the 1st harvest of the 2nd run when the plants were too small. Light absorptance was measured similarly to the

method described by Zhen et al. (2019). Three newly expanded leaves were selected from each chamber for light absorptance measurement. Light spectrums were measured by a spectroradiometer (PS-100, Apogee Instruments, Logan, UT). A LED light with multiple LEDs with different spectrums (GN-DMX512-D LED System, EyeHortilux, Mentor, Ohio) was used to provide light ranging from 400 to 770 nm. To measure light transmittance, the light spectrum of the LED light was first measured inside a dark room with the spectroradiometer directly under the LED light. Then, a lettuce leaf was placed between the LED light and the spectroradiometer, with the adaxial side facing up, to measure the transmitted light spectrum under the leaves. Light transmittance of the leaves was then calculated at 1 nm resolution as the transmitted spectrum divided by LED light spectrum. Light reflectance of leaves was measured using a fiber-optic cable facing perpendicular to the adaxial surface of lettuce leaves under the LED light. The reflectance spectrum was then divided by reflectance spectrum of a Halon white standard (AS-004, Apogee Instruments) to calculate the leaf reflectance. Leaf absorptance was calculated as 100% - reflectance - transmittance. The average absorptance spectrum of the three leaves from the same chamber was used for later analyses. The amount of ePAR photons absorbed leaves was calculated by multiplying the light spectrum of the grow light with the absorptance spectrum of the respective leaf.

Data analysis

The effect of the % FR in the growing spectrum on various parameters was tested in Excel (Microsoft, Seattle, WA) with regression analysis, with chamber temperature as a covariate since temperature varied among different chambers. Linear regression was conducted between total CCG of each run and total shoot dry weight in Excel as well. We

also tested the correlation between length the longest leaf and projected canopy size, light absorptance and SLW, and the correlation between P_g and PCS, amount of ePAR photons absorbed by leaves, and %FR. The multiple regression was carried out by JMP Pro 15 (SAS Institute, Cary, NC). The total PCS and the amount of the ePAR photons absorbed by leaves between the two runs were compared using a paired t-test in Excel.

Results and discussions

1. Far-red light-induced leaf expansion and hyponasty, increasing projected canopy size

Morphological changes in lettuce plants induced by far-red light were visible early on. In the first run, at 10 DAT, a greater %FR increased seedling height (Fig. S4.1A). In the second run, the effect of %FR was already visible at 7 DAT (Fig. S4.1B). The length of the longest leaf increased linearly with %FR in all harvests (Fig. 4.1). During the 1st run, we observed a 0.15 and 0.11 cm increase in longest leaf length for the 1st and 2nd harvest, respectively, with each 1% increase in %FR (Fig. 4.1A). The increase of the longest leaf length was more substantial in the 2nd run. With every 1% increase in %FR, the longest leaf length increased 0.15 cm for the 1st harvest and 0.20 cm for the 2nd harvest (Fig. 4.1B). The increase in plant height is likely a result of both an increase in leaf length and a change in leaf angle. Far-red light stimulates upward growth of leaves to form a steeper leaf angle, known as hyponasty. Our observations of taller plants and longer leaves align with the typical symptoms of a shade avoidance response (Gommers et al., 2013; Ruberti et al., 2012).

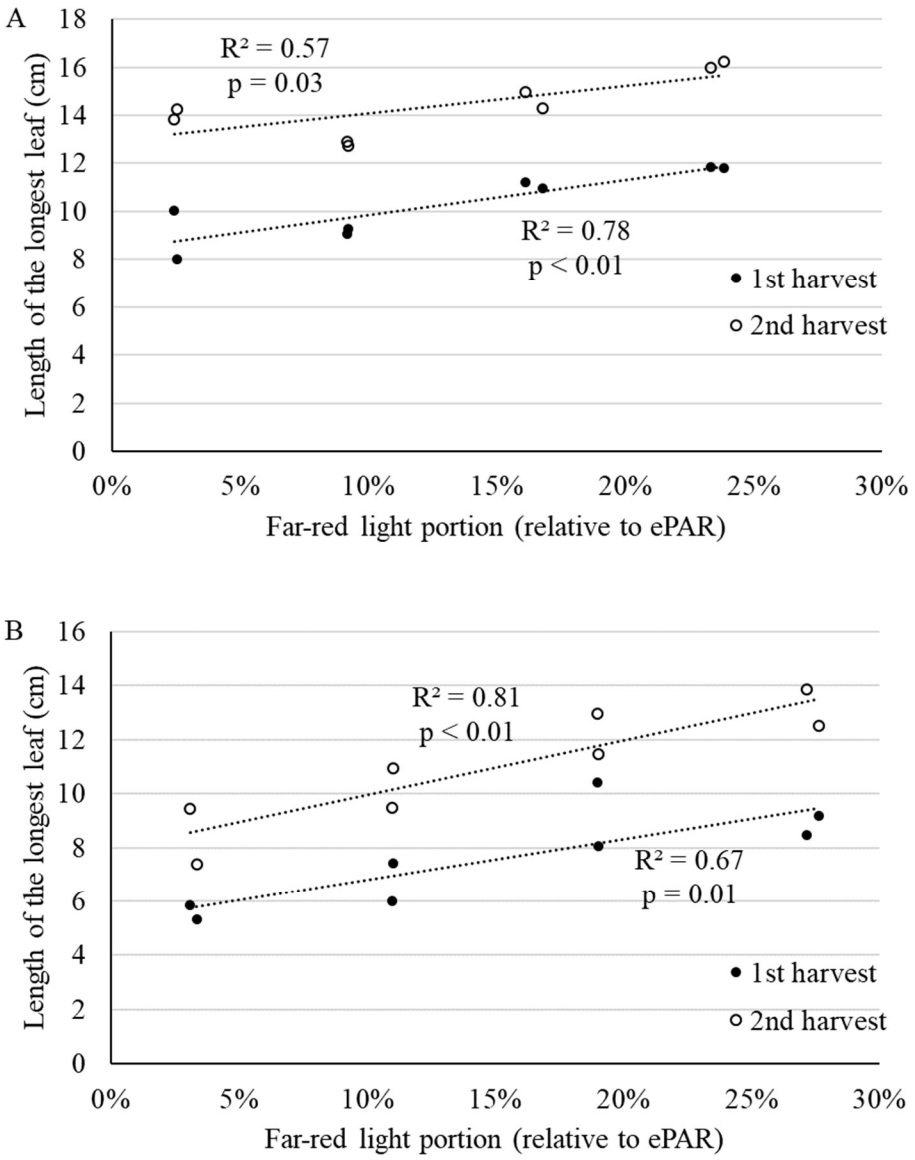

Figure 4.1. The length of the longest leaf of lettuce plants increased linearly with the %FR in the grow light spectrum at the 1st (22 DAT) and the 2nd (35 DAT) for the 1st run (A) and at the 1st (12 DAT) and the 2nd harvest (18 DAT) for the 2nd run (B).

The PCS during the 1st run was not increased by increasing %FR until 20 DAT (Fig. 4.2A), which was the last date that PCS was measured. With the %FR increasing from 2.5% to 23.6%, PCS increased from 137 to 164 $cm^2 \cdot plant^{-1}$ (20%) (Fig. 4.2A and

Fig. S4.2). For the 2nd run, PCS increased with increasing %FR starting from 18 DAT until the end of the study at 32 DAT (21 DAT in Fig. 4.2B and Fig. S4.2). In the 2nd run at 21 DAT, the increase in PCS was much greater (from 147 to 238 $cm^2 \cdot plant^{-1}$ or 61.6%) compared to the 1st run, despite similar %FR (from 3.2% to 27.4%) (Fig. 4.2B).

Previous studies showed that inclusion of far-red photons can induce leaf expansion and thus canopy enlargement. The canopy enlargement results in greater light interception by the crop, and higher biomass accumulation under sole-source lighting (Li and Kubota, 2009; Kubota et al., 2011; Park and Runkle, 2017; Craver et al., 2018; Hernandez and Spalholz, 2019; Meng and Runkle, 2019; Zou et al., 2019; Zhen and Bugbee, 2020a; b; Jin et al., 2021; Legendre and van Iersel, 2021). In our study, we similarly noted increased leaf expansion in response to %FR, as is evident from the greater length of the longest leaf (Fig. S4.2) and increased plant height (Fig. S4.1), although the effect on leaf expansion was greater in the 2nd run than in the 1st run (Fig. S4.2). The effect of the %FR on canopy enlargement also was more evident in the 2nd run (Fig. 4.2). We found a strong correlation between the PCS and the longest leaf length for both runs, which suggests that the treatment effects on canopy enlargement were a consequence of effects on leaf expansion. In the 1st run, with a 1 cm increase in the longest leaf length at 22 DAT, PCS at 20 DAT increased 3.7 $cm^2 \cdot plant^{-1}$ ($R^2 = 0.81$, $p < 0.01$). In the 2nd run, the PCS at 21 DAT also strongly correlated with the longest leaf length at the nearest harvest (18 DAT) ($R^2 = 0.78$, $p < 0.01$). Each centimeter increase in longest leaf length at 18 DAT was associated with an 18.8 $cm^2 \cdot plant^{-1}$ increase in PCS at 21 DAT, much higher than that in the 1st run. Our data showed that substitution of red photons with far-red photons resulted in increased leaf expansion and canopy size. The effect of far-red PFD on leaf length and canopy size was greater in the 2nd than in the 1st run.

The smaller effect of far-red substitution on leaf length and canopy enlargement in the 1st run than in the 2nd run may be related to plant density. Previous studies have found that high planting density can reduce the effect of far-red photons on crop growth and yield (Shibuya et al., 2020; Jin et al., 2021). At 20 DAT during the 1st run, we had not harvested any plants, so the plant density was 97 plant·m^{-2}. For the 2nd run, at 21 DAT, the lettuce plants had already gone through two rounds of harvesting (at 12 DAT and 18 DAT) and the plant density was reduced to 21.5 plant·m^{-2}. At high plant density, the canopy closes faster and there is limited benefit to making larger leaves with far-red photon substitution (Shibuya et al., 2020; Jin et al., 2021), since increased canopy size increases interplant competition for light. The effectiveness of far-red photon substitution on leaf expansion and canopy enlargement may be higher when plants do not receive any additional signal that also indicates shaded conditions (Shibuya et al., 2020; Jin et al., 2021). It is possible that, in our study, the difference in planting density, caused by different harvest times, between the two runs resulted in a greater effect of far-red photon substitution on leaf length and PCS in the 2nd run (Fig. 4.2).

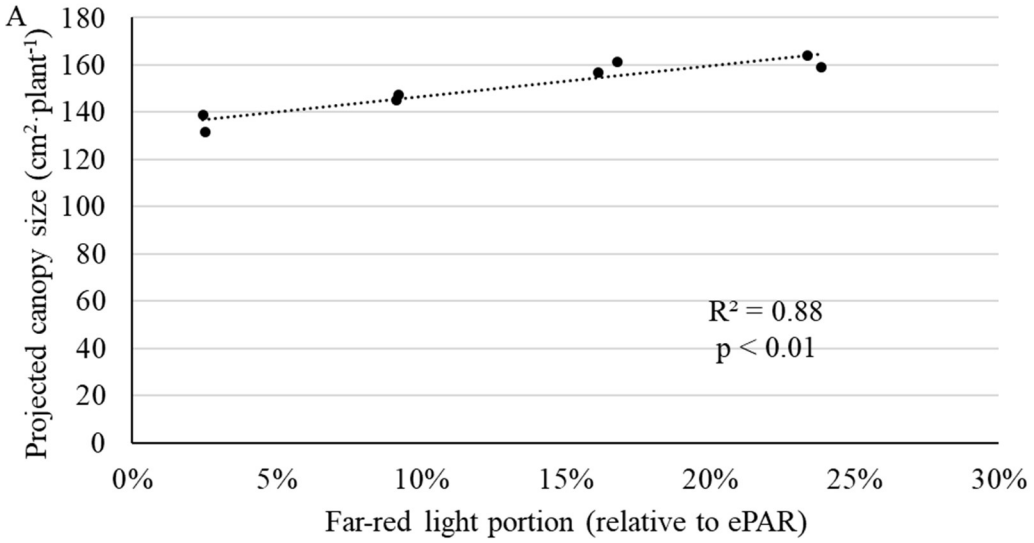

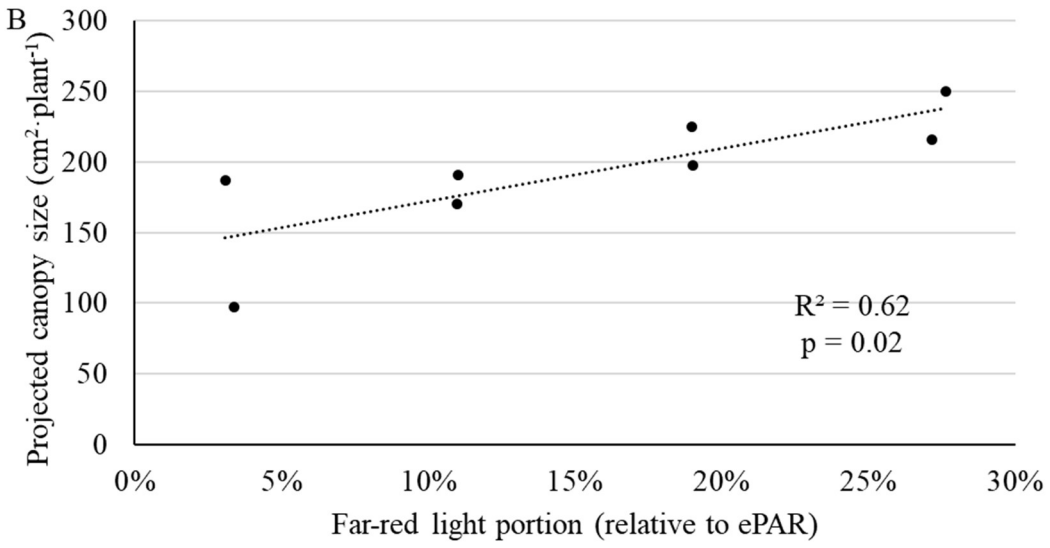

Figure 4.2. Projected canopy size increased with %FR in the grow light spectrum at 20 DAT for the 1st run (A) and at 21 DAT for the 2nd run (B).

2. Photosynthetic rate was affected by far-red PFD through effects on canopy enlargement and leaf absorptance

Crop gross photosynthetic rates did not consistently respond to %FR between the two runs (Fig. 4.3 and Fig. 4.4). In the 1st run, P_g decreased with increasing %FR at 7-10, 13-16 and 19-21 DAT. The negative effect of far-red photon substitution on P_g disappeared after the 1st harvest at 22 DAT. Nevertheless, in the 2nd run, P_g increased with %FR in ePAR from 21 to 25 DAT (Fig. 4.4). In the 1st run at 20 DAT, for example, when %FR increased from 2.5% to 23.6%, crop P_g decreased by 26.2% (Fig. 4.3A). In the 2nd run at 21 DAT, crop P_g increased linearly with %FR by 31.5% when %FR increased from 3.2% to 27.4% (Fig. 4.3B). In the 1st run, P_g significantly decreased with increasing %FR before the 1st harvest; that effect diminished after the 1st harvest (Fig. 4.4A and 4.4C). But for the 2nd run, the increased in P_g by far-red photon substitution was seen only from 21 to 25 DAT, after the 2nd harvest (Fig. 4.4B and 4.4D).

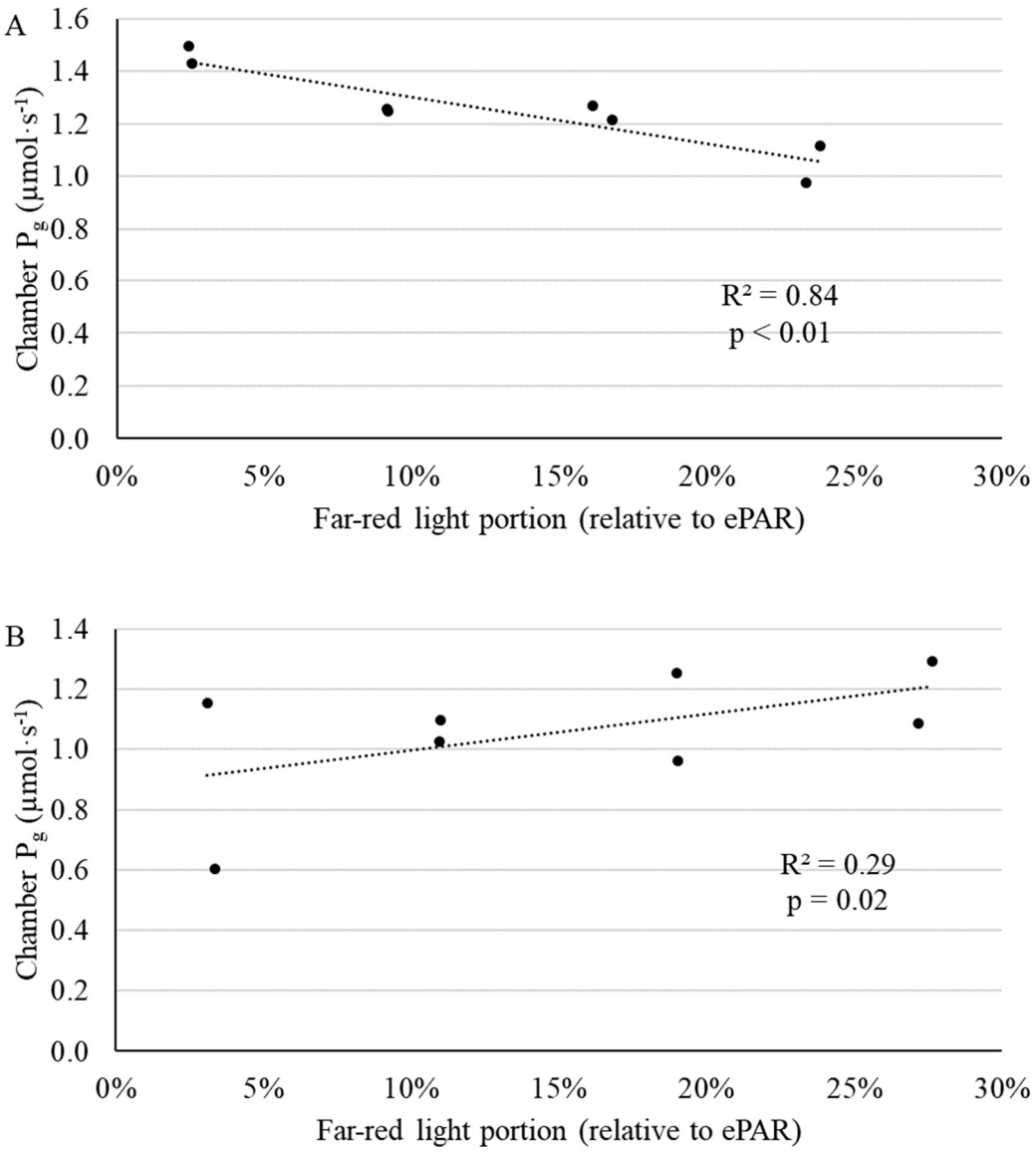

Figure 4.3. Crop P_g responded to the %FR differently in the two runs. At 20 DAT in the 1st run, two days before the 1st harvest, crop P_g decreased with increasing %FR (A), whereas at 21 DAT in the 2nd run, crop P_g increased with increasing %FR (B).

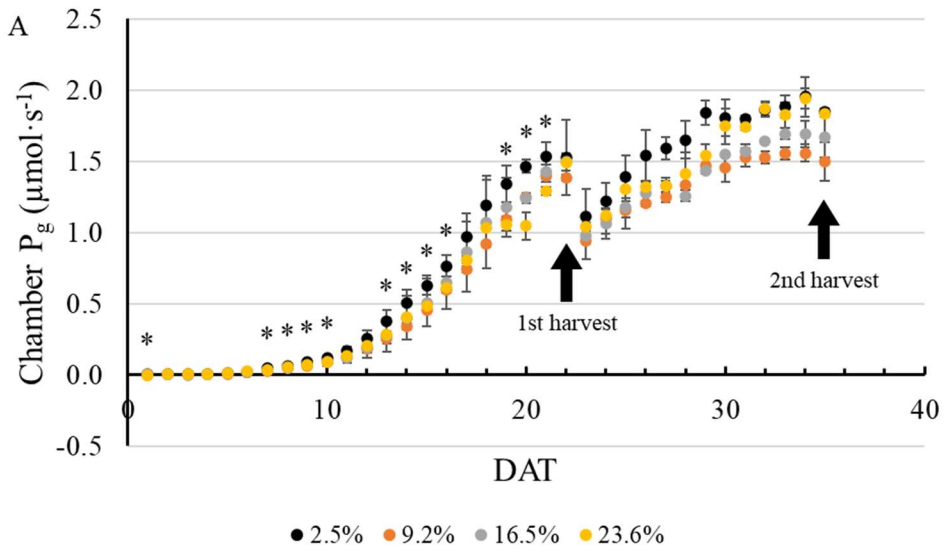
A
Chamber P_g (μmol·s^{-1})
2.5
2.0
1.5
1.0
0.5
0.0
-0.5
0
10
20
30
40
DAT
1st harvest
2nd harvest
2.5%
9.2%
16.5%
23.6%

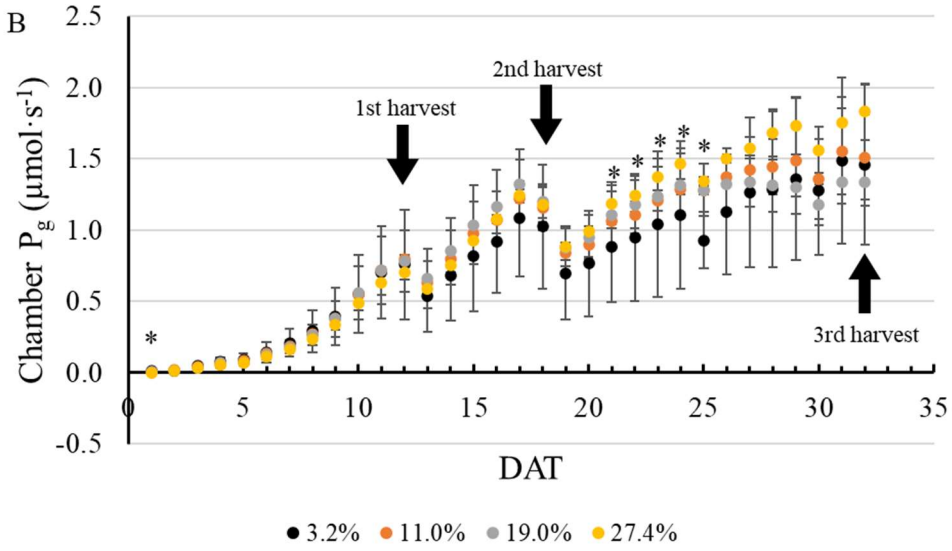
B
Chamber P_g (μmol·s^{-1})
2.5
2.0
1.5
1.0
0.5
0.0
-0.5
0
5
10
15
20
25
30
35
DAT
1st harvest
2nd harvest
3rd harvest
3.2%
11.0%
19.0%
27.4%

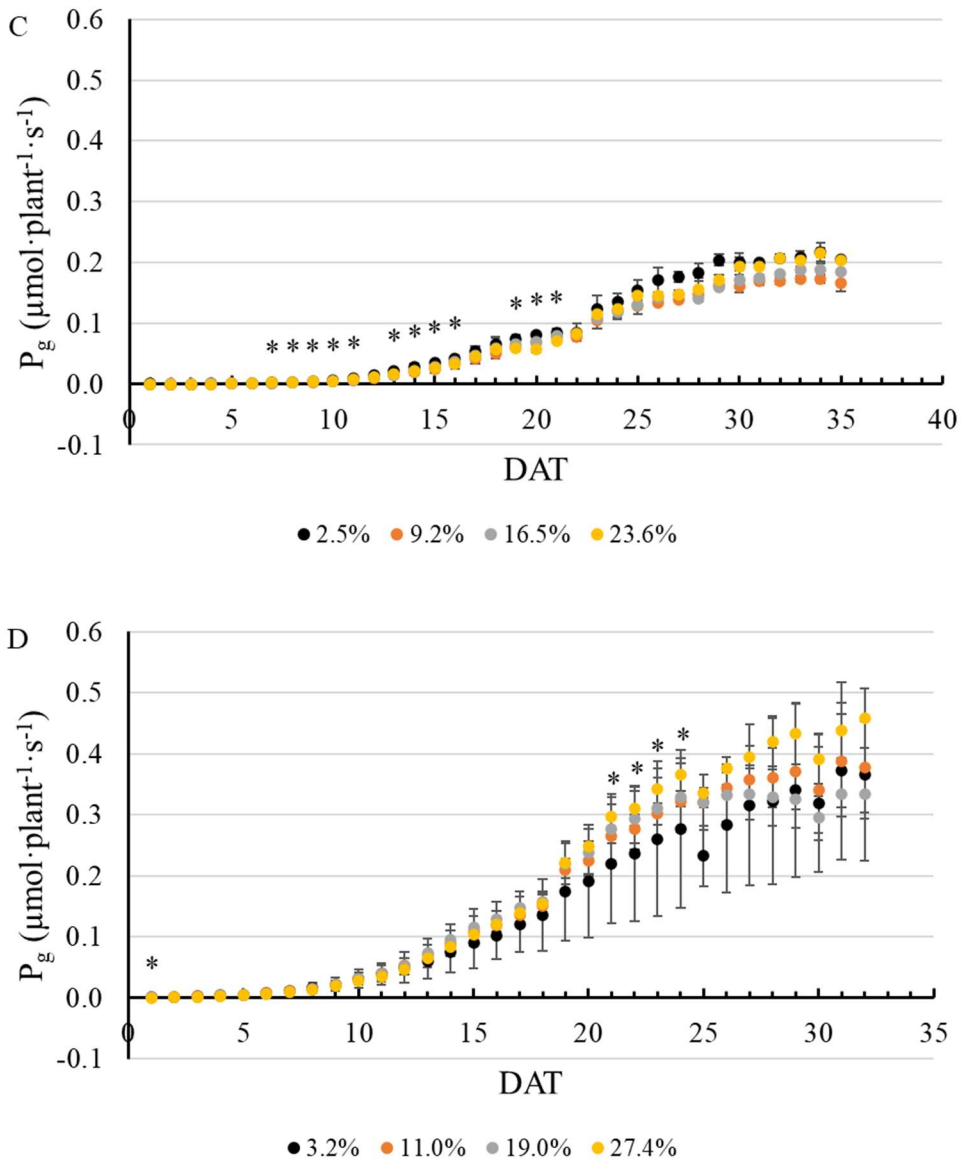

Figure 4.4. Crop P_g (A and B) and plant P_g (C and D) throughout the experiment for the 1st run (A and C) and the 2nd run (B and D). On days marked with a *, P_g was correlated with %FR (α = 0.05). In the 1st run, P_g decreased with increasing portion of far-red photons on days with a significant effect (A and C). In the 2nd run, increasing far-red PFD increased P_g, except for day 1, on which P_g decreased with increasing PFD (B and D).

The leaf level light absorptance of lettuce decreased with %FR only in the 1st harvest of the 1st run (Fig. 4.5 and Fig. S4.3). At this time, the decrease in leaf-level absorptance was not observed in the blue waveband (400 - 499 nm), while the light absorptance across the green (500 – 599 nm), red (600 – 699 nm), far-red (700 – 750 nm) and ePAR wavebands (400 – 750 nm) all decreased with increasing %FR (Fig. 4.5A and Fig. S4.3A). The difference in light absorptance of leaves in response to %FR was not observed in the 2nd harvest of the 1st run or in the two harvests of the 2nd run (Fig. 4.5B, C and D and Fig. S4.3B, C and D). Despite the inconsistent effect of far-red photon substitution on leaf-level light absorptance, lettuce leaves grown under higher %FR absorbed less ePAR photons, since red photons were substituted with more poorly-absorbed far-red photons.

We did not find any effect of far-red photon substitution on chlorophyll a and b concentration, total chlorophyll concentration, and chlorophyll a to b ratio in the 1st harvest of the 1st run (Fig. S4.5). The response of SLW to increasing %FR was strongest in younger plants and decreased with increasing %FR at the 1st harvest of the 1st run, and the first two harvests of the 2nd run (Fig. 4.6). For the last harvest of both runs, %FR no longer affected SLW (Fig. 4.6). Comparing the first two harvests of the 2nd run, the decrease in SLW was more significant at the 1st (0.36 $g \cdot m^{-2}$ decrease in SLW per 1% increase in %FR) than the 2nd harvest (0.25 $g \cdot m^{-2}$ decrease in SLW per 1% increase in %FR) (Fig. 4.6).

The leaf absorptance across the ePAR waveband at the 1st harvest of the 1st run was positively correlated with SLW ($r = 0.78$, $p = 0.02$). At the 2nd harvest of the 2nd run, SLW was similarly correlated with leaf absorptance across the ePAR region ($r = 0.70$, $p = 0.05$). However, for the last harvest of both runs, when far-red PFD no longer affected absorptance, SLW and absorptance were not correlated ($p \geq 0.50$).

Far-red photon substitution resulted in inconsistent effects on crop P_g in the two runs, owing to combined morphological and physiological changes induced by far-red photon substitution. In the 1st run, P_g was negatively correlated with %FR before the 1st harvest (Fig. 4.3 and Fig. 4.4), despite higher PCS at 20 DAT (Fig. 4.2). Multiple regression detected no correlation between crop P_g, PCS at 20 DAT, and the amount of ePAR photons absorbed by leaves. The increase in PCS and decrease in the amount of ePAR photons absorbed by leaves in response to %FR may have offset each other (PCS increased 19.7% while ePAR photons absorbed by leaves decreased 20.9% when %FR increased from 2.5% to 23.6%), possibly resulting in a similar amount of canopy light capture under different far-red PFD treatments. The lower P_g in response to higher %FR observed at 20 DAT in the 1st run may have been caused by lower leaf-level quantum yield of photosynthesis, which was previously observed in lettuce in response to far-red supplementation (Zou et al., 2019). That study found that lettuce leaves grown under supplemental far-red photons had a lower leaf level quantum yield of photosynthesis based on absorbed photons. Therefore, they had a lower net photosynthetic rate than leaves grown without supplemental far-red photons when absorbing the same amount of PAR (Zou et al., 2019).

In the 2nd run, %FR increased crop P_g from 21 to 25 DAT, contrary to the results from the 1st run (Fig. 4.3 and Fig. 4.4). Multiple regression indicated that crop P_g at 21 DAT was positively correlated with both PCS at 21 DAT ($p < 0.01$) and ePAR photons absorbed by leaves ($p < 0.01$). The positive correlation of PCS to crop P_g is consistent with the hypothesis that higher %FR promotes canopy enlargement, increases photon capture, and thus crop P_g. The positive correlation between crop P_g at 21 DAT and ePAR

photons absorbed by leaves (amount of ePAR photon absorbed by leaves under different %FR can be seen in Fig. S4.4) indicated that a lower amount of ePAR photons absorbed by leaves grown under higher %FR decreased the benefit of increased PCS on light capture and photosynthesis. But the lower amount of ePAR photons absorbed by leaves with %FR did not offset the higher light interception elicited by higher PCS, since P_g still increased with increasing %FR on this date (Fig. 4.3B and Fig. 4.4B): The PCS at 21 DAT increased 61.6% when %FR increased from 3.2% to 27.4% (see Fig. 4.2); while the amount of ePAR photons absorbed by leaves decreased by only 16.6% (see Fig. S4.4).

At 32 DAT in the 2nd run, when crop P_g no longer increased with increasing %FR, multiple regression showed that crop P_g was negatively correlated with %FR ($p = 0.01$), but positively correlated with PCS ($p < 0.01$). At this time, crop P_g no longer correlated with ePAR photons absorbed by leaves. The negative correlation between crop P_g and %FR suggest a lower quantum yield of photosynthesis to used absorbed photons of leaves grown under high %FR, similar to what was observed by Zou et al. (2019). This may explain why far-red photon substitution no longer increased crop P_g despite higher PCS. Also, at this stage, individual leaves grown under high %FR still absorbed fewer ePAR photons (Fig. S4.4). However, the plants had multiple leaf layers which may have diminished the difference in light capture induced by far-red photon substitution at the canopy level (Zhen and Bugbee, 2020b). Therefore, crop P_g was no longer correlated with the amount of ePAR photons absorbed by leaves.

In both runs, far-red photon substitution induced leaf expansion (Fig. 4.1), which increased PCS (Fig. 4.2 and Fig. S4.2). Far-red photon substitution also decreased ePAR photon absorbed by leaves in both runs (Fig. S4.4). Far-red photon substitution negatively affected crop P_g in the 1st run, but positively affected crop P_g in the 2nd run (Fig. 4.3 and Fig. 4.4). The

contradictory effects of far-red photon substitution on crop P_g between the two runs may be associated with differences in plant density. Between the two runs, plant density during the 2nd run after the 1st harvest (12 DAT) was lower than plant density at the same DAT during the 1st run. In the 1st run, since plant density, as well as light interception, was higher at 21 DAT than that at 20 DAT in the 2nd run, far-red photon substitution may have limited benefits on light interception through leaf expansion for the 1st run (19.7% increase in PCS when %FR increasing from 2.5% to 23.6% at 20 DAT in the 1st run vs 61.6% increase in PCS when %FR increased from 3.2% to 27.4% at 21 DAT in the 2nd run). The PCS of individual lettuce plants in the 1st run was consistently lower than the PCS of plants in the 2nd run at similar DAT (Fig. 4.2 and Fig. S4.2, note the difference in the scales of the y-axes). Crop P_g in the 1st run stopped increasing before the 1st harvest, but increased rapidly after the harvest reduced inter-plant competition (Fig. 4.4A). This validates the idea that, at high plant density, the effect of far-red photon substitution on light interception was limited. Also, the higher plant density during part of the 1st run created more intra-canopy shading than in the 2nd run (average total PCS was 1354 cm^2 at 20 DAT in the 1st run, which was larger than 767.1 cm^2 measured at 21 DAT in the 2nd run, $p < 0.01$), which induced a more dramatic reduction in ePAR photons absorbed by leaves and possibly lower quantum yield of photosynthesis of leaves to utilize absorbed photons. On average, leaves in the 1st run absorbed 4.7% fewer ePAR photons compared with leaves of a similar age under similar far-red PFD in the 2nd run (Fig. S4.4A, B, $p < 0.01$). Therefore, the higher plant density in the 1st run reduced the increase in PCS and magnified the reduction in light absorptance by %FR compared to the 2nd run. Consequentially, in the 1st run, the smaller increase in PCS failed to compensate for the

more dramatic decrease in leaf-level light absorptance and possibly lower quantum yield of photosynthesis of leaves at 20 DAT, which resulted in lower crop P_g with increased far-red photon substitution.

In short, P_g was positively correlated with PCS through the whole growing cycle, negatively correlated with the decreasing amount of absorbed ePAR photons, and possibly also negatively affected by other responses induced by far-red photon substitution, such as the lower quantum yield of photosynthesis of leaves based on absorbed photons, as previously observed in lettuce (Zou et al., 2019). But the effect of P_g was apparently dependent on planting density. In the 2nd run, with less inter-plant competition, P_g increased with increasing %FR from 21 to 25 DAT, while P_g decreased with increasing %FR during the 1st run before the 1st harvest at 22 DAT, when plant density and inter-plant competition for light were greater.

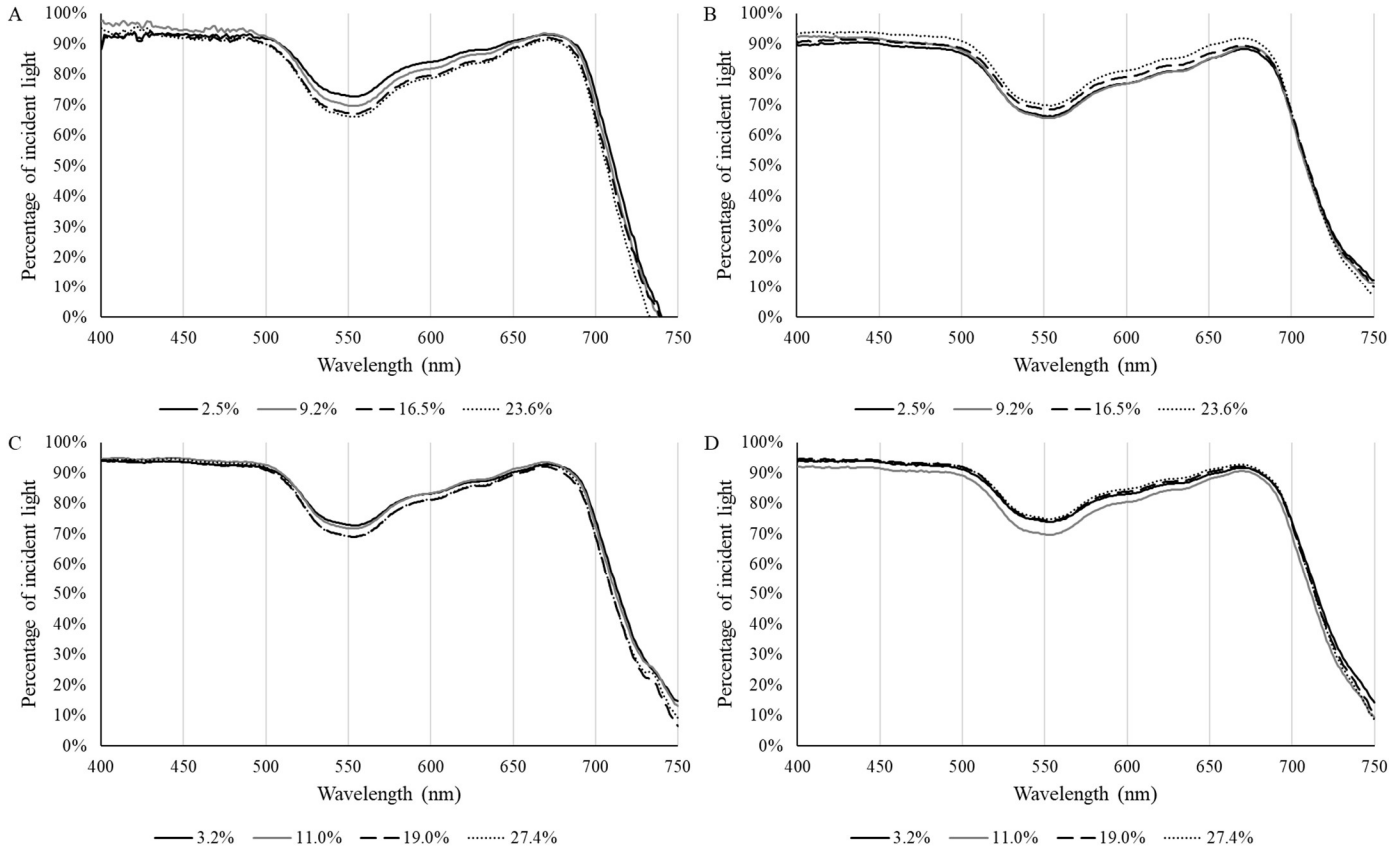

Figure 4.5. Leaf level light absorptance of lettuce plants grown with different %FR in the 1st harvest of the 1st run (A), 2nd harvest of the 1st run (B), 2nd harvest of the 2nd run (C) and 3rd harvest of the 2nd run (D). The %FR values are shown at the bottom of both graphs and with their corresponding line patterns.

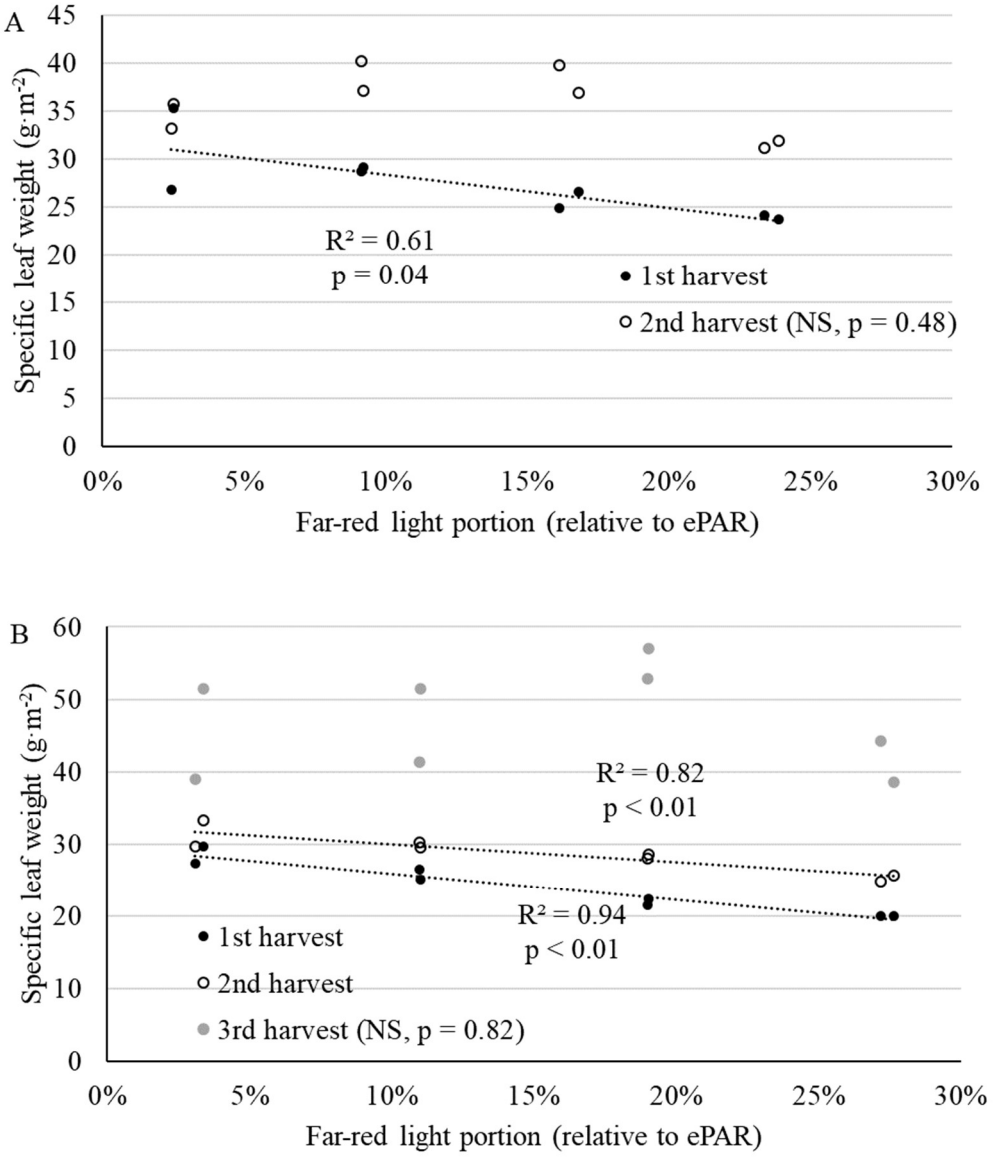

Figure 4.6. Specific leaf weight of lettuce decreased with increasing %FR at the 1st harvest of the 1st run (A) and the 1st and the 2nd harvest of the 2nd run (B), but not for the final harvest of both runs.

3. Far-red photons have lower photosynthetic activity than red photons

To quantify the photosynthetic activity of far-red photons at 21 DAT (Fig. S4.6) and 29 DAT of the 1st run and at 9 DAT and 32 DAT of the 2nd run, the far-red LEDs were turned off temporarily. At 32 DAT of the 2nd run, we also turned off the red LEDs to quantify the change in photosynthetic rate in response to red photons. P_g decreased when far-red LEDs were turned off and increased when they were turned back on, indicating that far-red photons had photosynthetic activity (Fig. S4.6). The change in P_g correlated with %FR (Fig. 4.7), with similar effects at 21 and 29 DAT in the 1st run. Similarly, the responses of P_g to far-red PFD being turned off were similar at 9 DAT and at 32 DAT in the 2nd run, so the data for different days within each run were pooled and analyzed together (Fig. 4.7). The slopes of the regression lines were 0.43 and 0.56 for the 1st and 2nd run, respectively. A slope of 1 would indicate that a 1% change in PFD decreases P_g by 1% and that the quantum yield of photosynthesis (moles of carbon assimilated per mole incident photons) of the light being turned off equaled the average quantum yield of all photons in the grow light spectrum. Thus, these data suggest that the photosynthetic efficacy of the far-red photons was approximately half of that of the average of all photons. At the end of the 2nd run, we also turned off the red LEDs, and P_g decreased by 0.98% for each 1% reduction in ePAR (Fig. 4.7C), suggesting that red photons had a quantum yield of photosynthesis close to the average of the entire spectrum. These results indicate that far-red photons had significant photosynthetic activity, but substantially lower than that of red photons.

The decrease in P_g in response to both red and far-red photon removal in our study was linear throughout the range of PFDs (0 – 51 $\mu mol \cdot m^{-2} \cdot s^{-1}$) (Fig. 4.7B); thus, it is likely that they were driving photosynthesis at their maximum quantum yield. The quantum yield of photosynthesis of red photons was 1.75 (0.98/0.56) times of that of far-red photon. The lower light absorptance of far-red photons may be responsible for the lower quantum yield of photosynthesis of far-red photons than of the red photons. The leaf level absorptance of red photons was 88.3 ± 3.3%, 1.97 times that of far-red photons (46.9 ± 3.0%) at the 3rd harvest of the 2nd run, although at the whole canopy level, the difference in absorptance between red and far-red photons would be smaller than at the leaf level. Another reason for the lower quantum yield of far-red photons is that only far-red photons absorbed by the light-harvesting complex surrounding PSI can be used for electron transport; far-red photons absorbed by the PSII light-harvesting complex cannot be used for photosynthesis.

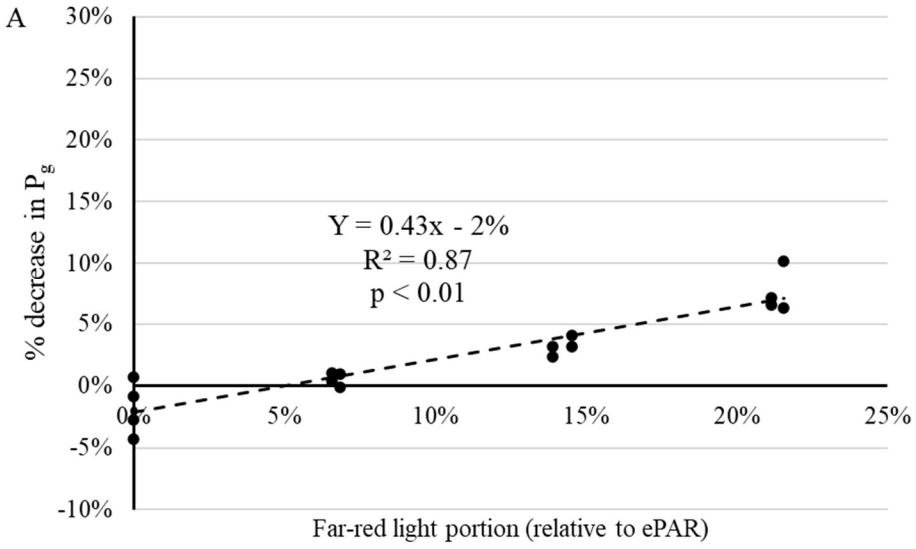

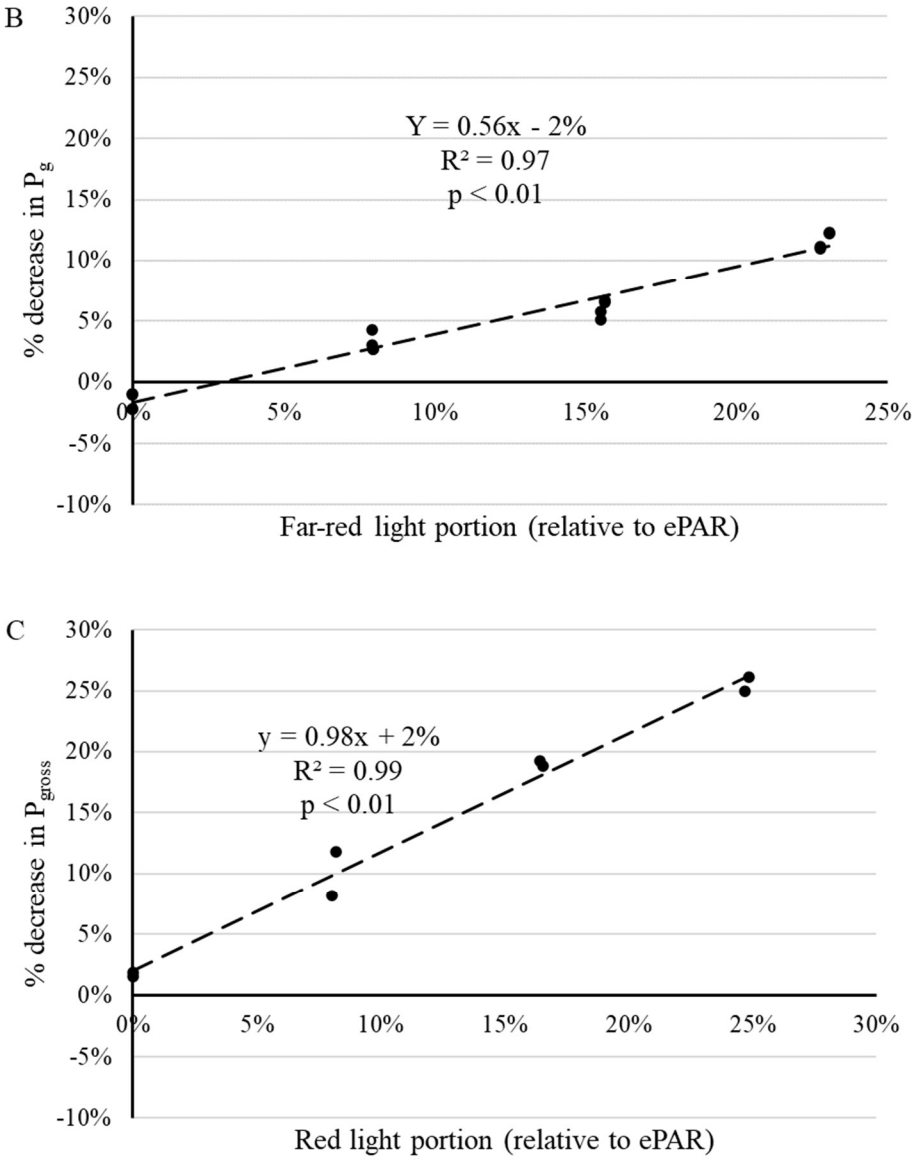

Figure 4.7. The relative decrease in P_g in response to far-red LEDs being turned off during the 1st run (A), and to far-red (B) and red LEDs (C) being turned off at the end of the 2nd run.

4. Far-red PFD did not affect carbon use efficiency

Not all carbon assimilated in photosynthesis is incorporated into biomass; some carbon is lost through respiration. The efficiency of converting assimilated carbon into biomass is referred to as carbon use efficiency (CUE). The CUE did not differ among treatments in either run (Fig.

4.8), despite differences in net photosynthetic rate (Fig. 4.3 and Fig. 4.4). A previous study also showed that far-red photon substitution failed to change the CUE of lettuce plants (Zhen and Bugbee, 2020b). CUE during both runs was low during the seedling stage and increased from 9 to 14 DAT as the plants grew. Low CUE during the seedling stage was previously recorded in marigold (*Tagetes patula*) seedlings (van Iersel, 2006), possibly as a result of the respiration of carbon reserves from seeds and low photosynthetic rate of seedlings. Similarly, in our study, CUE of lettuce reached a maximum around 15 DAT for the 1st run and 13 DAT for the 2nd run (21 days after sowing for both runs) (Fig. 4.7). CUE was relatively stable [0.67 ± 0.04 mol·mol^{-1} (average ± standard deviation) for the 1st run, and 0.65 ± 0.03 mol·mol^{-1} for the 2nd run] from 15 to 31 DAT during the 1st run and from 15 to 27 DAT during the 2nd run (Fig. 4.4), and similar to the 0.61 ± 0.02 measured by Zhen and Bugbee (2020b) and 0.62 measured by Frantz et al. (2004). Towards the end of the growing cycle, CUE slowly decreased.

Despite occasional differences in gross photosynthetic rate, no difference was detected in CUE of lettuce plants grew under different %FR (Fig. 4.8). Our finding that far-red photon substitution of red photons had no effect on CUE on lettuce aligns with the similar CUE of lettuce grown with or without far-red photon substitution observed by Zhen and Bugbee (2020b).

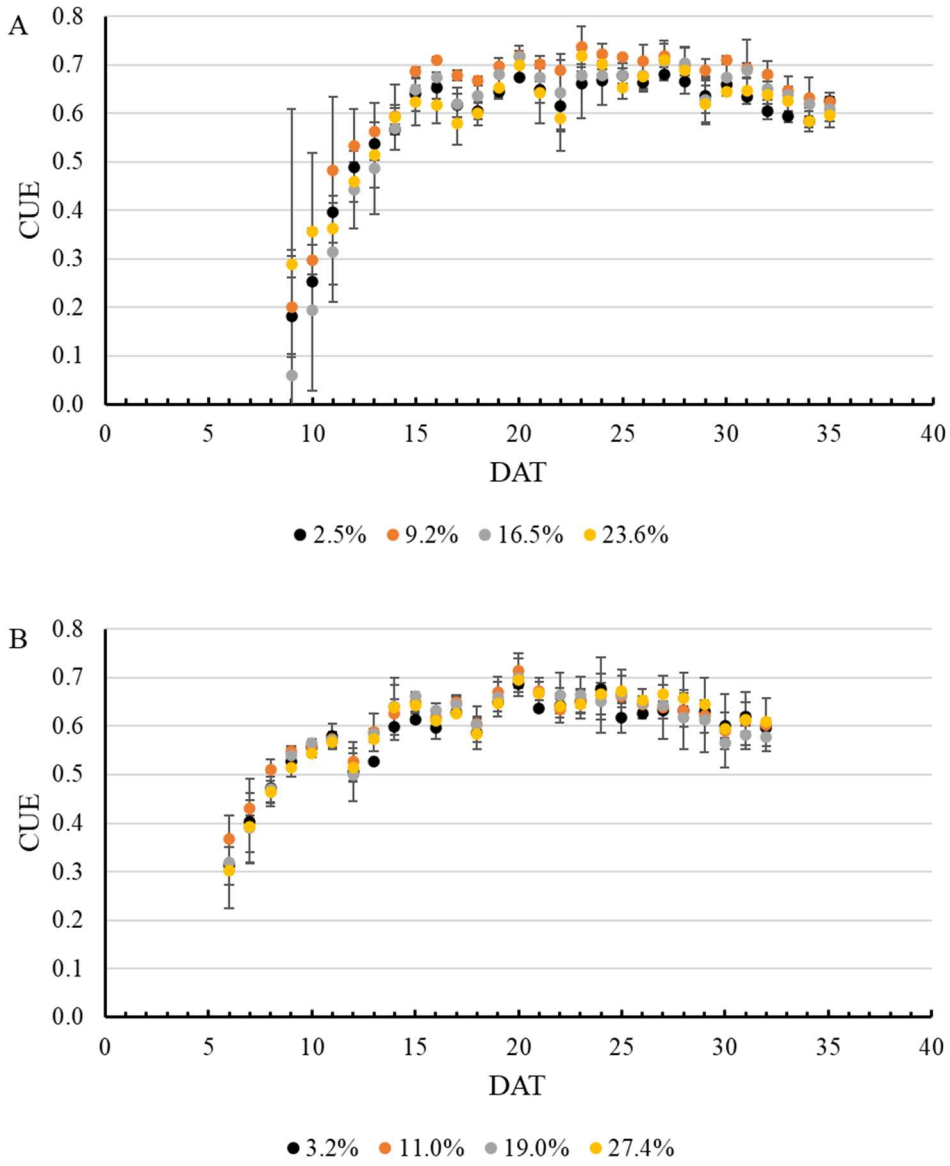

Figure 4.8. Lettuce CUE did not change in response to %FR during the 1st (A) and 2nd run (B). Error bars represent the standard deviation (n = 2). The %FR is shown at the bottom of both graphs.

5. Yield of lettuce was not affected by far-red PFD

The final dry weight of lettuce was not affected by %FR (Fig. 4.9). The CCG was closely correlated with total shoot dry weight, summed over all harvests, for both runs (Fig. 4.10) and was not affected by %FR ($p = 0.17$ for the 1st run and $p = 0.09$ for the 2nd run). Apparently, the

change in canopy carbon assimilation in response to far-red PFD was too small to have a significant effect on shoot dry weight.

CCG calculated from canopy photosynthesis measured by the whole-plant gas exchange system correlated strongly with the final dry weight of lettuce plants (Fig. 4.10), indicating that the whole-plant gas exchange system provided a reliable measurement of carbon assimilation of lettuce plants. The slope of the regression equations was 24.4 $g \cdot mol^{-1}$ for the 1st run and 29.4 $g \cdot mol^{-1}$ for the 2nd run (Fig. 4.10). Assuming that root tissue made up for 10% of total dry weight, then we can estimate that, per mole of assimilated carbon, the total dry weight of lettuce plant increased by 24.4 $g \cdot mol^{-1}$ / 0.9 = 27.1 $g \cdot mol^{-1}$ for the 1st run and 29.4 $g \cdot mol^{-1}$ / 0.9 = 32.7 $g \cdot mol^{-1}$ for the 2nd run. Carbon content of plants in the two runs can then be estimated as 12 $g \cdot mol^{-1}$ / 27.1 $g \cdot mol^{-1}$ = 0.443 $g \cdot g^{-1}$ for the 1st run and 12 $g \cdot mol^{-1} \div 32.7$ $g \cdot mol^{-1}$ = 0.367 $g \cdot g^{-1}$ for the 2nd run, close to the typical shoot carbon content of 0.40 – 0.42 $g \cdot g^{-1}$ (unpublished results).

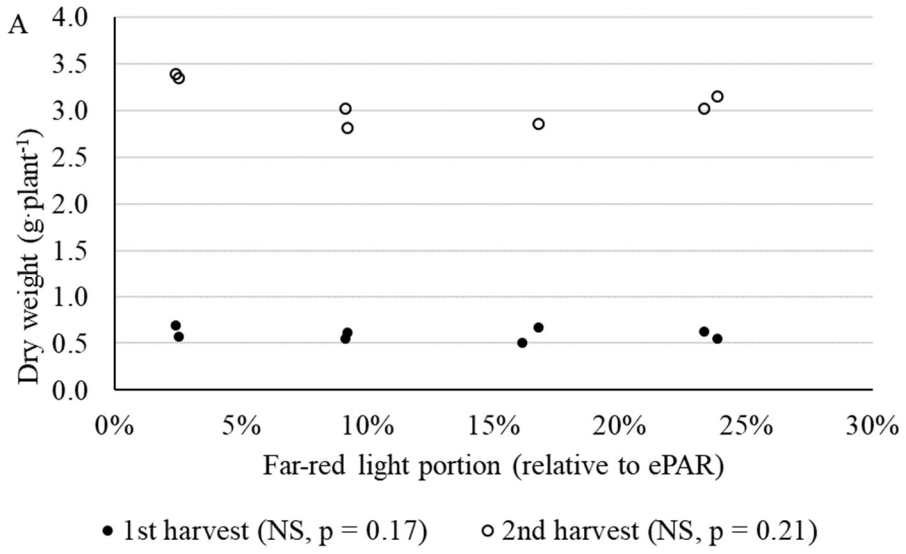

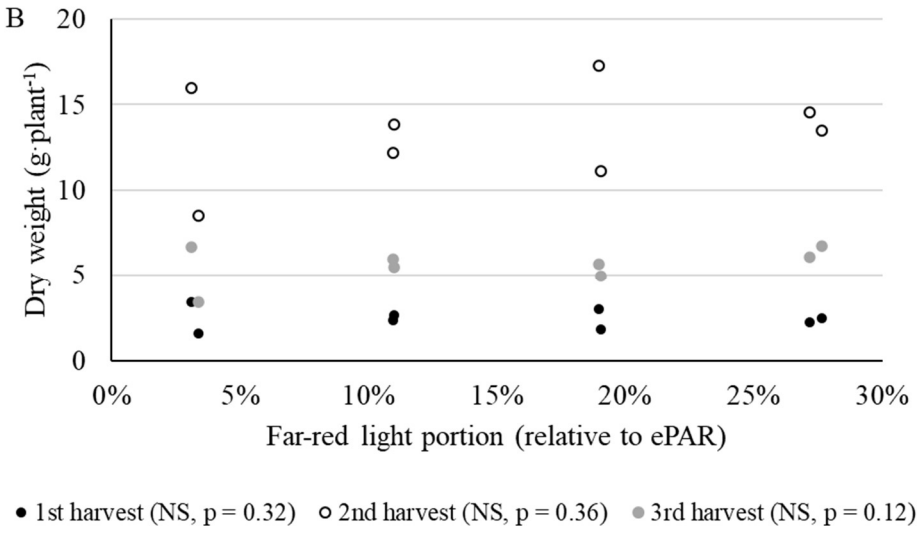

Figure 4.9. Shoot dry weight of 'Little Gem' lettuce did not respond to %FR at any harvest during the 1st (A) or 2nd run (B) of the experiment.

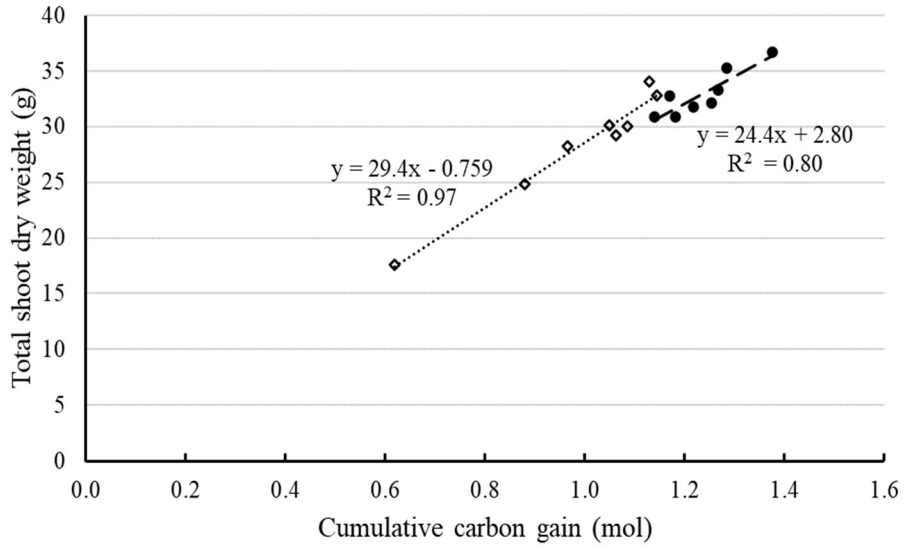

Figure 4.10. Cumulative carbon gain of lettuce plants through the whole growing cycle strongly correlated to the total shoot dry weight of both runs (solid dots for the 1st run and the open circles for the 2nd run). The R^2 and p values for regression are shown in the graph.

In our study, far-red photon substitution induced leaf expansion and canopy enlargement, which increased canopy light interception. Far-red photon substitution also reduced the amount of ePAR photons leaves absorbed, simply because we replaced strongly-absorbed red photons with less absorbed far-red photons. This reduction in absorbed ePAR photons by leaves decreased the light energy available for photosynthesis and thus negatively impacted photosynthetic rates. In the 1st run, the reduction in the amount of ePAR absorbed by leaves possibly negated the benefit of larger PCS on canopy level photosynthesis. But in the 2nd run, larger canopy size increased canopy level P_g, despite lower leaf level ePAR photon absorptance with far-red photon substitution. The different effect of far-red photon substitution on crop P_g between the two runs is likely a result of different plant densities: high plant density during much of the 1st run limited the increase in canopy size while aggravating the reduction in light absorptance. Furthermore, far-red photons had photosynthetic activity when applied with blue and white background light but had substantially lower photosynthetic activity than red photons. The canopy-level quantum yield of photosynthesis of red photons was 1.75 times that of far-red photons. Despite the effect on carbon assimilation, far-red photon substitution did not affect carbon use efficiency of lettuce plants, consistent with a previous study (Zhen and Bugbee, 2020b). The final dry weight and cumulative carbon gain of lettuce plants were not affected by %FR in either run. It is worth noting that these observations may be limited to 'Little Gem' lettuce, since the response to far-red photon inclusion is cultivar-specific, as seen in Chapter 3. Our results suggest a potential cost-saving opportunity for growers. Since far-red LEDs have higher efficacy of converting

electricity to photon output (Kusuma et al., 2020), replacing LEDs that provide PAR with far-red LEDs can reduce energy consumption without a negative impact on crop growth.

References:

Bugbee, B., and Monje, O. (1992). The Limits of Crop Productivity. *BioScience* 42(7), 494-502. doi: 10.2307/1311879.

Cannell, M.G.R., and Thornley, J.H.M. (2000). Modelling the Components of Plant Respiration: Some Guiding Principles. *Annals of Botany* 85(1), 45-54. doi: 10.1006/anbo.1999.0996.

Craver, J.K., Boldt, J.K., and Lopez, R.G. (2018). Radiation Intensity and Quality from Sole-source Light-emitting Diodes Affect Seedling Quality and Subsequent Flowering of Long-day Bedding Plant Species. *HortScience* 53(10), 1407-1415.

Dewar, R.C., Medlyn, B.E., and McMurtrie, R.E. (1998). A mechanistic analysis of light and carbon use efficiencies. *Plant, Cell & Environment* 21(6), 573-588. doi: https://doi.org/10.1046/j.1365-3040.1998.00311.x.

Emerson, R. (1957). Dependence of yield of photosynthesis in long-wave red on wavelength and intensity of supplementary light. *Science* 125(3251), 746-746. doi: 10.1126/science.125.3251.746.

Emerson, R., and Lewis, C.M. (1943). The dependence of the quantum yield of Chlorella photosynthesis on wave length of light. *American Journal of Botany* 30(3), 165-178.

Emerson, R., and Rabinowitch, E. (1960). Red drop and role of auxiliary pigments in photosynthesis. *Plant physiology* 35(4), 477.

Engineers, A.S.o.A.a.B. (2017). Quantities and Units of Electromagnetic Radiation for Plants (Photosynthetic Organisms). *ANSI/ASABE S640. 12 p.*

Evans, J. (1987). The dependence of quantum yield on wavelength and growth irradiance. *Functional Plant Biology* 14(1), 69-79. doi: 10.1071/PP9870069.

Frantz, J.M., Cometti, N.N., and Bugbee, B. (2004). Night temperature has a minimal effect on

respiration and growth in rapidly growing plants. *Annals of Botany* 94(1)**,** 155-166.

Gifford, R. (1994). The global carbon cycle: a viewpoint on the missing sink. *Functional Plant Biology* 21(1)**,** 1-15.

Gommers, C.M.M., Visser, E.J.W., Onge, K.R.S., Voesenek, L.A.C.J., and Pierik, R. (2013). Shade tolerance: when growing tall is not an option. *Trends in Plant Science* 18(2)**,** 65-71. doi: 10.1016/j.tplants.2012.09.008.

Hernandez, R., and Spalholz, H. (Year). "Characterization of Solar Radiation Spectral Contribution in Lettuce Bolting and Flowering Using LEDs in an Indoor Setting", in: *2019 ASHS Annual Conference*: ASHS).

Holmes, M., and Smith, H. (1977). The function of phytochrome in the natural environment—II. The influence of vegetation canopies on the spectral energy distribution of natural daylight. *Photochemistry and Photobiology* 25(6)**,** 539-545.

Jin, W., Urbina, J.L., Heuvelink, E., and Marcelis, L.F.M. (2021). Adding Far-Red to Red-Blue Light-Emitting Diode Light Promotes Yield of Lettuce at Different Planting Densities. *Frontiers in Plant Science* 11(2219). doi: 10.3389/fpls.2020.609977.

Kim, C., and van Iersel, M.W. (2022). Morphological and Physiological Screening to Predict Lettuce Biomass Production in Controlled Environment Agriculture. *Remote Sensing* 14(2)**,** 316.

Kubota, C., Chia, P., Yang, Z., and Li, Q. (Year). "Applications of far-red light emitting diodes in plant production under controlled environments", in: *International Symposium on Advanced Technologies and Management Towards Sustainable Greenhouse Ecosystems: Greensys2011 952*), 59-66.

Kusuma, P., and Bugbee, B. (2021). Far-red Fraction: An Improved Metric for Characterizing

Phytochrome Effects on Morphology. *Journal of the American Society for Horticultural Science J. Amer. Soc. Hort. Sci.* 146(1)**,** 3. doi: 10.21273/jashs05002-20.

Kusuma, P., Pattison, P.M., and Bugbee, B. (2020). From physics to fixtures to food: current and potential LED efficacy. *Horticulture Research* 7(1)**,** 56. doi: 10.1038/s41438-020-0283-7.

Legendre, R., and van Iersel, M.W. (2021). Supplemental Far-Red Light Stimulates Lettuce Growth: Disentangling Morphological and Physiological Effects. *Plants* 10(1)**,** 166.

Li, Q., and Kubota, C. (2009). Effects of supplemental light quality on growth and phytochemicals of baby leaf lettuce. *Environmental and Experimental Botany* 67(1)**,** 59-64.

McCree, K.J. (1971). The action spectrum, absorptance and quantum yield of photosynthesis in crop plants. *Agricultural Meteorology* 9(Supplement C)**,** 191-216. doi: 10.1016/0002-1571(71)90022-7.

McCree, K.J. (1972). Test of current definitions of photosynthetically active radiation against leaf photosynthesis data. *Agricultural Meteorology* 10**,** 443-453. doi: 10.1016/0002-1571(72)90045-3.

Meng, Q., and Runkle, E.S. (2019). Far-red radiation interacts with relative and absolute blue and red photon flux densities to regulate growth, morphology, and pigmentation of lettuce and basil seedlings. *Scientia Horticulturae* 255**,** 269-280. doi: 10.1016/j.scienta.2019.05.030.

Monje, O., and Bugbee, B. (1998). Adaptation to high CO2 concentration in an optimal environment: radiation capture, canopy quantum yield and carbon use efficiency. *Plant, Cell & Environment* 21(3)**,** 315-324. doi: https://doi.org/10.1046/j.1365-3040.1998.00284.x.

Myers, J. (1971). Enhancement studies in photosynthesis. *Annual Review of Plant Physiology* 22(1)**,** 289-312.

Park, Y., and Runkle, E.S. (2017). Far-red radiation promotes growth of seedlings by increasing leaf expansion and whole-plant net assimilation. *Environmental and experimental botany* 136**,** 41-49. doi: 10.1016/j.envexpbot.2016.12.013.

Reich, P.B., Walters, M.B., Ellsworth, D.S., Vose, J.M., Volin, J.C., Gresham, C., et al. (1998). Relationships of leaf dark respiration to leaf nitrogen, specific leaf area and leaf life-span: a test across biomes and functional groups. *Oecologia* 114(4)**,** 471-482. doi: 10.1007/s004420050471.

Ruberti, I., Sessa, G., Ciolfi, A., Possenti, M., Carabelli, M., and Morelli, G. (2012). Plant adaptation to dynamically changing environment: the shade avoidance response. *Biotechnology advances* 30(5)**,** 1047-1058.

Sager, J., Smith, W., Edwards, J., and Cyr, K. (1988). Photosynthetic efficiency and phytochrome photoequilibria determination using spectral data. *Transactions of the ASAE* 31(6)**,** 1882-1889. doi: 10.13031/2013.30952.

Shibuya, T., Endo, R., Kitaya, Y., and Tsuchida, M. (2020). Far-red Light Interacts with Plant Density to Change Photosynthate Allocation of Cucumber Seedlings and Their Subsequent Early Growth after Transplanting. 1. doi: 10.21273/hortsci15159-20.

Valladares, F., and Niinemets, Ü. (2008). Shade Tolerance, a Key Plant Feature of Complex Nature and Consequences. *Annual Review of Ecology, Evolution, and Systematics* 39(1)**,** 237-257. doi: 10.1146/annurev.ecolsys.39.110707.173506.

van Iersel, M.W. (2006). Respiratory Q10 of marigold (Tagetes patula) in response to long-term temperature differences and its relationship to growth and maintenance respiration.

Physiologia Plantarum 128(2)**,** 289-301. doi: 10.1111/j.1399-3054.2006.00743.x.

van Iersel, M.W., and Bugbee, B. (2000). A Multiple Chamber, Semicontinuous, Crop Carbon Dioxide Exchange System: Design, Calibration, and Data Interpretation. *Journal of the American Society for Horticultural Science* 125(1)**,** 86-92.

Zhen, S., and Bugbee, B. (2020a). Far‐red photons have equivalent efficiency to traditional photosynthetic photons: implications for redefining photosynthetically active radiation. *Plant, Cell & Environment*.

Zhen, S., and Bugbee, B. (2020b). Substituting Far-Red for Traditionally Defined Photosynthetic Photons Results in Equal Canopy Quantum Yield for CO2 Fixation and Increased Photon Capture During Long-Term Studies: Implications for Re-Defining PAR. *Frontiers in Plant Science* 11(1433). doi: 10.3389/fpls.2020.581156.

Zhen, S., Haidekker, M., and van Iersel, M.W. (2019). Far‐red light enhances photochemical efficiency in a wavelength‐dependent manner. *Physiologia plantarum* 167(1)**,** 21-33. doi: 10.1111/ppl.12834.

Zhen, S., van Iersel, M., and Bugbee, B. (2021). Why Far-Red Photons Should Be Included in the Definition of Photosynthetic Photons and the Measurement of Horticultural Fixture Efficacy. *Frontiers in Plant Science* 12**,** 1158.

Zhen, S., and van Iersel, M.W. (2017). Far-red light is needed for efficient photochemistry and photosynthesis. *Journal of Plant Physiology* 209**,** 115-122. doi: http://dx.doi.org/10.1016/j.jplph.2016.12.004.

Zou, J., Zhang, Y., Zhang, Y., Bian, Z., Fanourakis, D., Yang, Q., et al. (2019). Morphological and physiological properties of indoor cultivated lettuce in response to additional far-red light. *Scientia Horticulturae* 257**,** 108725. doi: 10.1016/j.scienta.2019.108725.

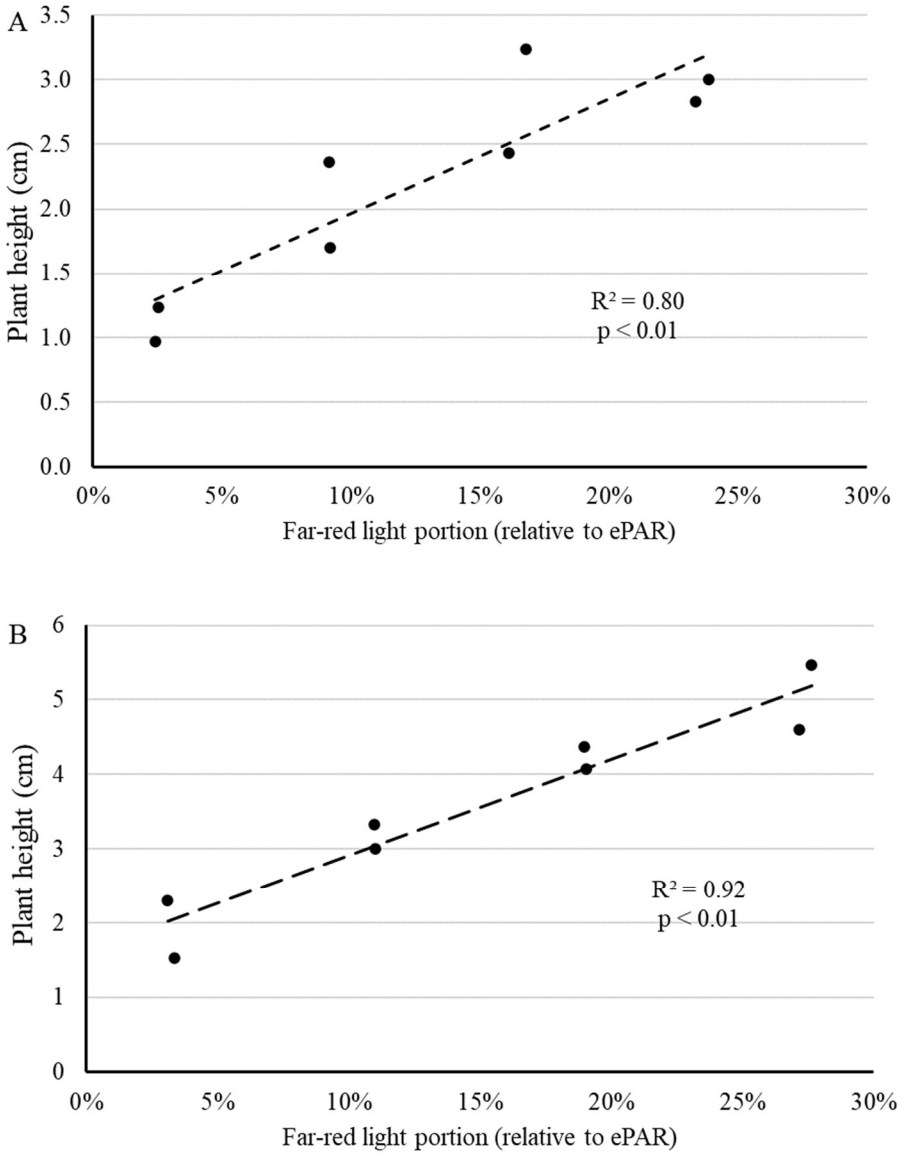

Figure S4.1. Lettuce height increased linearly with %FR at 10 DAT for the 1st run (A) and at 7 DAT for the 2nd run (B).

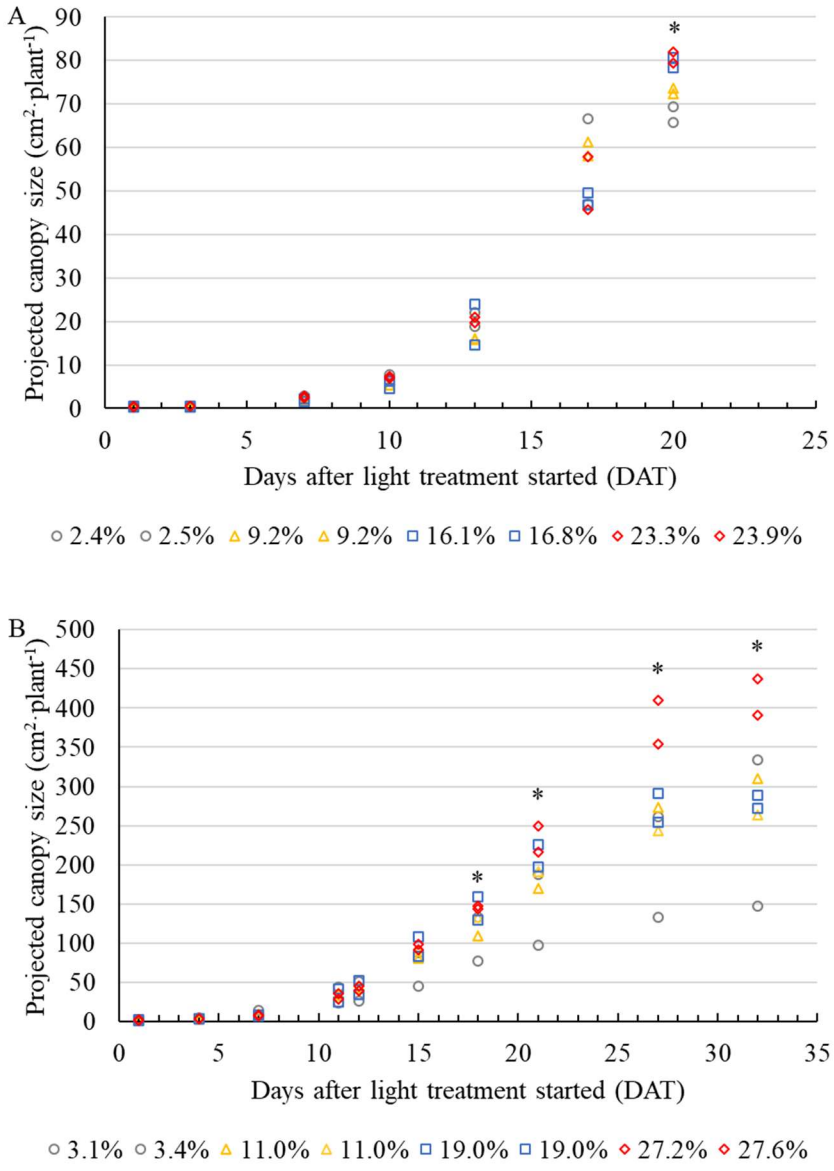

Figure S4.2. Projected canopy size from 1 to 20 DAT during the 1st run (A) and throughout the experiment in the 2nd run (B) per plant. On days marked with a *, PCS increased with increasing %FR (shown in the legend) ($\alpha = 0.05$).

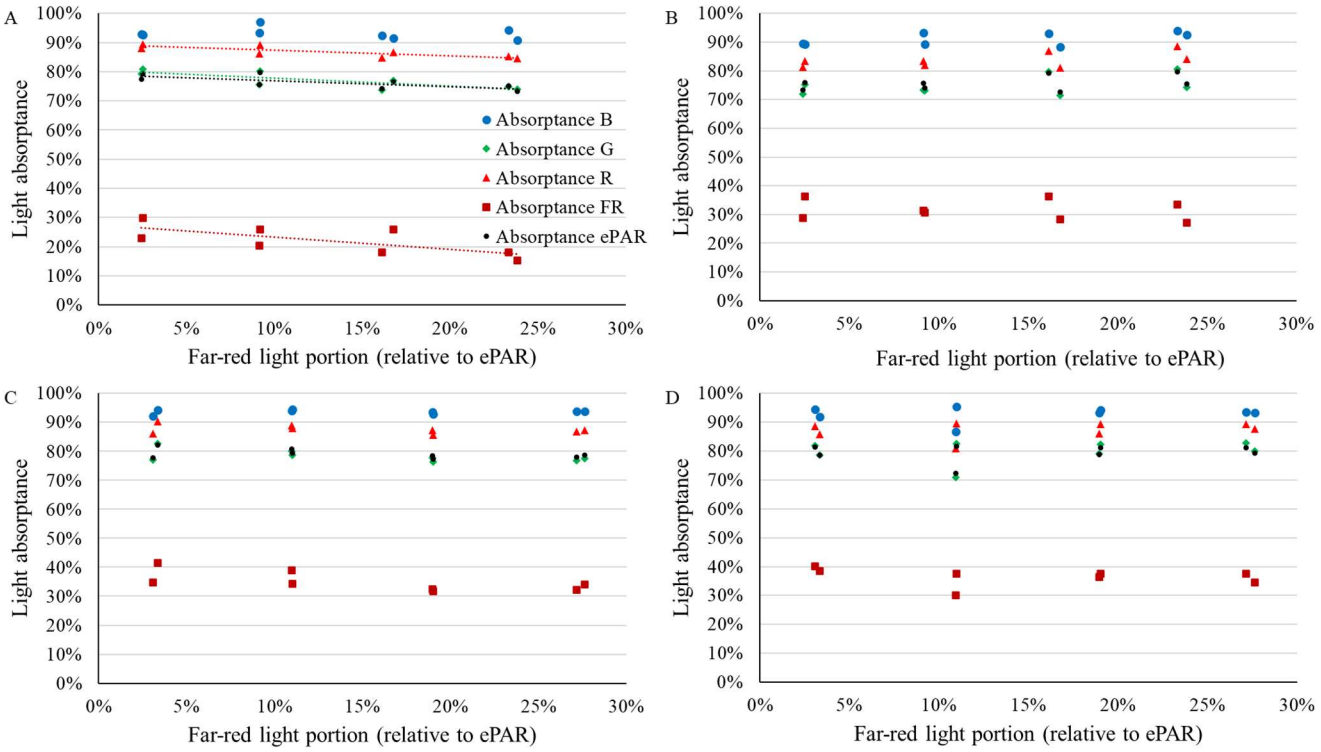

Figure S4.3. The response of lettuce leaf absorptance of blue (400 – 499 nm, solid blue circles), green (500 – 599 nm, green diamonds), red (600- 699 nm, red triangles), far red (700 – 750 nm, dark red squares) and ePAR photons (400 – 750 nm, black dots) in response to %FR at the 1st harvest of the 1st run (A), 2nd harvest of the 1st run (B), 2nd harvest of the 2nd run (C) and 3rd harvest of the 2nd run (D). A higher %FR linearly decreased absorptance of green, red and far-red photons only in the 1st harvest of the 1st run (A), as indicated by the regression lines.

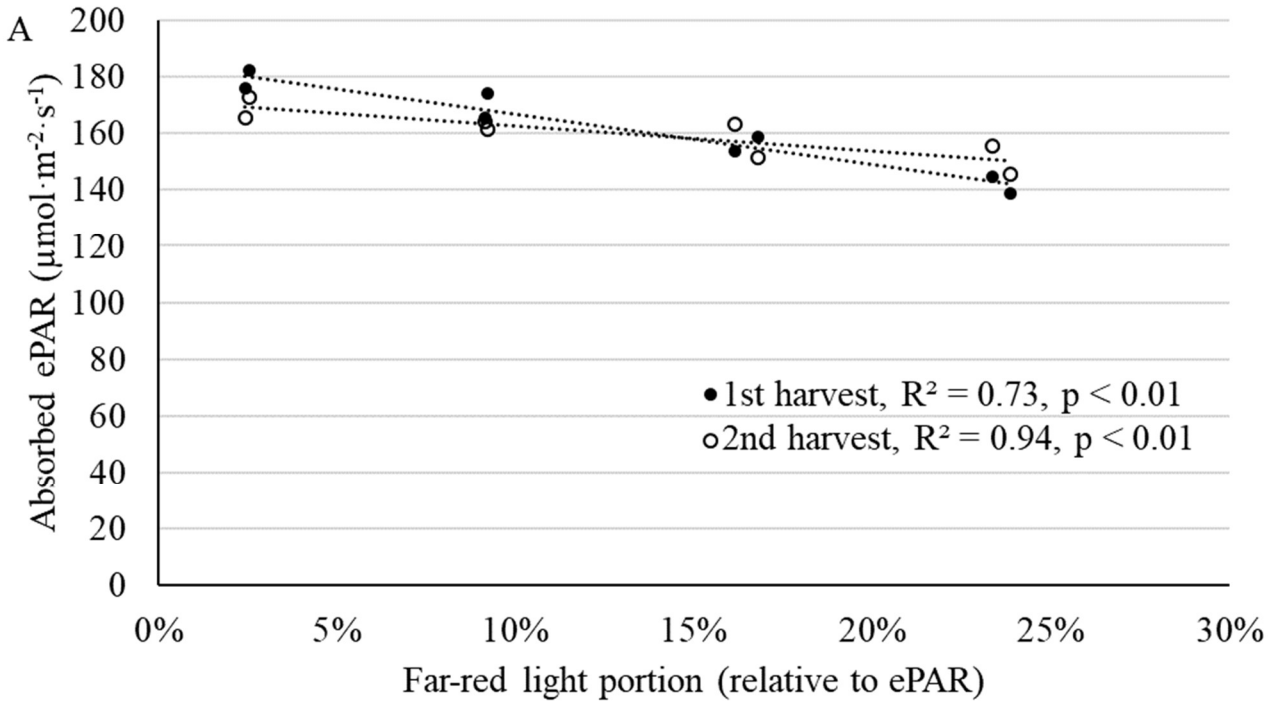
A
Absorbed ePAR (µmol·m-2·s-1)
200
180
160
140
120
100
80
60
40
20
0
0%
5%
10%
15%
20%
25%
30%
Far-red light portion (relative to ePAR)
1st harvest, R² = 0.73, p < 0.01
2nd harvest, R² = 0.94, p < 0.01

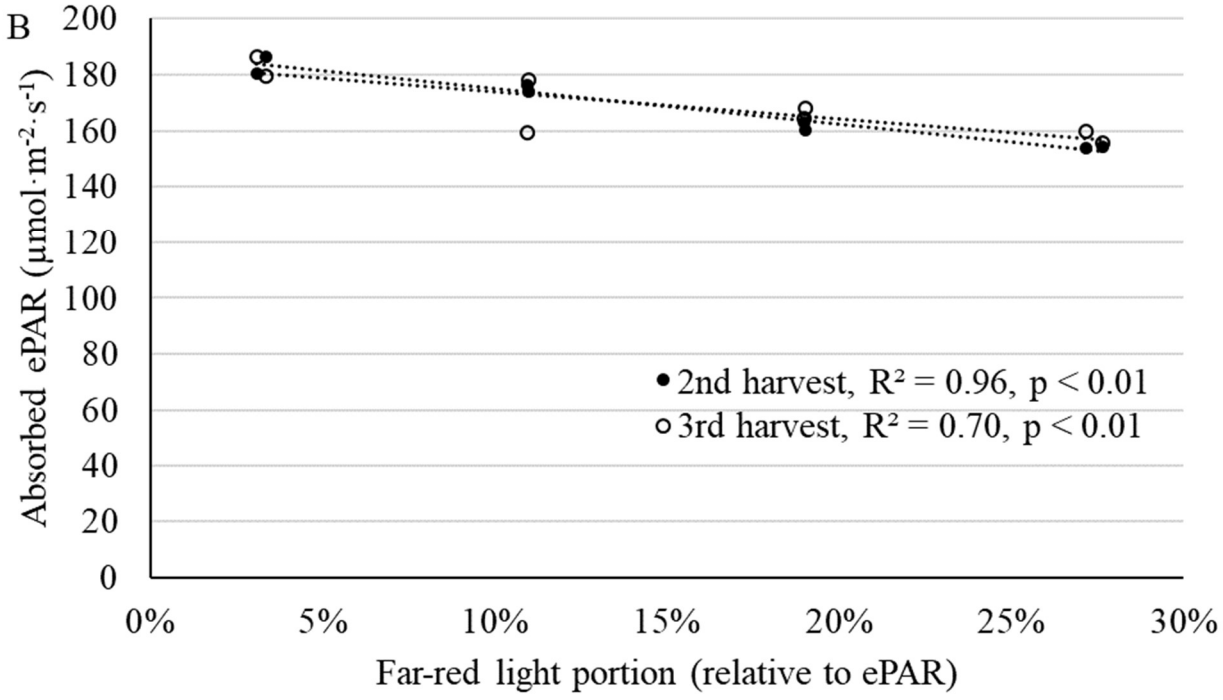
B
Absorbed ePAR (µmol·m-2·s-1)
200
180
160
140
120
100
80
60
40
20
0
0%
5%
10%
15%
20%
25%
30%
Far-red light portion (relative to ePAR)
2nd harvest, R² = 0.96, p < 0.01
3rd harvest, R² = 0.70, p < 0.01

Figure S4.4. The amount of ePAR photons by absorbed lettuce leaves decreased with increasing %FR in the 1st (A) and 2nd run (B). The main reason for this decrease is the lower absorptance of far-red photons (see Fig. 4.5).

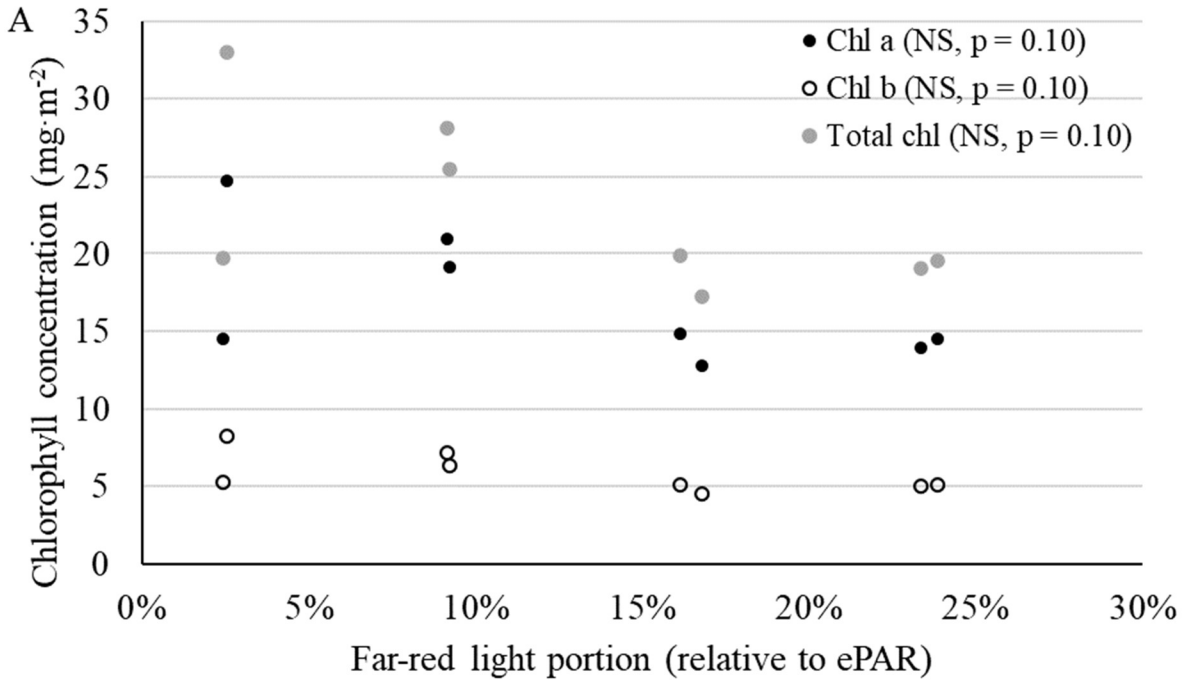

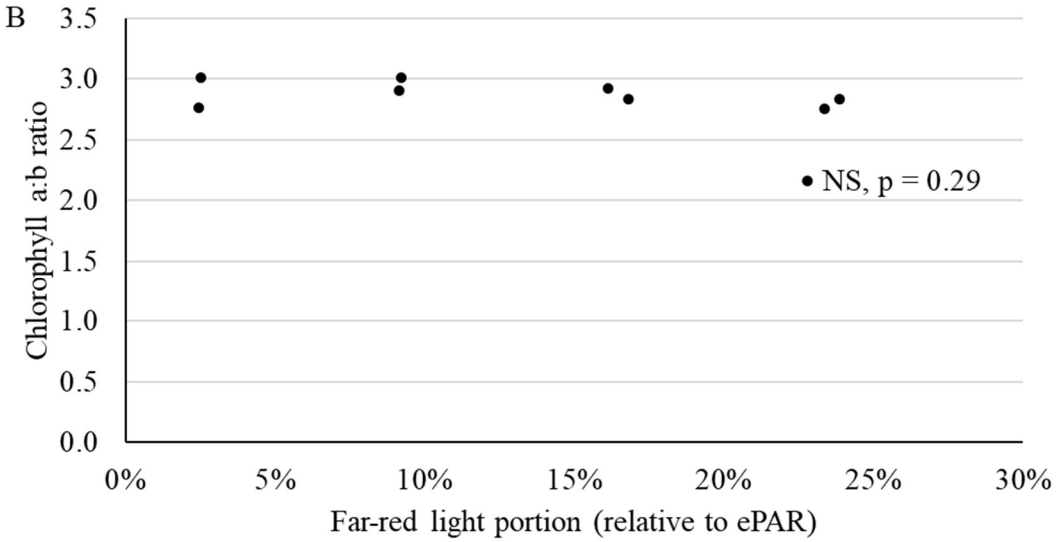

Figure S4.5. The chlorophyll a and b concentration, total chlorophyll concentration and chlorophyll a:b ratio were not affected by increasing %FR in the 1st run.

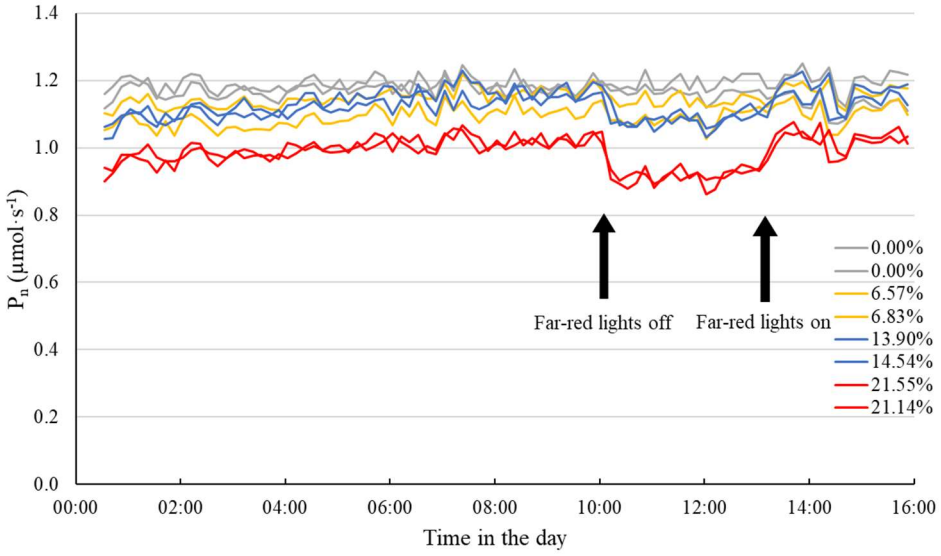

Figure S4.6. Example of raw P_n data at 21 DAT of the 1st run. Far-red lights were turned off at 10:02 and turned back on at 13:02. The %FR of each treatment is listed with their corresponding line color.

Table S4.1. Light spectrum and average temperature in each gas exchange chamber in both runs

Chamber No.		Blue PFD (µmol·m^{-2}·s^{-1})	Green PFD (µmol·m^{-2}·s^{-1})	Red PFD (µmol·m^{-2}·s^{-1})	Far-red PFD (µmol·m^{-2}·s^{-1})	ePAR PFD (µmol·m^{-2}·s^{-1})	Fraction of far-red photons in ePAR	Light spectrum	Temperature (°C)
1st run	2	70.2	39.2	62.7	34.8	206.9	16.8%	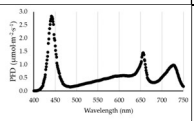	26.6
	3	68.6	37.1	91.0	4.9	201.6	2.4%	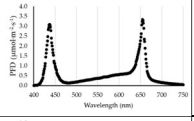	26.3
	4	71.4	37.0	76.3	18.6	203.3	9.2%	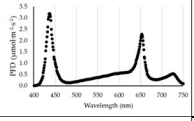	20.2
	5	71.3	38.2	45.8	48.6	203.9	23.9%	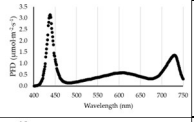	22.4
	7	72.5	38.3	45.8	47.7	204.4	23.3%	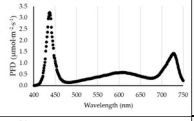	26.7
	8	67.8	40.1	78.9	18.9	205.7	9.2%	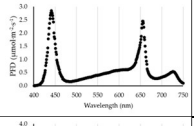	20.8
	9	71.0	37.7	92.9	5.2	206.9	2.5%	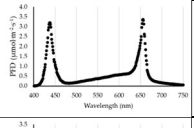	23.0
	10	72.8	38.0	60.7	33.0	204.4	16.1%	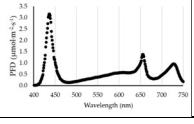	20.8

Table S4.1. Light spectrum and average temperature in each gas exchange chamber in both runs (cont.)

Chamber No.		Blue PFD (µmol·m^{-2}·s^{-1})	Green PFD (µmol·m^{-2}·s^{-1})	Red PFD (µmol·m^{-2}·s^{-1})	Far-red PFD (µmol·m^{-2}·s^{-1})	ePAR PFD (µmol·m^{-2}·s^{-1})	Fraction of far-red photons in ePAR	Light spectrum	Temperature (°C)
2nd run	2	71.5	38.2	45.4	54.2	209.3	27.6%	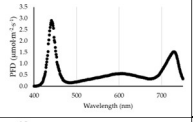	25.5
	3	73.3	36.6	61.3	36.7	207.9	19.0%	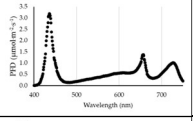	24.2
	4	73.1	36.7	93.2	5.4	208.3	3.4%	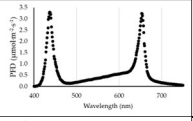	20.1
	5	74.0	37.0	76.1	20.8	207.9	11.0%	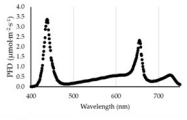	22.0
	7	73.5	38.2	92.9	5.0	209.6	3.1%	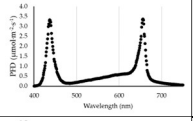	26.8
	8	72.4	37.5	61.0	36.7	207.5	19.0%	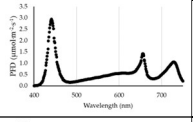	21.0
	9	73.7	36.2	45.5	53.5	208.9	27.2%	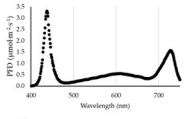	20.5
	10	73.3	37.3	75.9	20.8	207.4	11.0%	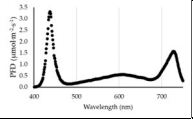	23.0

CHAPTER 5

CARBON USE EFFICIENCY OF LETTUCE DECREASES AS MAINTENANCE RESPIRATION DIVERTS CARBON AWAY FROM GROWTH

Introduction

Plants assimilate carbon through photosynthesis. But not all assimilated carbon is incorporated into biomass. A fraction of the assimilated carbon is lost through respiration, which supplies energy and metabolic intermediates to support growth and maintenance of plants' living tissues. Therefore, it is important to include a respiration component to estimate plant growth from photosynthesis and in modeling crop carbon balance and growth. The efficiency with which plant incorporate assimilated carbon into their biomass is referred to as carbon use efficiency (CUE). CUE is calculated as ratio of carbon that is retained in biomass to the total assimilated carbon (Monje and Bugbee, 1998). On the other hand, 1-CUE quantifies the ratio of carbon lost through respiration to the total assimilated carbon, often referred as the R:P ratio. CUE has been reported to be fairly consistent (0.4-0.6) among different species (Gifford, 1994; Reich et al., 1998; Cannell and Thornley, 2000). Previous studies showed that the CUE of plants that adapted to different environmental conditions (for example, temperature, CO_2 concentration, nutrient concentration and light spectrum) shifted slightly within the range of 0.4-0.6 (Gifford, 1994; Monje and Bugbee, 1998; van Iersel and Kang, 2002; Frantz et al., 2004; Zhen and Bugbee, 2020). However, CUE can vary largely with the developmental stage. Studies in wheat (*Triticum aestivum*), vinca (*Catharanthus roseus*), marigold (*Tagetes patula*), and lettuce (*Lactuca sativa*) found that CUE was low during the seedling stage and increased as the photosynthetic machinery

developed (Monje and Bugbee, 1998; van Iersel and Seymour, 2000; van Iersel and Seymour, 2002; Zhen and Bugbee, 2020). As plants grew, the CUE reached its maximum during the vegetative stage, then declined as the plant matured (Monje and Bugbee, 1998; van Iersel and Seymour, 2002; van Iersel, 2003; Zhen and Bugbee, 2020). With the large variation in CUE throughout the life cycle of crop, knowledge of CUE is critical to estimate growth rates from photosynthesis measurements and to accurately model plant growth.

To better understand CUE changes over time, it is important to understand the underlying reasons for how much of the fixed carbohydrates are allocated to respiration. To do so, it is useful to separate respiration into growth (R_g) and maintenance respiration (R_m), although these two types of respiration do not have a distinct biochemical difference (Bugbee and Monje, 1992; Cannell and Thornley, 2000). R_g is the respiration associated with production of new biomass, which supplies energy and organic compounds to growth-related processes, such as synthesizing new biomass, nutrient uptake, and nitrate and sulfate reduction. Growth respiration can be calculated as the growth respiration coefficient (g_r) multiplied by the growth rate. g_r is often assumed to be constant through the life cycle of a plant (van Iersel, 2003), especially if the composition of the plant material does not change drastically over time, as is the case with leafy greens like lettuce. R_m is associated with the maintenance of the existing biomass, which includes processes such as protein turnover and maintaining ion homeostasis (Cannell and Thornley, 2000). Maintenance respiration can similarly be calculated as the maintenance respiration coefficient (m_r) multiplied by the plant size. The plant size is typically expressed as dry weight of the plant. m_r of plants often experiences changes with the developmental stage of plants, if the composition of the plant material changes during their life cycle. For lettuce, m_r can

be assumed to be constant, since lettuce plants likely do not undergo major changes in chemical composition during their vegetative growth (van Iersel, 2003).

There are different approaches to quantify R_g and R_m. van Iersel and Seymour (2000) showed that by using a semi-continuous, whole-plant CO_2 exchange, R_g and R_m can be quantified in a non-destructive manner. In their approach, the newly incorporated carbon each day, daily carbon gain (DCG, mmol·plant^{-1}·d^{-1}), was used as a proxy of growth rate. The cumulative carbon a plant has incorporated into its biomass, cumulative carbon gain (CCG, mmol·plant^{-1}), was used as a proxy of plant size. Thus, respiration be calculated as $R = R_g + R_m = f_1(DCG) + f_2(CCG)$ (van Iersel and Seymour, 2000). If g_r and m_r are assumed to be constant through the life cycle of a plant, the respiration can simply be expressed as $R = g_r \times DCG + m_r \times CCG$. The approach has been successfully applied to study the effect of temperature on respiration (van Iersel, 2006) and the effect of respiration and growth on CUE (van Iersel, 2003).

In this study, we measured gas exchange rates of lettuce from young seedlings to mature plants in a whole-plant gas exchange system. From the gas exchange data, the growth and maintenance respiration of lettuce plants were calculated from the seedling stage to mature stage. We tracked the changes in photosynthesis, maintenance and growth respiration, daily carbon gain and CUE throughout the life cycle of lettuce plants, and discussed the impact of changes in different physiological processes on CUE.

Materials and methods

We used the same data set described in chapter 4. We measured CO_2 exchange of lettuce at the whole-plant level from the seedling stage (7 days-old plants from sowing in the 1st run and 9 day-old plants in the 2nd run) to mature stage (41 day-old plants in both runs). Gas exchange rate was collected semi-continuously every 10 min in the 1st run and every 20 min in the 2nd run.

Eight gas exchange chambers illuminated by LED light with different red to far-red ratio were used with 18 plants in each chamber at the start of the measurements. The ePAR (400 – 750 nm) in all chambers was ~200 $\mu mol \cdot m^{-2} \cdot s^{-1}$ with a photoperiod of 16 h. In the 1st run, nine plants were harvested when plants were 28 days old and the rest of plants were harvested at the end of the 1st run. In the 2nd run, 9, 5 and 4 plants were harvested when plants were 20, 27 and 41 days old, respectively. The harvested plants were dried at 80 °C for at least 72 h and measured for dry weight. The daily P_n, gross photosynthetic rate per plant (P_g) and R_d per plant (unit: $\mu mol \cdot d^{-1} \cdot plant^{-1}$) were obtained from chapter 4.

The $R_{d,day}$ ($mmol \cdot plant^{-1} \cdot d^{-1}$) is the total respiration of a plant in a day, calculated as $R_d \times 24\ h \cdot d^{-1} \times 3600\ s \cdot h^{-1}$, assuming that the respiration rate during the daytime and in the dark were similar. Daily carbon gain (DCG, $mmol \cdot plant^{-1} \cdot d^{-1}$), cumulative carbon gain (CCG, the running total of DCG, $mmol \cdot plant^{-1}$) and CUE were also obtained from the data in the previous chapter. We estimated the growth respiration coefficient, g_r ($mol \cdot mol^{-1}$) and maintenance respiration coefficient, m_r ($mol \cdot mol^{-1} \cdot day^{-1}$), based on the equation: $R_{d,day} = g_r \times DCG + m_r \times (CCG) + a$. The intercept existed because the collection of gas exchange data started with seedlings, so the CCG we measured during this study was lower than the actual carbon content of the lettuce plants, since we did not take into account the seedling carbon content. The intercept 'a' is thus an estimate of the R_m of the seedling biomass. The estimation of g_r of and m_r was done using regression analysis (Microsoft Excel, Microsoft, Seattle, WA). The two components of respiration, R_g and R_m, were calculated as $R_g = g_r \times DCG$ and $R_m = m_r \times CCG + a$. Since we did not detect any effect of far-red substitution or temperature on CUE, CCG, g_r and m_r, the data from eight gas exchange chambers were pooled and analyzed together for both runs.

We tested the relationship between total CCG and the total shoot dry weight by summing the dry weight from plants at the different harvests. Linear regressions between total CCG and total dry weight of the lettuce harvested in both runs were conducted in Microsoft Excel. Non-linear regressions were carried out using SigmaPlot 11 (Systat Software, San Jose, CA).

Results and discussions

The total raw CCG through the whole growing cycle linearly correlated with the total dry weight of all lettuce harvested in both runs (Fig. 5.1). Lettuce plants gained 29.4 and 24.4 g biomass for every mole of carbon assimilated during the 1st and 2nd run, respectively. The strong correlation between CCG and the final dry weight indicated that the whole-plant gas exchange system provided reliable CO_2 exchange and growth measurements.

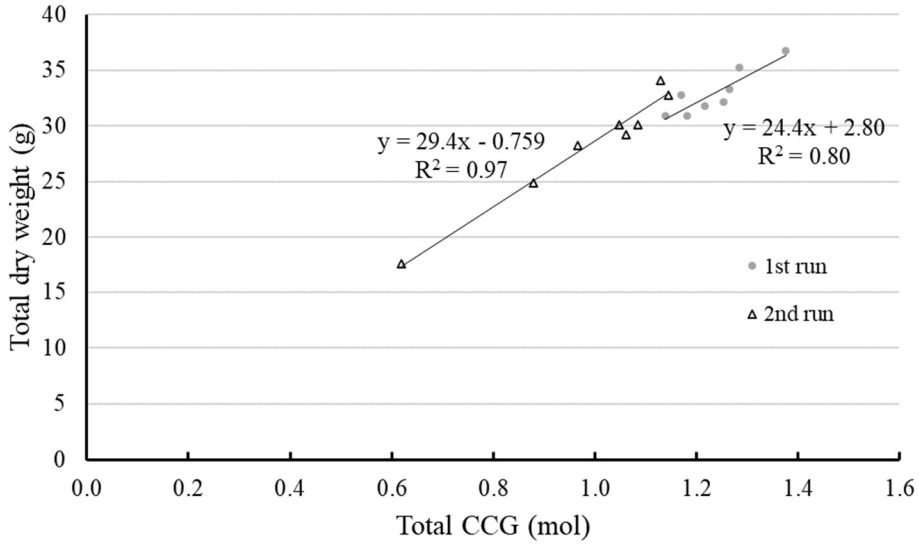

Figure 5.1. Total CCG of plants in each gas exchange chamber correlated with the total dry weight of lettuce plants harvested from the same chamber in both runs, which suggested that CCG is a good approximation of lettuce size.

During the 1st run, the average daily $P_{g,day}$ and $P_{n,day}$ increased with time until ~27 days old (Fig. 5.2A), after which $P_{g,day}$ and $P_{n,day}$ plateaued. The plateau in $P_{g,day}$ and $P_{n,day}$ indicates that the canopy had reached the maximum size the gas exchange chambers allowed for and the lettuce plants intercepted almost all available light. For the 2nd run, $P_{g,day}$ and $P_{n,day}$ increased throughout their life cycle without reaching a plateau (Fig. 5.2B), since some of the lettuce plants were harvested throughout the study to minimize canopy overlap among plants. R_d increased (more negative) over time for both runs, as the lettuce plants got larger (Fig. 5.2A and 2B). When plotted as a function of CCG, $P_{g,day}$ and $P_{n,day}$ increased asymptotically (Fig. 5.2C and 2D). $P_{g,day}$ and $P_{n,day}$ started to level off when the canopy grew large enough to intercept almost all light available in the gas exchange chamber.

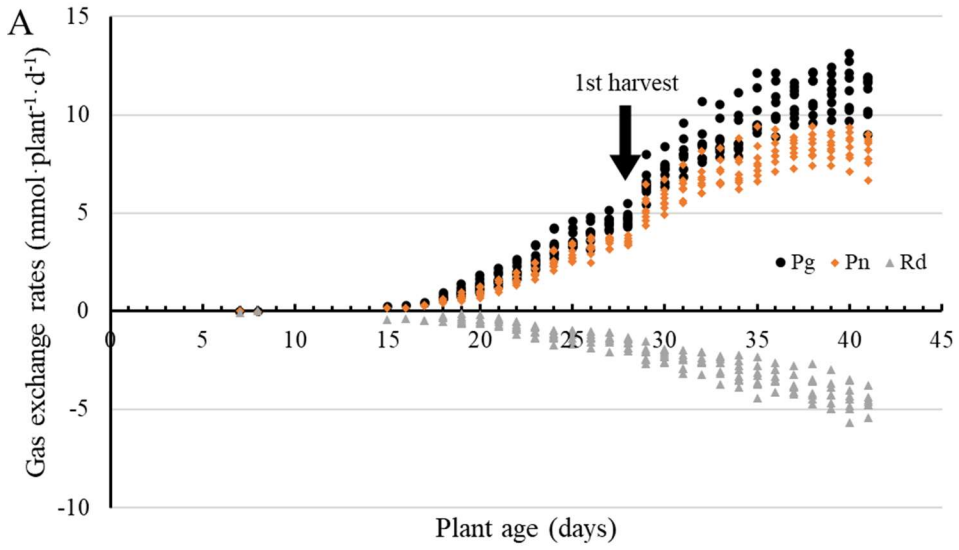

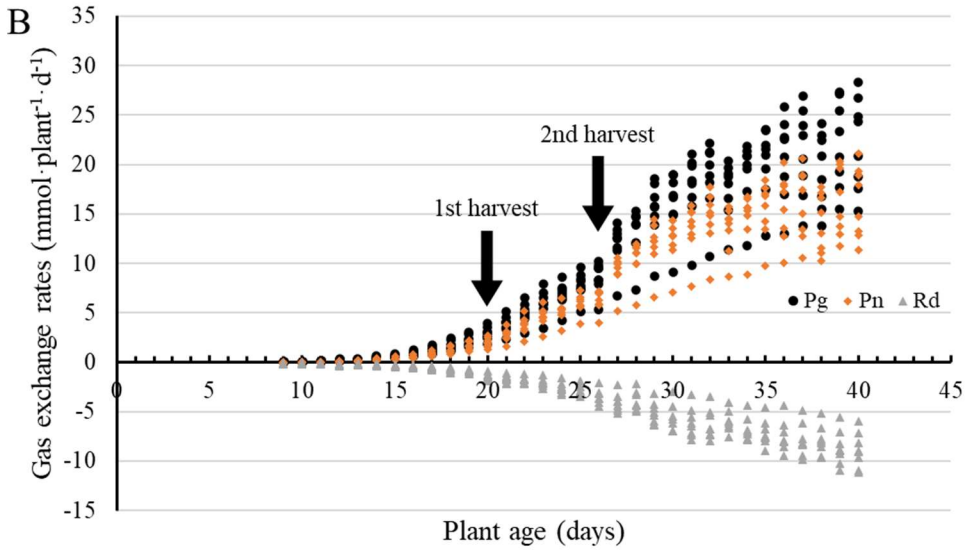
B
Gas exchange rates (mmol·plant-1·d-1)
35
30
25
20
15
10
5
0
-5
-10
-15
0
5
10
15
20
25
30
35
40
45
1st harvest
2nd harvest
Pg
Pn
Rd
Plant age (days)

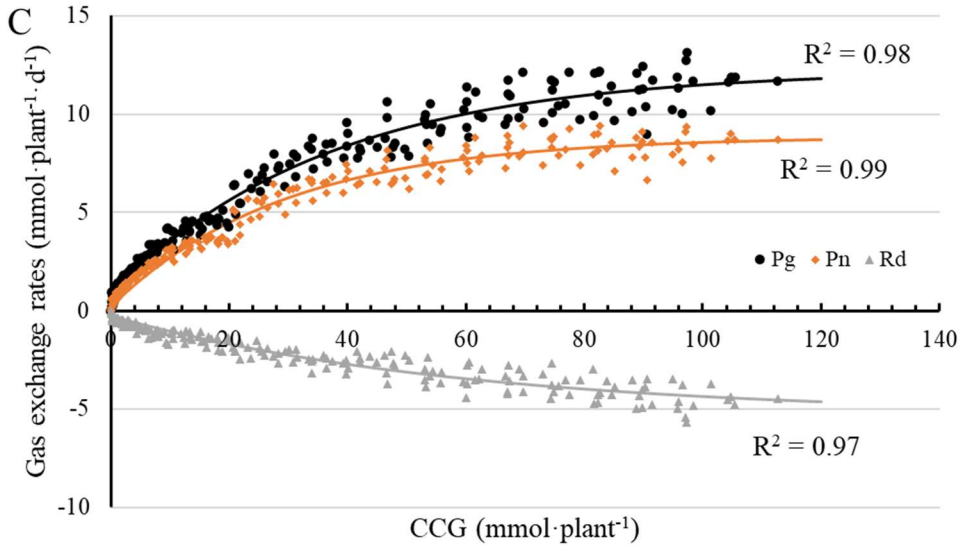
C
Gas exchange rates (mmol·plant-1·d-1)
15
10
5
0
-5
-10
0
20
40
60
80
100
120
140
R² = 0.98
R² = 0.99
R² = 0.97
Pg
Pn
Rd
CCG (mmol·plant-1)

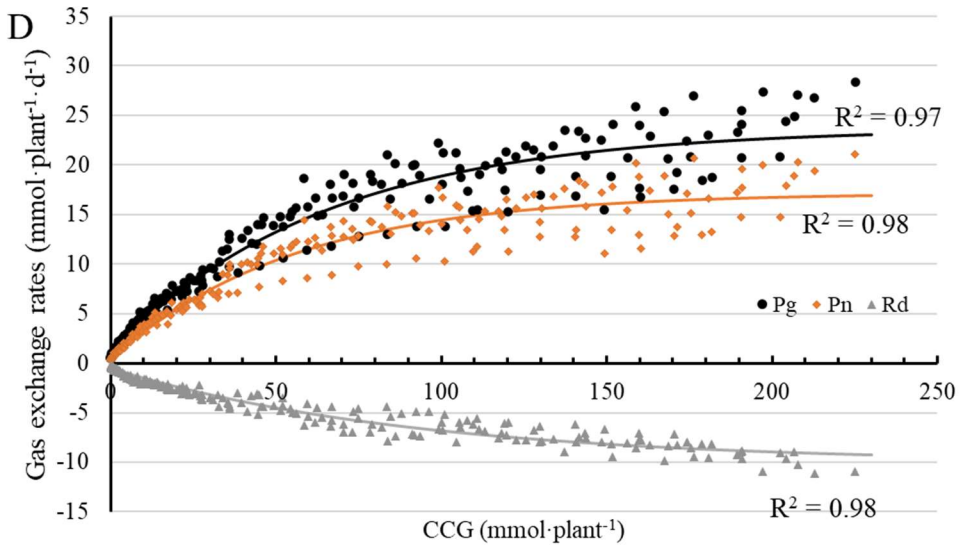

Figure 5.2. Lettuce $P_{g,day}$, $P_{n,day}$ and $R_{d,day}$ as functions of plant age (A and B) and CCG (C and D) the 1st run (A) and the 2nd run (B). For each run, data from lettuce plants in eight gas exchange chambers were pooled and plotted together. $P_{g,day}$, $P_{n,day}$, and $R_{d,day}$ followed an exponential rise to maximum function when regressed against CCG (Table S5.1). R^2 values of each regression are shown in the graph.

DCG is a measure of growth rate and increased asymptotically with CCG for both runs (Fig. 5.3A and 5.3B). The DCG reached a plateau, likely when light availability limited further increases in $P_{g,day}$. van Iersel and Seymour (2002) showed that as lettuce plants grew larger in size, and the fraction of maintenance respiration in total respiration further increased (will be discussed later), DCG decreased with plant size.

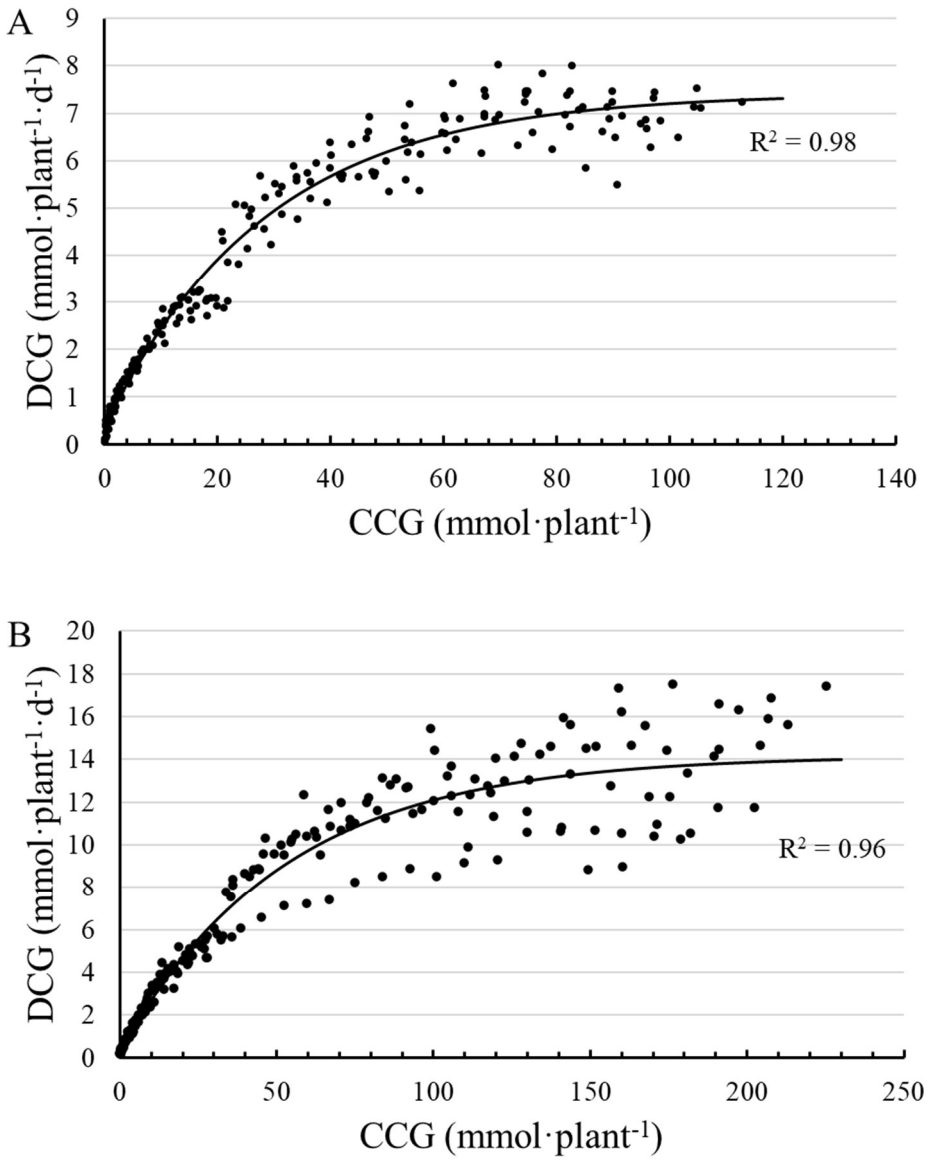

Figure 5.3. Daily carbon gain (DCG, a proxy for growth rate) increased with cumulative carbon gain (CCG, a proxy for plant size), but the increase slowed down as plants grew larger during the 1st (A) and the 2nd run (B). For each run, data from lettuce plants in eight gas exchange chambers were pooled and plotted together. DCG followed an exponential rise to maximum function against CCG. The regression equations can be found in Table S5.1. R^2 values of each regression are shown in the graph.

CUE of lettuce plants was low during the seedling stage (Fig. 5.4A) and increased sharply from 15 to 20 days during the 1st run and 13 to 22 days during the 2nd run. The initial sharp increase in CUE occurred when CCG was less than 20 mmol (Fig. 5.4B). The low CUE of young plants, which was also seen in marigolds (van Iersel and Seymour, 2002; van Iersel, 2006), is possibly due to the respiration of carbon reserves from the seeds and low photosynthetic rate of young seedlings. The increase in CUE was potentially due to the increasing photosynthetic rate of lettuce plants after the initial leaves became physiologically mature. CUE then remained relatively stable at 0.67 ± 0.04 $mol \cdot mol^{-1}$ (average ± SD) from 21 to 37 days during the 1st run, and at 0.65 ± 0.03 $mol \cdot mol^{-1}$ from 23 to 35 days during the 2nd run (Fig. 5.4A). These values are similar to the 0.61 and 0.62 $mol \cdot mol^{-1}$ reported by Zhen and Bugbee (2020) and Frantz et al. (2004) for actively growing lettuce plants. CUE of lettuce slowly decreased after 37 days in the 1st run and 35 days in the 2nd run with time (Fig. 5.4A). When plotted against CCG, the decrease was more noticeable when plant CCG exceeded 50 mmol for both runs (Fig. 5.4B). This indicates that, as lettuce plants grew, a greater fraction of assimilated carbohydrates was lost through respiration. A similar decrease in CUE as plants grew bigger was observed in wheat, marigold, and lettuce (Monje and Bugbee, 1998; van Iersel and Seymour, 2002; van Iersel, 2003; Zhen and Bugbee, 2020).

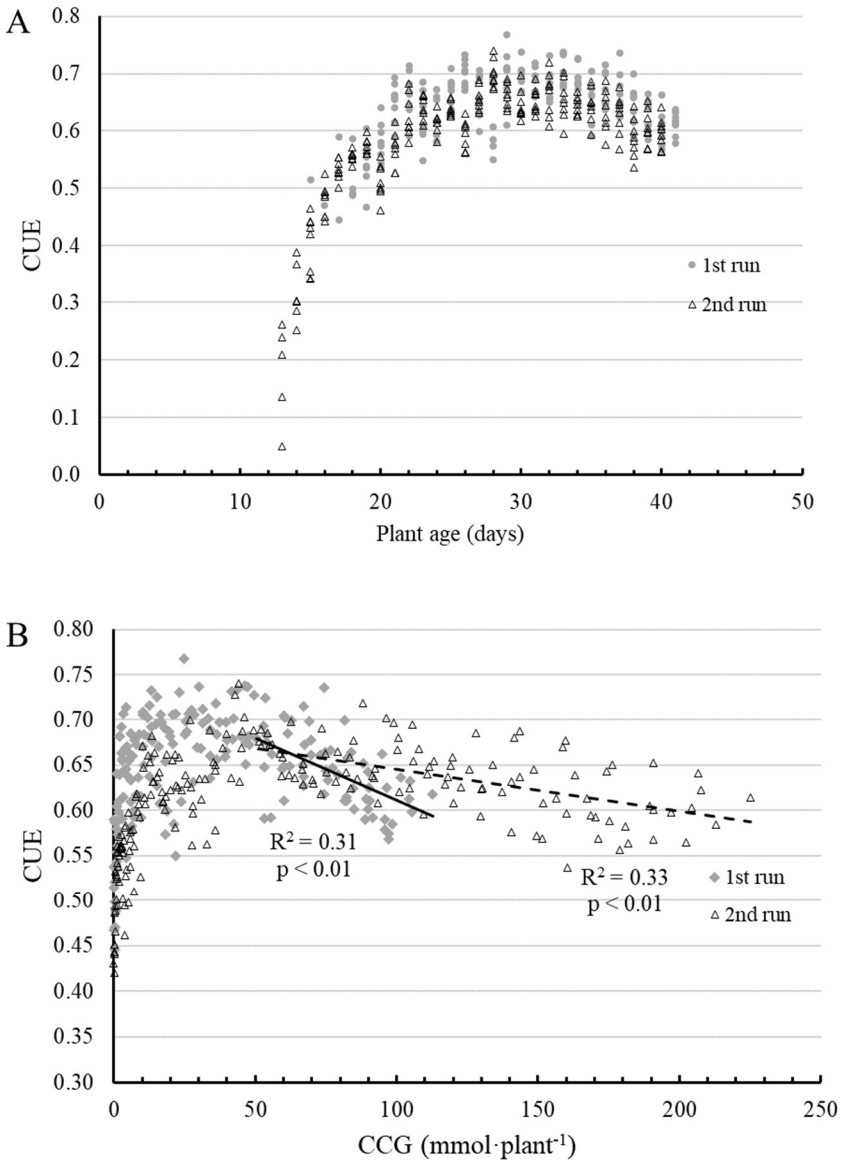

Figure 5.4. CUE followed a similar trend against time (A) and plant size (B) in both runs. For each run, data from lettuce plants in eight gas exchange chambers were pooled and plotted together. When CCG was greater than 50 mmol per plant, CUE decreased linearly with increasing CCG in both runs (B). R^2 and p values of each regression are shown in the graph.

We used multiple linear regression to estimate the g_r and m_r ($R^2 = 0.96$ for the 1st run and $R^2 = 0.97$ for the 2nd run). The estimated g_r was 0.28 mol·mol^{-1} for the 1st run and 0.34 mol·mol^{-1} for

the 2nd run. The m_r was estimated as 22.9 mmol·mol^{-1}·d^{-1} for the 1st run and 20.9 mmol·mol^{-1}·d^{-1} for the 2nd run. The m_r values in our study are lower than previously reported in lettuce (van Iersel, 2003), but still within the range of previously reported values for m_r (van Iersel, 1998; van Iersel and Seymour, 2000). The growth respiration coefficient, g_r, can be used to estimate the theoretical maximum CUE. Assuming that R_m is negligible, maximum CUE can be calculated as $1/(1+g_r)$. In our study, the maximum CUE was estimated to be 0.78 and 0.75 mol·mol^{-1} for the 1st and 2nd run, respectively. The difference between measured CUE and the theoretical maximum CUE is due to carbon lost through maintenance respiration. The difference between measured CUE and maximum CUE was large in very young plants and also increased when CCG was greater than 50 mmol, indicating that more carbon was allocated to R_m (Fig. 5.4B).

R_g increased over time until plants were 26 days old, then leveled off until the 1st harvest which occurred two days later (Fig. 5.5A). The stable R_g indicates that the growth of lettuce plants had plateaued as well, possibly because the lettuce plants had reached canopy closure, at which point light interception limits growth. R_m continued to increase over time and accounted for an increasingly higher percentage of R_d, leaving less carbon available for growth. Therefore, growth rate and R_g leveled off at this point. After the 1st harvest when removing half plants created gaps in the canopies, R_g continued to increase until plants were 35 days old, after which R_g decreased with time (Fig. 5.5A). This decrease in R_g was likely similarly due to canopy closure. R_g continuously increased with time in the 2nd run (Fig. 5.5B), since we harvested lettuce plants more frequently in the 2nd run to minimize leaf overlap among plants. As a result, the growth of lettuce plants in the 2nd run continued to increase light interception and carbon assimilation. The increase in R_g with increasing CCG was faster when lettuce was small (Fig. 5.5C and 5.5D). R_m increased exponentially with time for both runs (Fig. 5.5A and 5.5B) and increased linearly with

CCG (Fig. 5.5C and 5.5D), as m_r was assumed to be constant throughout the study. The percentage of R_m in total respiration (R_d) increased with plant size (Fig. 5.6). However, the percentage of R_m measured at CCG < 10 mmol was difficult to estimate due to small values and, thus, this data was excluded from the graph. For young plants, R_m made up ~40% of R_d in the 1st run and ~30% of R_d in the 2nd run, when CCG was ~10 mmol per plant (Fig. 5.6). When plants reached full size, R_m made up ~60% and 50% of R_d in the 1st and the 2nd run, respectivey. (Fig. 5.6). Therefore, R_m accounted for an increasing percentage of R_d. In the 1st run, R_m exceeded R_g towards the end of the growth cycle (Fig. 5.5A, 6). Similar patterns in R_m and R_g in response to plant size were previously observed (van Iersel and Seymour, 2000; van Iersel, 2003). CUE decreased when CCG was larger than 50 mmol per plant (Fig. 5.4B), a consequence of the increasing R_m percentage diverting assimilated carbon away from growth and R_g.

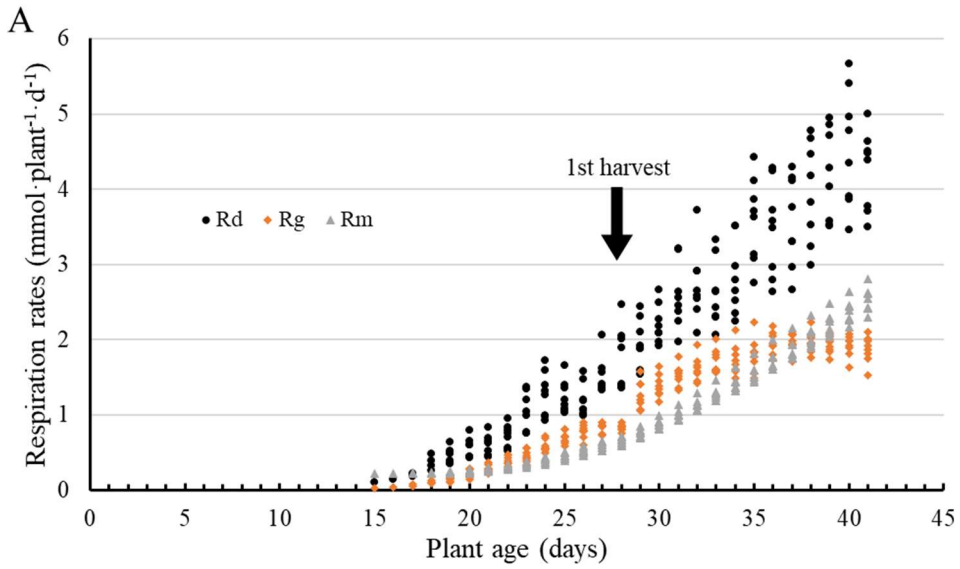

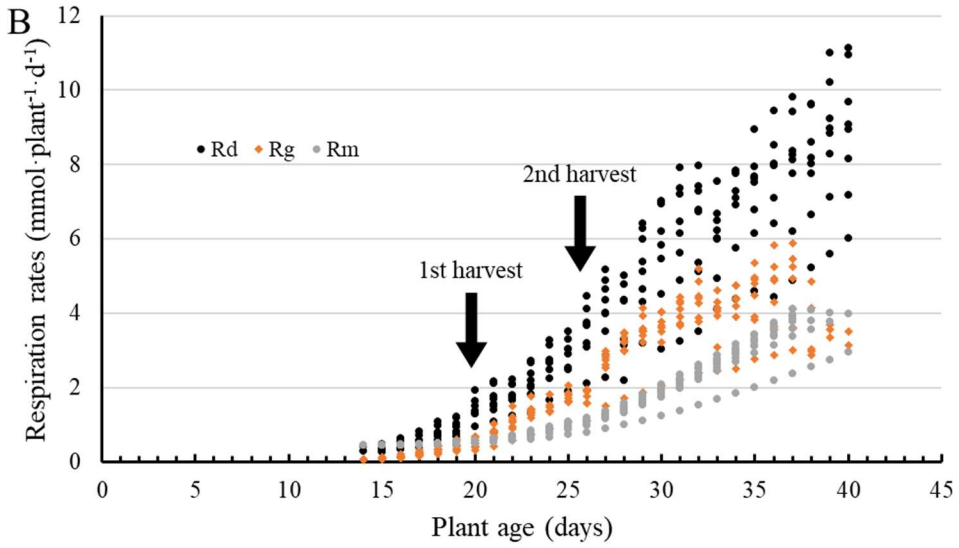
B
Respiration rates (mmol·plant-1·d-1)
Rd
Rg
Rm
1st harvest
2nd harvest
Plant age (days)

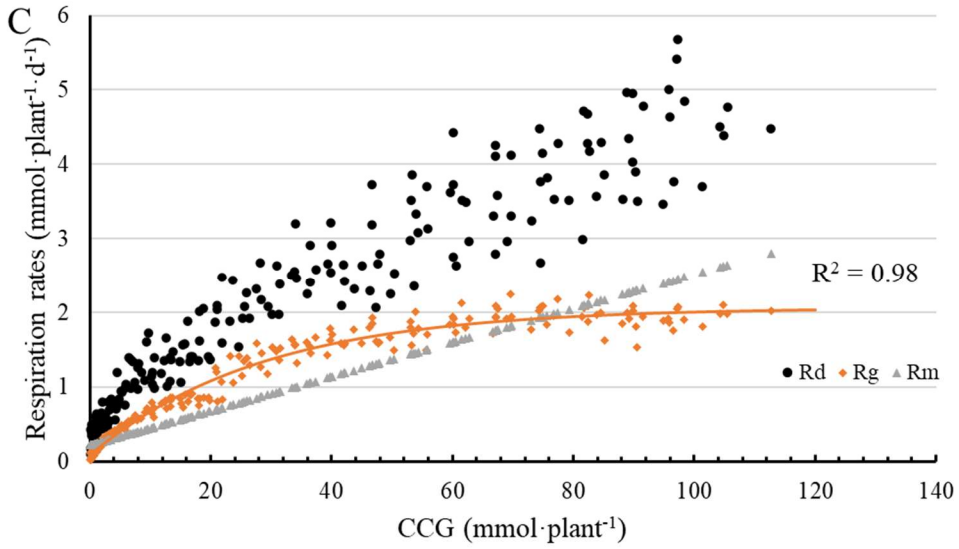
C
Respiration rates (mmol·plant-1·d-1)
R2 = 0.98
Rd
Rg
Rm
CCG (mmol·plant-1)

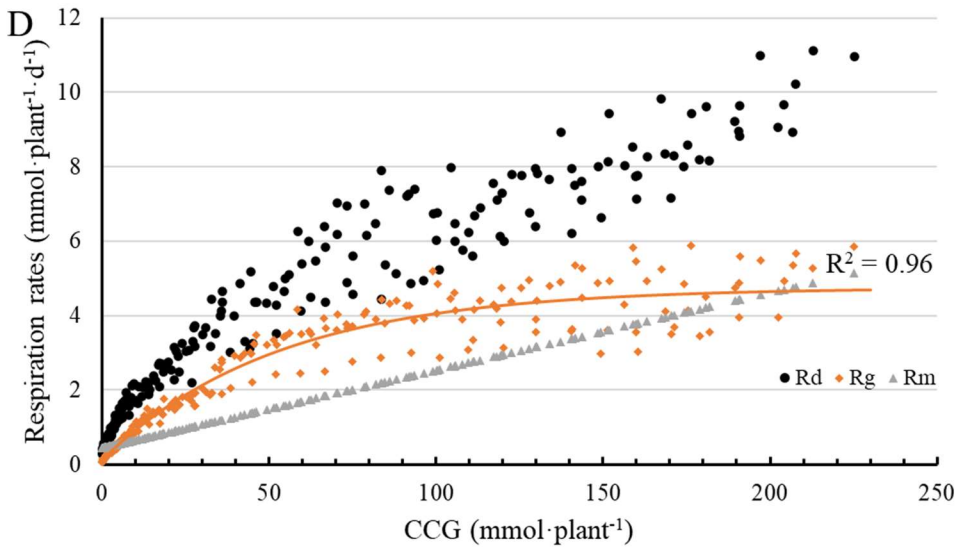

Figure 5.5. R_m increased exponentially with time in both runs (A and B). R_g of lettuce plants showed a stepwise increased with time in the 1st run (A) and continuously increased with time in the 2nd run (B). R_m linearly with plant size, while increase of R_g slowed down with plant size and reached a maximum for the 1st run (C) and the 2nd run (D). For each run, data from lettuce plants in eight gas exchange chambers were pooled and plotted together. R_g followed an exponential rise to maximum function against CCG. The regression equations can be found in Table S5.1. R^2 values of each regression are shown in the graph.

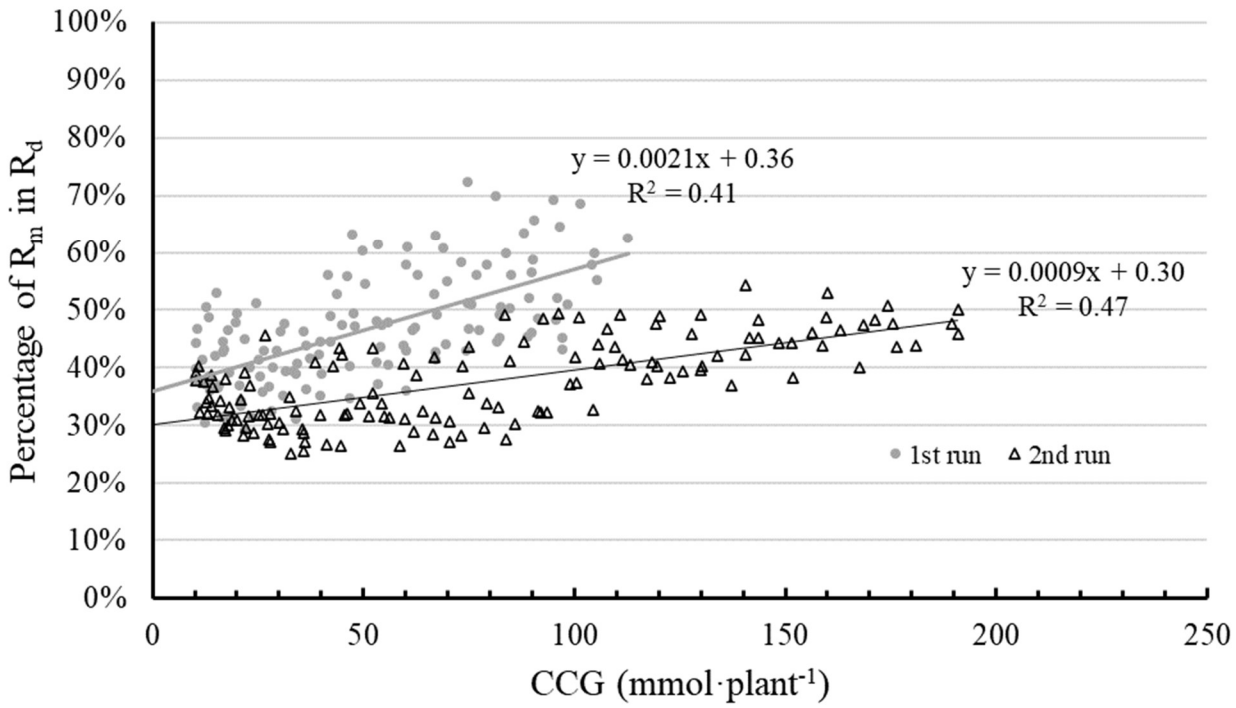

Figure 5.6. Percentage of R_m in total respiration increase with increasing CCG for lettuce. For each run, data from lettuce plants in eight gas exchange chambers were pooled and plotted together. Percentage of R_m in R_d increased linearly with CCG.

Conclusions

Plant growth is driven by carbon assimilation through photosynthesis and carbon loss through respiration. In this study, we recorded a CUE range of lettuce from 0.05 to 0.76 mol·mol^{-1} from the seedling stage to mature stage, implying that 95 to 24% of the assimilated carbon was lost through respiration during the life cycle of lettuce. Carbon loss through respiration is important in driving growth, suggesting that growth rates cannot be estimated solely from photosynthesis measurements or models. It is important to include CUE to connect carbon assimilation and plant growth to accurately estimate growth rates. In this study, we found that when CCG of lettuce

plants increased, $P_{g,day}$ and $P_{n,day}$ and DCG followed an exponential rise to a maximum pattern (Fig. 5.2 and 3). The plateau of $P_{g,day}$ and $P_{n,day}$ and DCG was likely due to the crops reaching canopy closure, after which further growth has little effect on light interception, photosynthesis, and growth rate. R_g followed an asymptotic increase when plotted against CCG, identical to the pattern between DCG and CCG. R_m, on the other hand, increased linearly with CCG. CUE increased with increasing CCG when plants were small, then steadily decreased when CCG was larger than 50 mmol per plant. This steady decrease in CUE was due to the increasing percentage of R_m in R_d, which competed with growth and R_g for carbon. The change in CUE at different developmental stages should be accounted for when modeling carbon balance and growth in plants.

References:

Bugbee, B., and Monje, O. (1992). The Limits of Crop Productivity. *BioScience* 42(7)**,** 494-502. doi: 10.2307/1311879.

Cannell, M.G.R., and Thornley, J.H.M. (2000). Modelling the Components of Plant Respiration: Some Guiding Principles. *Annals of Botany* 85(1)**,** 45-54. doi: 10.1006/anbo.1999.0996.

Frantz, J.M., Cometti, N.N., and Bugbee, B. (2004). Night temperature has a minimal effect on respiration and growth in rapidly growing plants. *Annals of Botany* 94(1)**,** 155-166.

Gifford, R. (1994). The global carbon cycle: a viewpoint on the missing sink. *Functional Plant Biology* 21(1)**,** 1-15.

Monje, O., and Bugbee, B. (1998). Adaptation to high CO2 concentration in an optimal environment: radiation capture, canopy quantum yield and carbon use efficiency. *Plant, Cell & Environment* 21(3)**,** 315-324. doi: https://doi.org/10.1046/j.1365-3040.1998.00284.x.

Reich, P.B., Walters, M.B., Ellsworth, D.S., Vose, J.M., Volin, J.C., Gresham, C., et al. (1998). Relationships of leaf dark respiration to leaf nitrogen, specific leaf area and leaf life-span: a test across biomes and functional groups. *Oecologia* 114(4)**,** 471-482. doi: 10.1007/s004420050471.

van Iersel, M. (Year). "Growth and maintenance respiration of Catharanthus roseus L. estimated from CO2 exchange", in: *XXV International Horticultural Congress, Part 9: Computers and Automation, Electronic Information in Horticulture 519*), 133-140.

van Iersel, M., and Seymour, L. (Year). "Temperature effects on photosynthesis, growth respiration, and maintenance respiration of marigold", in: *XXVI International Horticultural Congress: Elegant Science in Floriculture 624*), 549-554.

van Iersel, M.W. (2003). Carbon use efficiency depends on growth respiration, maintenance respiration, and relative growth rate. A case study with lettuce. *Plant, Cell & Environment* 26(9)**,** 1441-1449. doi: doi:10.1046/j.0016-8025.2003.01067.x.

van Iersel, M.W. (2006). Respiratory Q10 of marigold (Tagetes patula) in response to long-term temperature differences and its relationship to growth and maintenance respiration. *Physiologia Plantarum* 128(2)**,** 289-301. doi: 10.1111/j.1399-3054.2006.00743.x.

van Iersel, M.W., and Kang, J.-G. (2002). Nutrient solution concentration affects whole-plant CO2 exchange and growth of subirrigated pansy. *Journal of the American Society for Horticultural Science* 127(3)**,** 423-429.

van Iersel, M.W., and Seymour, L. (2000). Growth Respiration, Maintenance Respiration, and Carbon Fixation of Vinca: A Time Series Analysis. *Journal of the American Society for Horticultural Science* 125(6)**,** 702-706.

Zhen, S., and Bugbee, B. (2020). Substituting Far-Red for Traditionally Defined Photosynthetic Photons Results in Equal Canopy Quantum Yield for CO2 Fixation and Increased Photon Capture During Long-Term Studies: Implications for Re-Defining PAR. *Frontiers in Plant Science* 11(1433). doi: 10.3389/fpls.2020.581156.

Supplemental table 5.1. Details of regression equations used in this study. In all cases cumulative carbon gain (CCG, mmol·plant^{-1}) is the independent variable.

Graph	Dependent variable	unit	Regression equation	y0	a	b
2C	$P_{g,day}$	mmol·plant^{-1}·d^{-1}	$y = y0 + a \times (1 - e^{-bx})$	0.812	12.9	0.0273
2C	$P_{n,day}$	mmol·plant^{-1}·d^{-1}	$y = y0 + a \times (1 - e^{-bx})$	0.253	5.0	0.0341
2C	$R_{d,day}$	mmol·plant^{-1}·d^{-1}	$y = y0 + a \times (1 - e^{-bx})$	-0.285	-11.4	0.0167
2D	$P_{g,day}$	mmol·plant^{-1}·d^{-1}	$y = y0 + a \times (1 - e^{-bx})$	1.094	33.9	0.0155
2D	$P_{n,day}$	mmol·plant^{-1}·d^{-1}	$y = y0 + a \times (1 - e^{-bx})$	0.351	25.2	0.0182
2D	$R_{d,day}$	mmol·plant^{-1}·d^{-1}	$y = y0 + a \times (1 - e^{-bx})$	-0.501	-9.5	0.0108
3A	DCG	mmol·plant^{-1}·d^{-1}	$y = y0 + a \times (1 - e^{-bx})$	0.353	7.1	0.0349
3B	RGR	mol·mol^{-1}·d^{-1}	$y = y0 + a \times e^{-bx}$	0.122	0.546	0.1616
3C	DCG	mmol·plant^{-1}·d^{-1}	$y = y0 + a \times (1 - e^{-bx})$	0.339	13.8	0.0190
3D	RGR	mol·mol^{-1}·d^{-1}	$y = y0 + a \times e^{-bx}$	0.119	0.349	0.0915
5A	R_m	mmol·plant^{-1}·d^{-1}	$y = y0 + a \times (1 - e^{-bx})$	0.315	1.97	0.0350
5B	R_m	mmol·plant^{-1}·d^{-1}	$y = y0 + a \times (1 - e^{-bx})$	0.549	4.65	0.0190

CHAPTER 6

CONCLUSION

Traditionally, photosynthetically active radiation (PAR) was defined as light within the range of 400-700 nm. Any light with wavelength out of this range was considered photosynthetically ineffective. Even within the PAR, not all photons are used by plants to drive photosynthesis at equal efficiency. Since green photons (500 - 600 nm) had lower absorptance by green leaves than blue (400 - 500 nm) and red photons (600 - 700 nm), green photons were shown to have a lower quantum yield of CO_2 assimilation (moles of CO_2 assimilation per mole of photons) than blue and red photons (McCree, 1971). However, this conclusion was drawn at low photosynthetic photon flux density (*PPFD*) and on incident photon base. We found that at low *PPFD*, despite the lower absorptance, green photons were used as efficiently as red photon at driving photosynthesis and were more efficiently than blue photons. At high *PPFD*, green photons resulted in higher quantum yield of CO_2 assimilate than both red and blue photons. Since green photons were less strongly absorptance by green leaves, energy of green photons was distribution more evenly across whole depth of leaves and excited more reaction centers for photosynthesis than blue and red photons. We also demonstrated that the interactive effect of *PPFD* and light spectrum on photosynthesis was due to changes in electron transport but not on Calvin cycle. Light of different wavebands with PAR also did no interacted with each other on driving photosynthesis.

Far-red photons (700 - 750 nm) falls outside of the PAR range and were traditionally thought to have extremely low photosynthetic activity. However, when far-red photons were applied with PAR photons, far-red photons were shown to drive photosynthesis just as efficiently

as PAR photons (Zhen and van Iersel, 2017; Zhen and Bugbee, 2020). Far-red photons had also shown to increase light interception by promoting canopy expansion, thus increased dry mass of many vegetable and ornamental crops under sole-source light (Li and Kubota, 2009; Kubota et al., 2011; Park and Runkle, 2017; Craver et al., 2018; Hernandez and Spalholz, 2019; Meng and Runkle, 2019; Zou et al., 2019; Legendre and van Iersel, 2021). However, the optimal amount of far-red light to apply with PAR light to elicit the full benefit of far-red lights inclusion on crops is unclear. We grew 'Cherokee', 'Green Saladbowl' and 'Little Gem' lettuces under 16 different supplemental far-red *PFD*s (photosynthetic flux density), ranging from 0 to 70.4 umol·m^{-2}·s^{-1}, with a background of 204 umol·m^{-2}·s^{-1} white light. Supplemental far-red photons induced leaf expansion in all three cultivars, which resulted in increased projected canopy size (PCS) in a cultivar-dependent manner. Supplemental far-red photons increased light interception of 'Cherokee' throughout the whole production cycle and resulted in higher shoot fresh and dry weight. The increase in light interception caused by supplemental far-red photons was transient for 'Green Saladbowl' and 'Little Gem', and the transient benefits of increased light interception translated to higher shoot dry weight for 'Little Gem', but not for 'Green Saladbowl'. Supplemental far-red light resulted in lower chlorophyll concentration for all three cultivars and lower anthocyanin content for the red lettuce 'Cherokee'. Those changes in pigmentation did not significantly affect Φ_{PSII}. In summary, adding far-red light in indoor production increased light interception of lettuce seedlings, but did not significantly affect leaf photosynthesis, and resulted in linear increases of biomass, up to 70.4 umol·m^{-2}·s^{-1} in two of the three cultivars tested.

To further disentangle the effect of far-red photon inclusion on crop growth through increased light interception by leaf expansion and canopy enlargement and through Emerson

enhancement effect, we grew 'Little Gem' lettuces under four light treatments of the same ePAR but with far-red photons progressively substituted red photons in the spectrum. We found that far-red photon substitution increased canopy light interception through leaf expansion and canopy enlargement. The effect of far-red photon substitution on canopy light depended on plant density: at low plant density, since light interception was low, leaf expansion and canopy enlargement greatly increased light interception; while at high plant density, lettuce plants quickly reached canopy closure and the effect of far-red photon substitution on light interception was limited. Far-red photon substitution also reduced the amount of ePAR photons leaves absorbed, simply because we replaced strongly-absorbed red photons with less absorbed far-red photons. At high plant density (the 1st run), the reduction in amount of ePAR absorbed by leaves possibly negated the benefit of larger PCS on canopy level photosynthesis. But at low plant density (the 2nd run), larger canopy size increased canopy level P_g, despite lower leaf level ePAR photon absorptance with far-red photon substitution. Furthermore, far-red photons had photosynthetic activity when applied with blue and white background light, but had substantially lower photosynthetic activity than red photons. The canopy-level quantum yield of photosynthesis of red photons was 1.75 times that of far-red photons. The lower quantum yield of photosynthesis of far-red photons were due lower leaf absorptance and likely incapability of far-red photons to excite PSII. Despite the effect on carbon assimilation, far-red photon substitution did not affect the final dry weight and cumulative carbon gain of the plants. Our results suggest a potential cost-saving opportunity for growers. Since far-red LEDs have higher efficacy of converting electricity to photon output (Kusuma et al., 2020), replacing LEDs that provide PAR with far-red LEDs can reduce energy consumption without a negative impact on

crop growth. Overall, far-red photon inclusion increased crop growth mostly through increase in light interception while canopy-level quantum yield of photosynthesis of far-red photons was lower than PAR photons. Far-red photon inclusion also likely benefits crops with less vigorous growing habit and at low plant density.

Carbon use efficiency (CUE) is an important component in modelling plant growth, changes in canopy-level gross photosynthetic rate of 'Little Gem' lettuce failed to induce changes in dry weight as seen in Chapter 4. We recorded a wide CUE range of lettuce: from 0.05 to 0.76 $mol \cdot mol^{-1}$ from the seedling stage to mature stage, implying that 95% to 24% of the assimilated carbon was lost through respiration during the life cycle of lettuce. CUE initially increased with plant size potentially due to respiration of carbon preserve in seeds. CUE then steadily decreased with plant size after cumulative carbon gain of lettuce plants was larger than 50 mmol. Photosynthesis of lettuce plants carried out through the day increased asymptotically as plants grew bigger in size. Growth respiration similarly followed an asymptotic increase with plant size. But maintenance respiration increased linearly with plant size after the seedling stage. This steady decrease in CUE was due to the increasing percentage of maintenance respiration in total respiration, which competed with growth and growth respiration for carbon. The change in CUE at different developmental stages should be accounted for when modeling carbon balance and growth in plants.

References:

Craver, J.K., Boldt, J.K., and Lopez, R.G. (2018). Radiation Intensity and Quality from Sole-source Light-emitting Diodes Affect Seedling Quality and Subsequent Flowering of Long-day Bedding Plant Species. *HortScience* 53(10)**,** 1407-1415.

Hernandez, R., and Spalholz, H. (Year). "Characterization of Solar Radiation Spectral Contribution in Lettuce Bolting and Flowering Using LEDs in an Indoor Setting", in: *2019 ASHS Annual Conference*: ASHS).

Kubota, C., Chia, P., Yang, Z., and Li, Q. (Year). "Applications of far-red light emitting diodes in plant production under controlled environments", in: *International Symposium on Advanced Technologies and Management Towards Sustainable Greenhouse Ecosystems: Greensys2011 952*), 59-66.

Kusuma, P., Pattison, P.M., and Bugbee, B. (2020). From physics to fixtures to food: current and potential LED efficacy. *Horticulture Research* 7(1)**,** 56. doi: 10.1038/s41438-020-0283-7.

Legendre, R., and van Iersel, M.W. (2021). Supplemental Far-Red Light Stimulates Lettuce Growth: Disentangling Morphological and Physiological Effects. *Plants* 10(1)**,** 166.

Li, Q., and Kubota, C. (2009). Effects of supplemental light quality on growth and phytochemicals of baby leaf lettuce. *Environmental and Experimental Botany* 67(1)**,** 59-64.

McCree, K.J. (1971). The action spectrum, absorptance and quantum yield of photosynthesis in crop plants. *Agricultural Meteorology* 9(Supplement C)**,** 191-216. doi: 10.1016/0002-1571(71)90022-7.

Meng, Q., and Runkle, E.S. (2019). Far-red radiation interacts with relative and absolute blue

and red photon flux densities to regulate growth, morphology, and pigmentation of lettuce and basil seedlings. *Scientia Horticulturae* 255**,** 269-280. doi: 10.1016/j.scienta.2019.05.030.

Park, Y., and Runkle, E.S. (2017). Far-red radiation promotes growth of seedlings by increasing leaf expansion and whole-plant net assimilation. *Environmental and experimental botany* 136**,** 41-49. doi: 10.1016/j.envexpbot.2016.12.013.

Zhen, S., and Bugbee, B. (2020). Far‐red photons have equivalent efficiency to traditional photosynthetic photons: implications for redefining photosynthetically active radiation. *Plant, Cell & Environment*.

Zhen, S., and van Iersel, M.W. (2017). Far-red light is needed for efficient photochemistry and photosynthesis. *Journal of plant physiology* 209**,** 115-122. doi: 10.1016/j.jplph.2016.12.004.

Zou, J., Zhang, Y., Zhang, Y., Bian, Z., Fanourakis, D., Yang, Q., et al. (2019). Morphological and physiological properties of indoor cultivated lettuce in response to additional far-red light. *Scientia Horticulturae* 257**,** 108725. doi: 10.1016/j.scienta.2019.108725.